Dusty Plasmas in the Solar System

Mihaly Horanyi
Department of Physics and LASP, U. of Colorado

Outline:

1) Motivation
2) Dusty plasma primer
3) Dust in magnetospheres: transport, capture, ejection

---

4) Dusty plasmas on the surfaces of airless bodies
5) Dusty plasmas in comets
6) Dust in the heliosphere: interstellar dust, nano-dust

Where do we find plasmas?

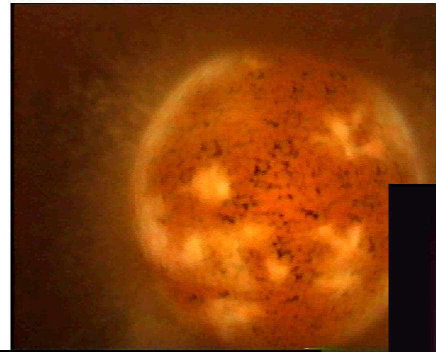
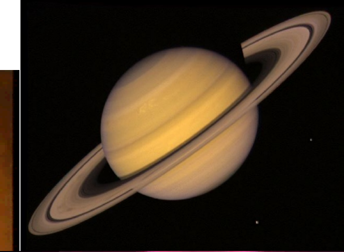
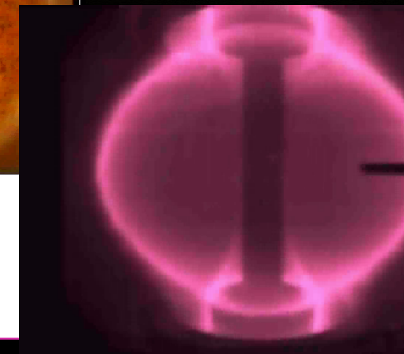

- 99% of the visible matter in the universe is ´plasma´.
- A large fraction of this plasma is ´dusty´:

Galaxies, interstellar clouds, star formation regions, planetary disks, comets, our atmosphere, planetary rings, all plasma processing devices, even plasma fusion reactors, etc.

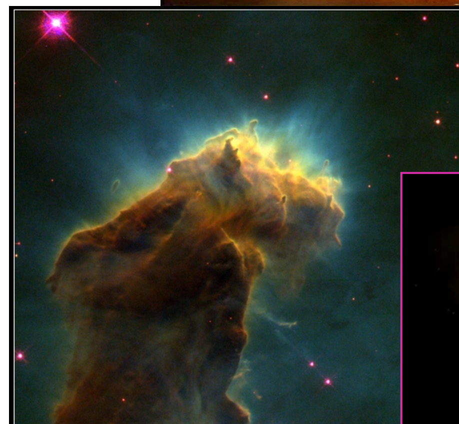
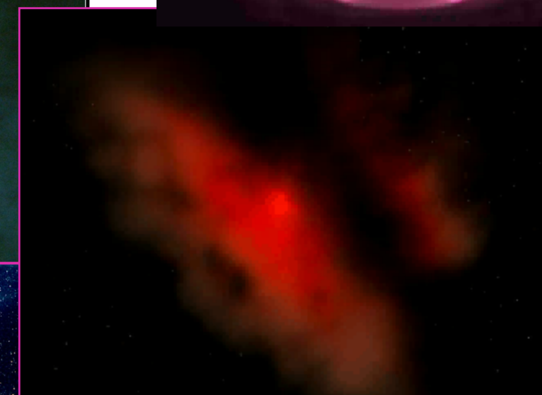




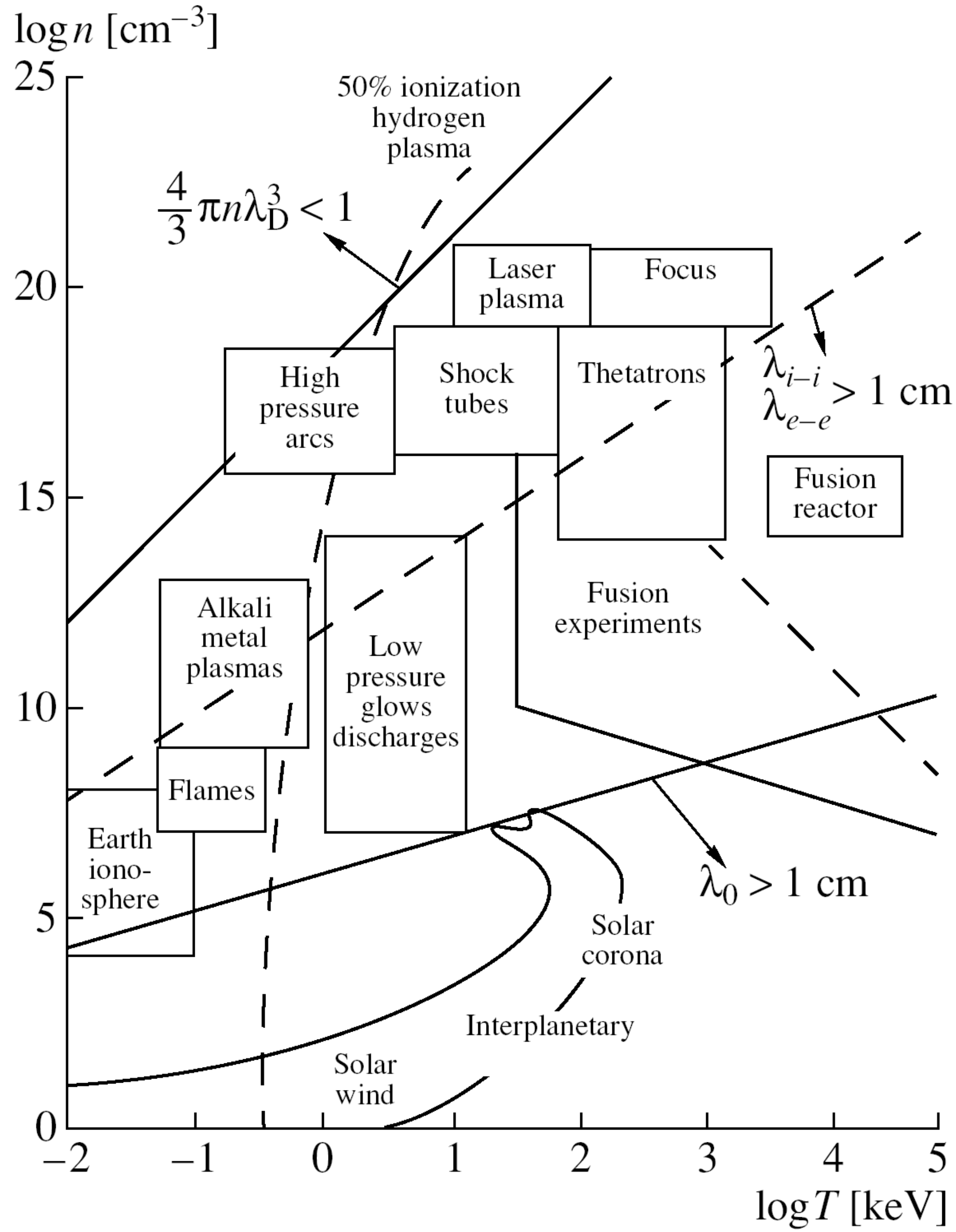

log n [cm−3]
50% ionization hydrogen plasma
4/3 πnλD3 < 1
Laser plasma
Focus
High pressure arcs
Shock tubes
Thetatrons
λi−i
λe−e > 1 cm
Fusion reactor
Fusion experiments
Alkali metal plasmas
Low pressure glows discharges
Flames
Earth ionosphere
λ0 > 1 cm
Solar corona
Interplanetary
Solar wind
log T [keV]

- Plasmas - Encyclopaedia Britannica:

- A collection of positive and negative charges, about equal in number or density and forming a neutrally charged distribution of matter.

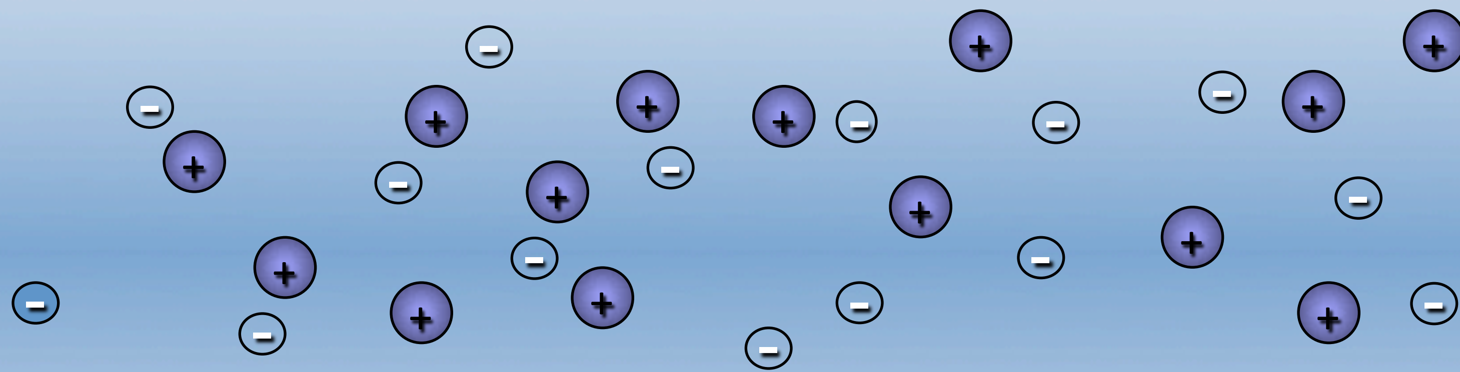

- Plasma state is called the fourth state of matter and is unique in the way in which it interacts with itself, with electric and magnetic fields, and with its environment.

- Dusty Plasmas

- A collection of positive and negative charges, and macroscopic objects, forming a neutrally charged distribution of matter.

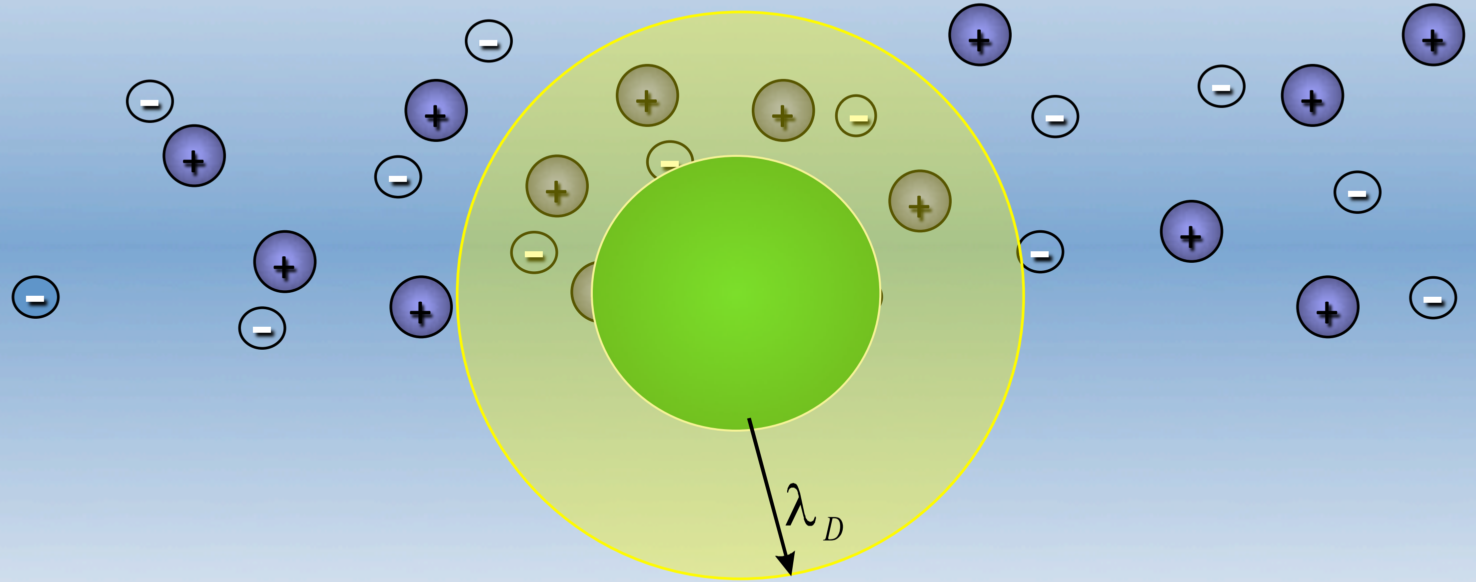

Small particles absorb electron and ions and become charged

- Dusty Plasmas

- A collection of positive and negative charges, and macroscopic objects, forming a neutrally charged distribution of matter.

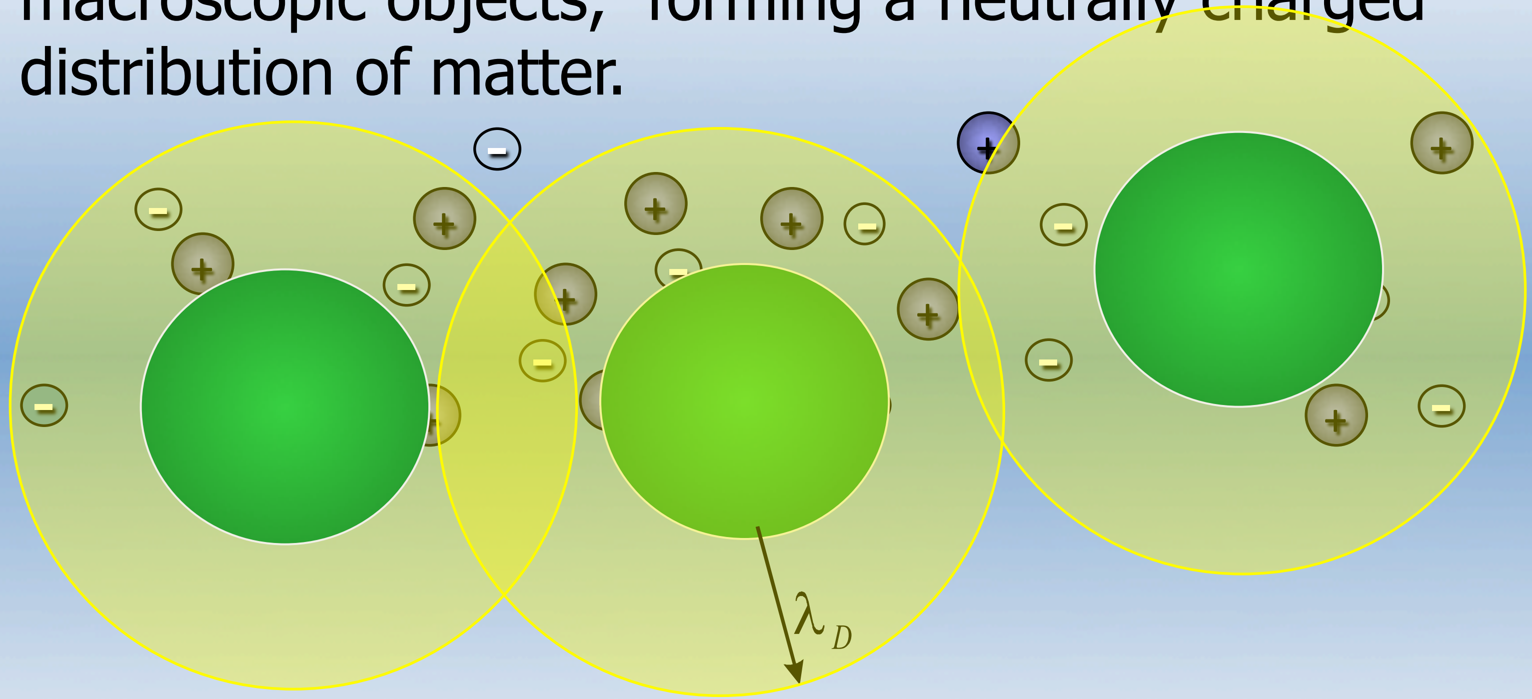

Small particles absorb electron and ions and become charged

Types of Dusty Plasmas:

$e, i_1, i_2, \ldots\ldots i_n$ and dust$^+$/dust$^-$ (comets, rings)

e and dust$^+$ (moon, asteroid surface)

dust$^+$ and dust$^-$ (sand storms)

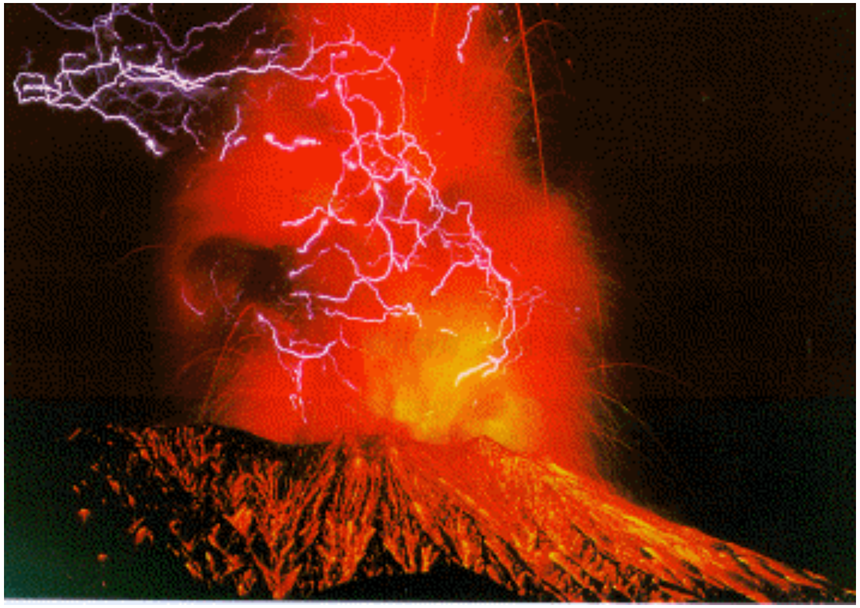

New physics:

Dust is many orders of magnitude heavier than ions and can carry many orders of magnitude larger + or - time dependent charge.

new spatial scales

new time scales

unusual dynamics

new waves & instabilities

Dust charge:

electron and ion fluxes

secondary and photoelectrons

dust – dust collisions

Dust - acoustic wave

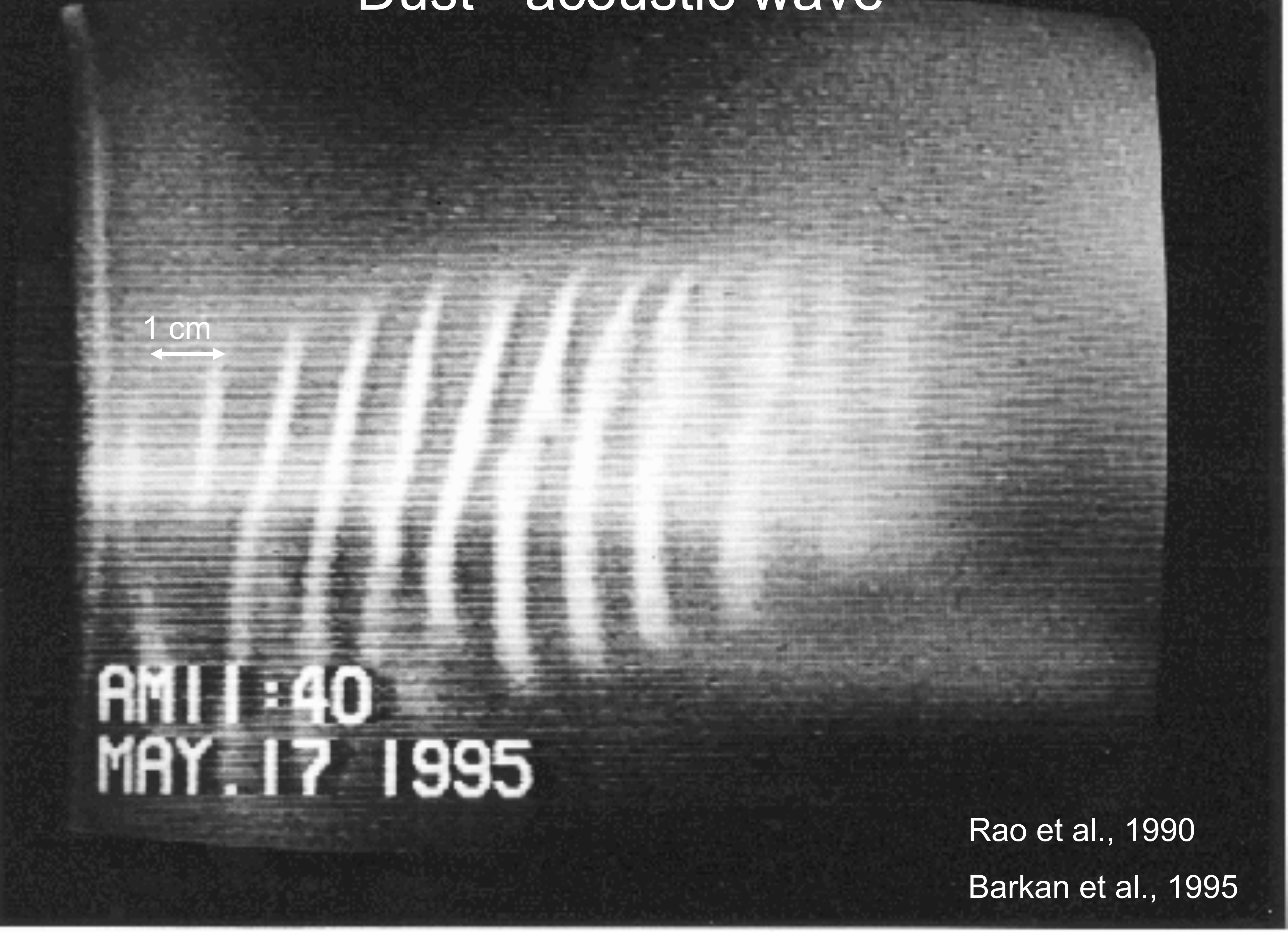

Rao et al., 1990

Barkan et al., 1995

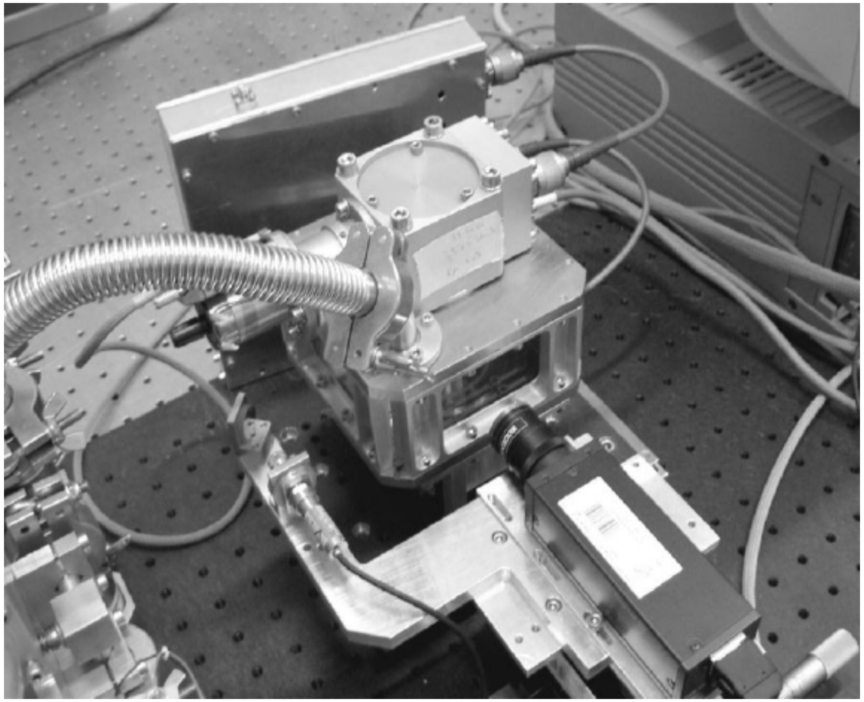

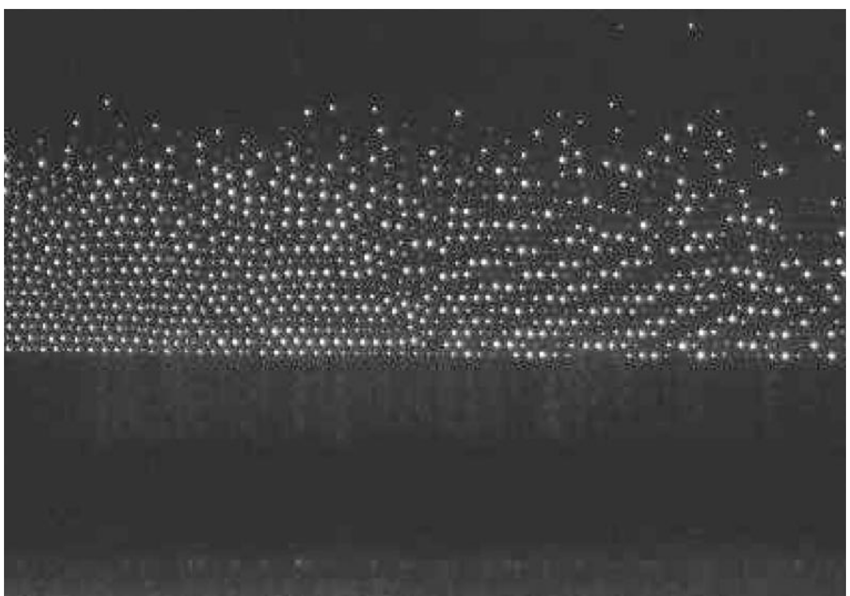
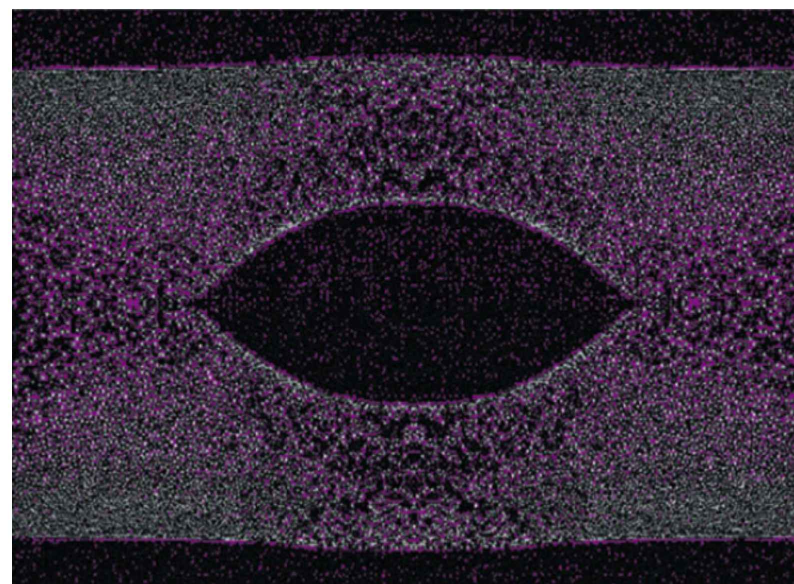

2) Dusty plasma primer

Dust Charging Processes

- electron and ion collection
- secondary emission
- UV induced photoelectron emission
- ....

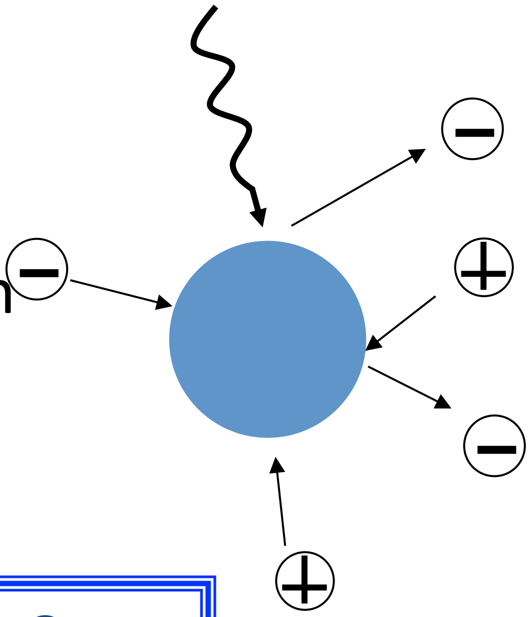

Total current to a grain = 0

$$\Sigma I = I_e + I_i + I_{sec} + I_{pe} = 0$$

The Charge on a Dust Grain

In typical lab plasmas $I_{sec} = I_{pe} = 0$

Electron thermal speed >> ion thermal speed so the grains charge to a negative potential V_S relative to the plasma, until the condition $I_e = I_i$ is achieved.

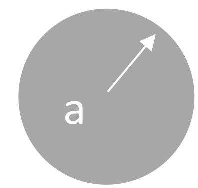

electron repulsion

$$I_e = en_e\sqrt{\frac{kT_e}{m_e}}\;\boxed{\exp\left(\frac{eV_S}{kT_e}\right)}\;\pi a^2$$

$$I_i = en_i\sqrt{\frac{kT_i}{m_i}}\;\boxed{\left(1-\frac{eV_S}{kT_i}\right)}\;\pi a^2$$

ion enhancement

$$\boxed{\begin{aligned} Q &= (4\pi\varepsilon_o a)\, V_S \\ Q_e &= 700\, a_\mu V_S \end{aligned}}$$

Typically V_S is independent of a

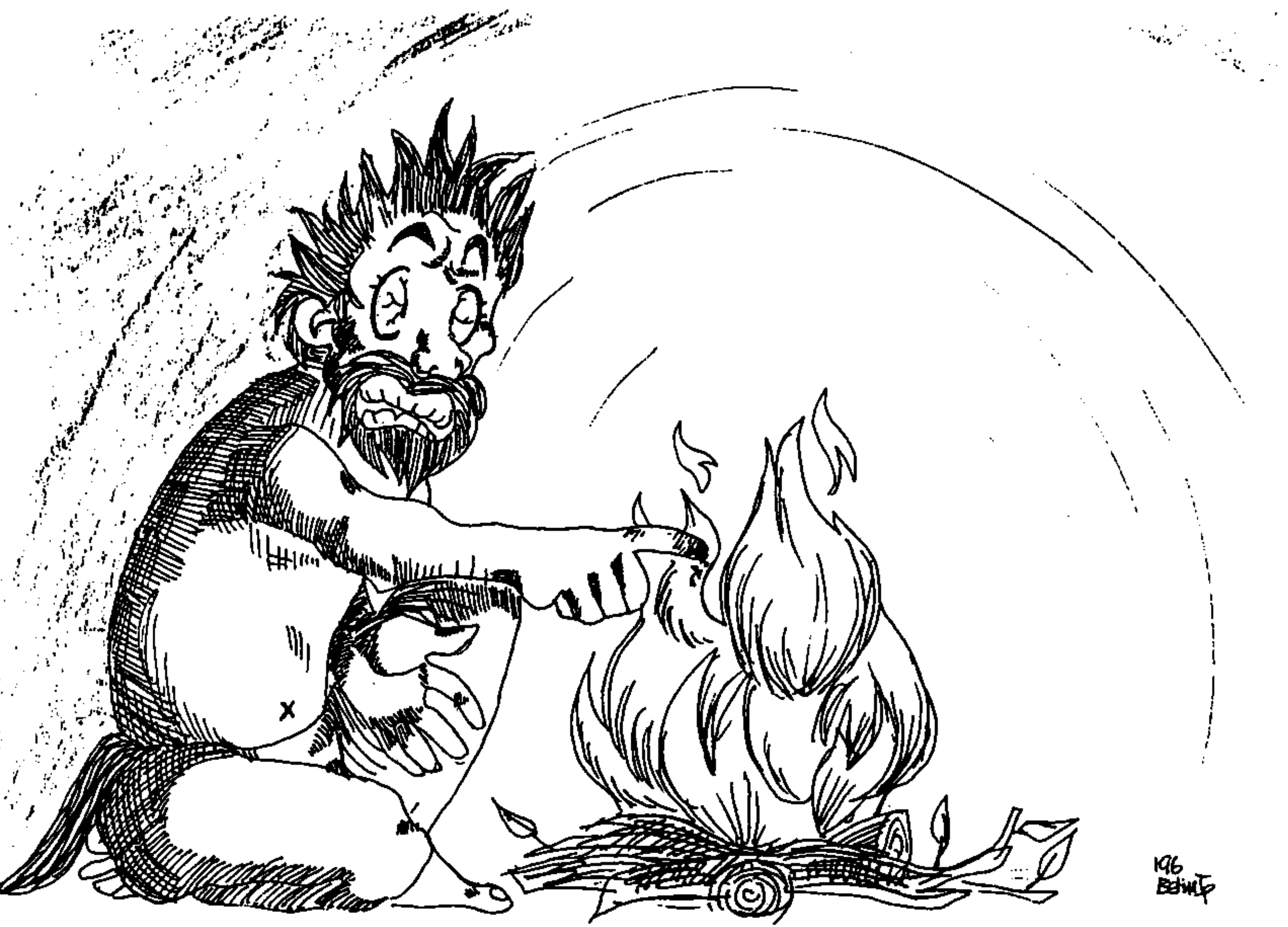

Dust Charge Measurements

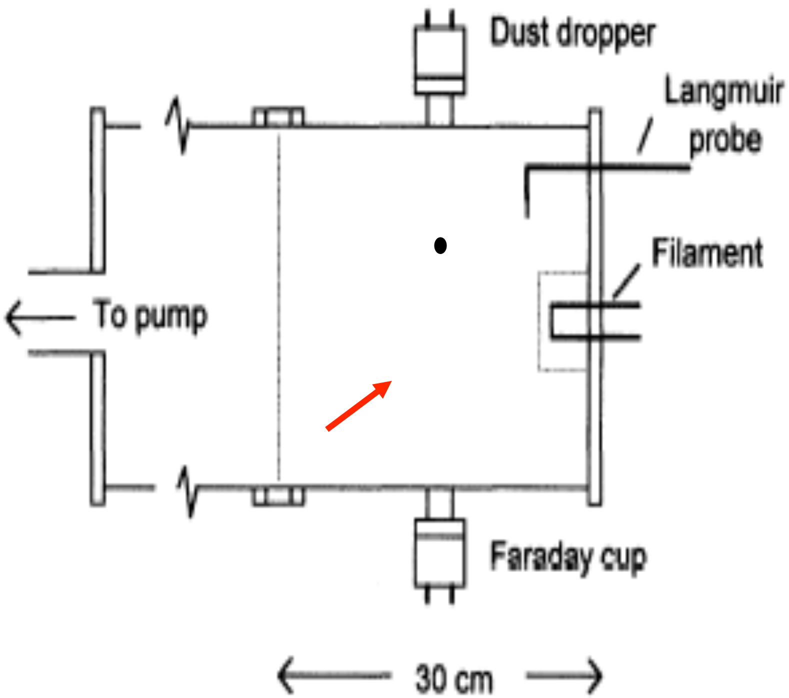

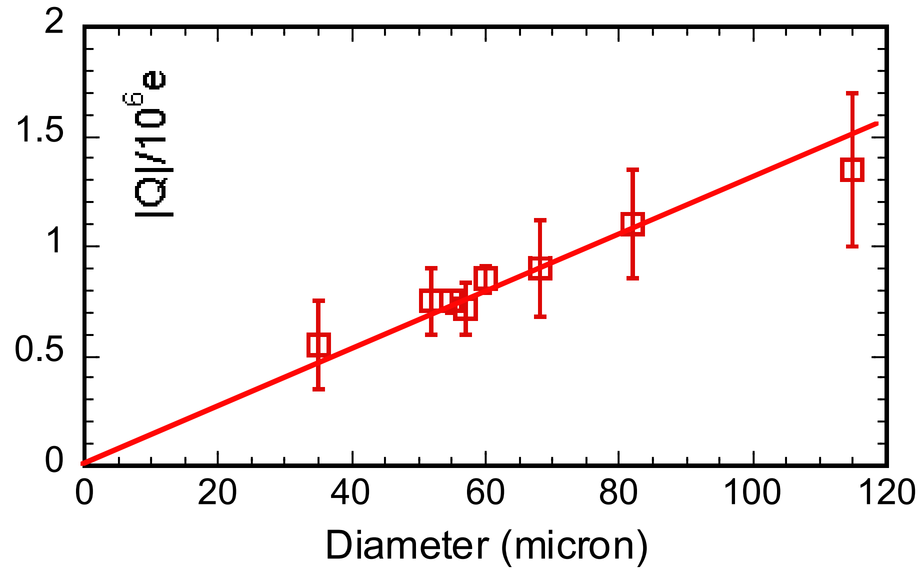

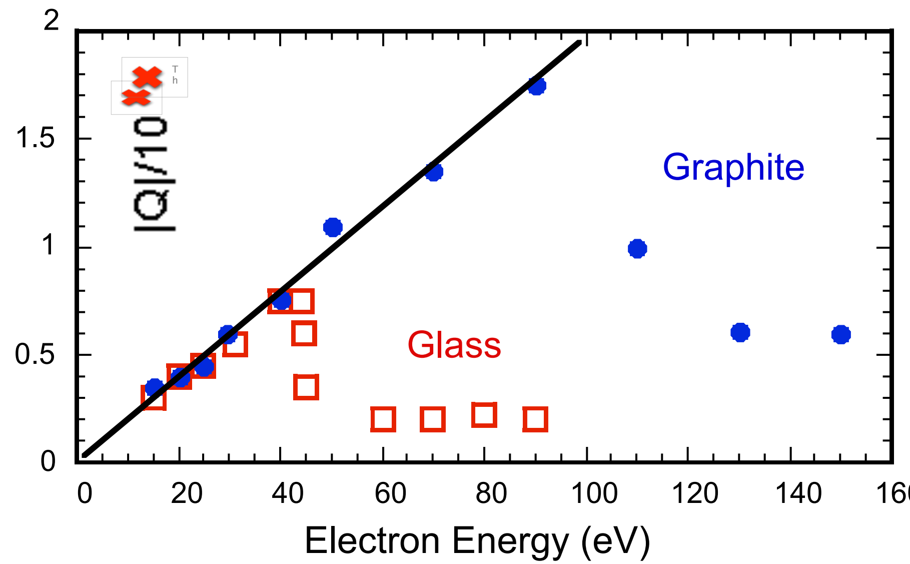

UV charging (I)

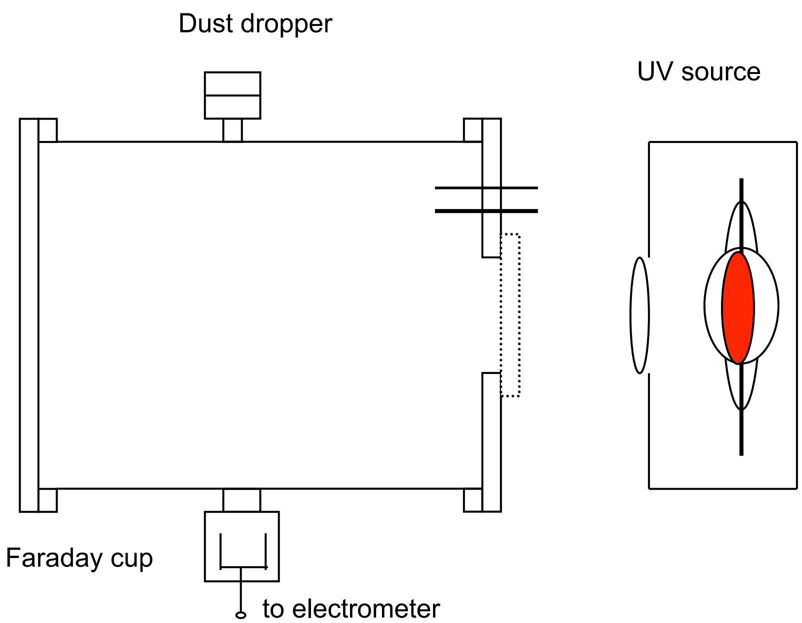

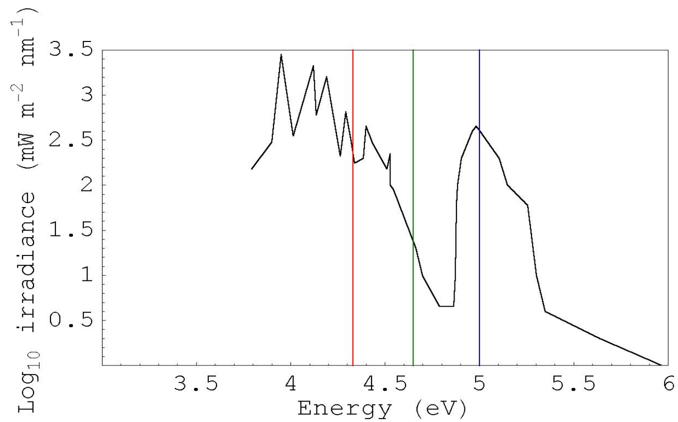

Spectral irradiance curve at 0.5 m for the 1kW Hg-Xe arc lamp.

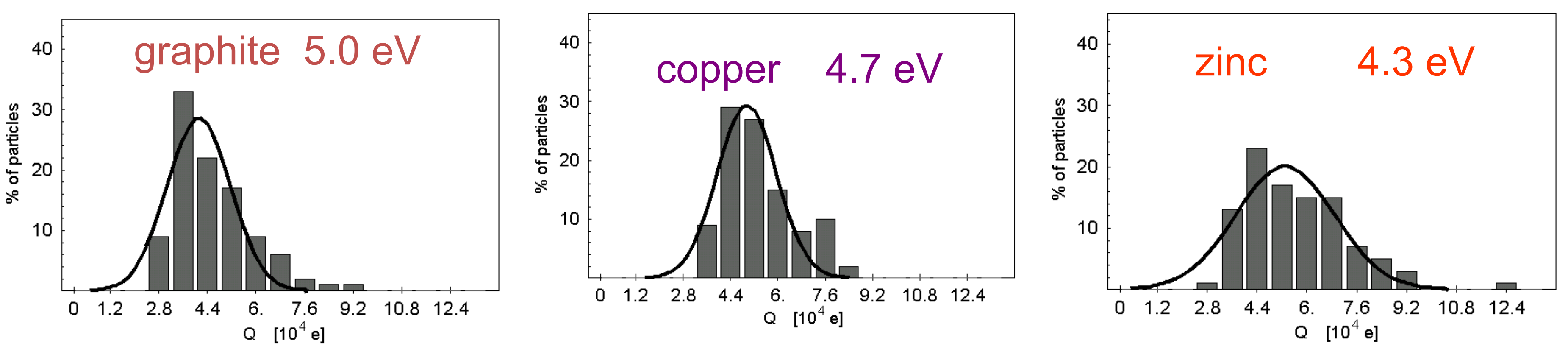

3) Dust in magnetospheres: transport, capture, ejection

Motion of a charged grain is followed by:

$$\ddot{\mathbf{r}} = -GM_J \nabla \left(\frac{1}{r} + \frac{R_J^2}{r^3} J_2 P_2 + \frac{R_J^4}{r^5} J_4 P_4 \right) + \frac{Q}{m} \left(\frac{\dot{\mathbf{r}}}{c} \times \mathbf{B} + \mathbf{E}_c \right)$$

Its charge:

$$\frac{dQ}{dt} = \sum_i I_i$$

Limits:

Q/m << 1

Gravity dominates

(Kepler orbits)

Q/m >> 1

E&M dominates

(adiabatic motion of e, i)

1 MeV proton @ Earth's synchronous radius

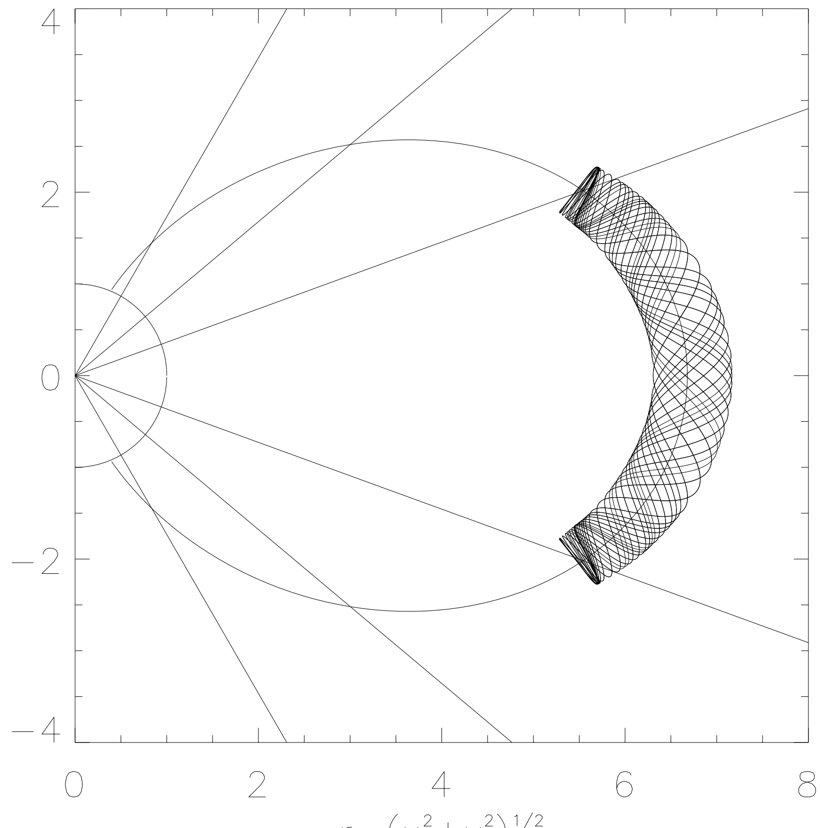

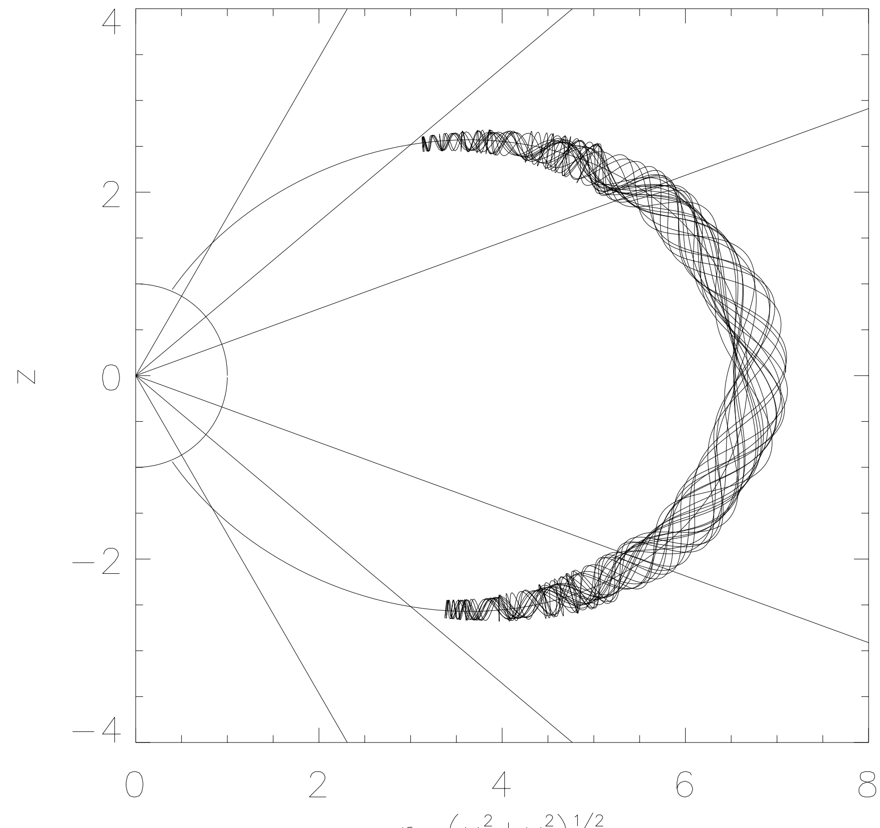

Saturn

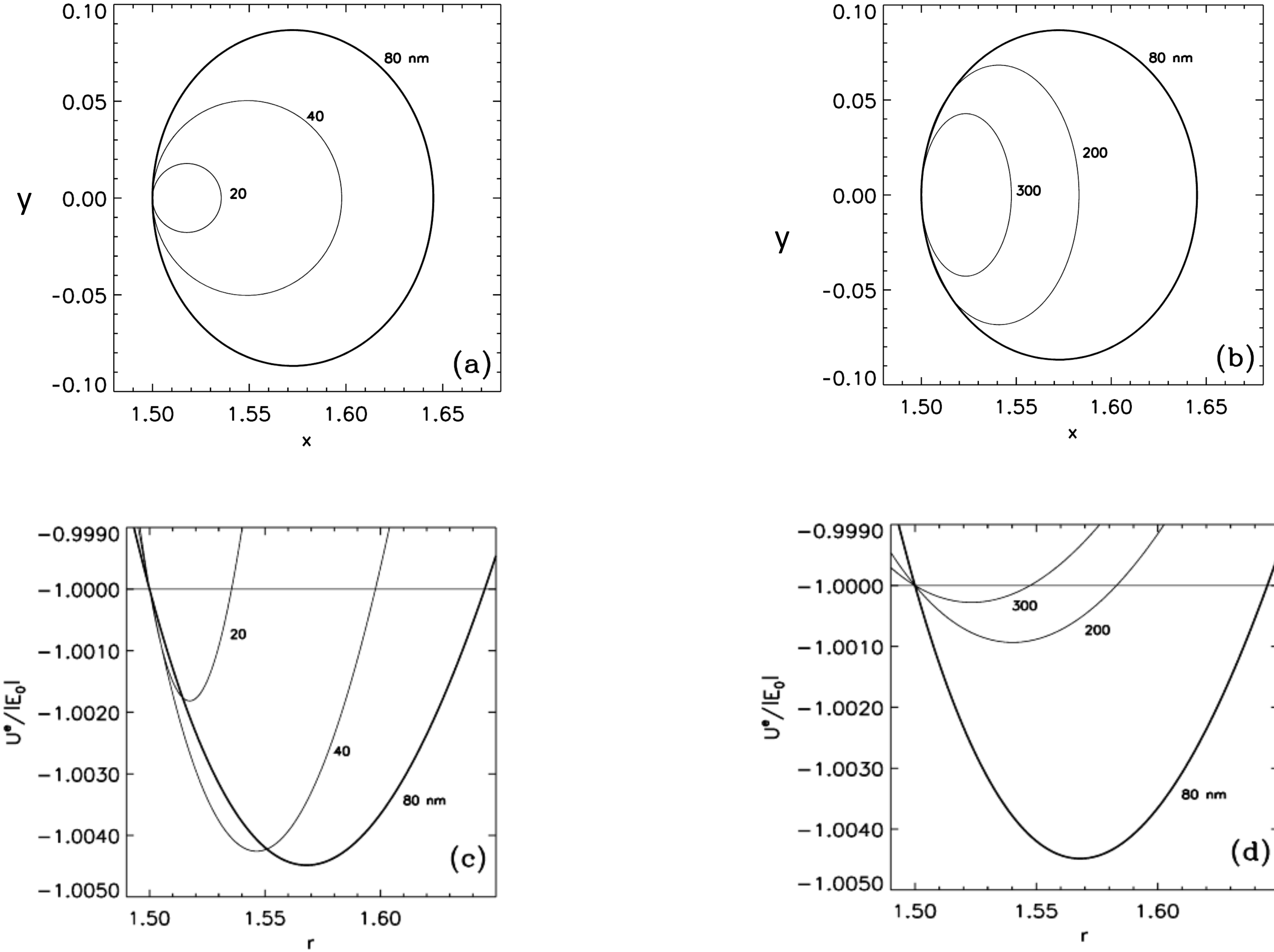

$\phi = -10$ V   Kepler start, inside synchronous radius

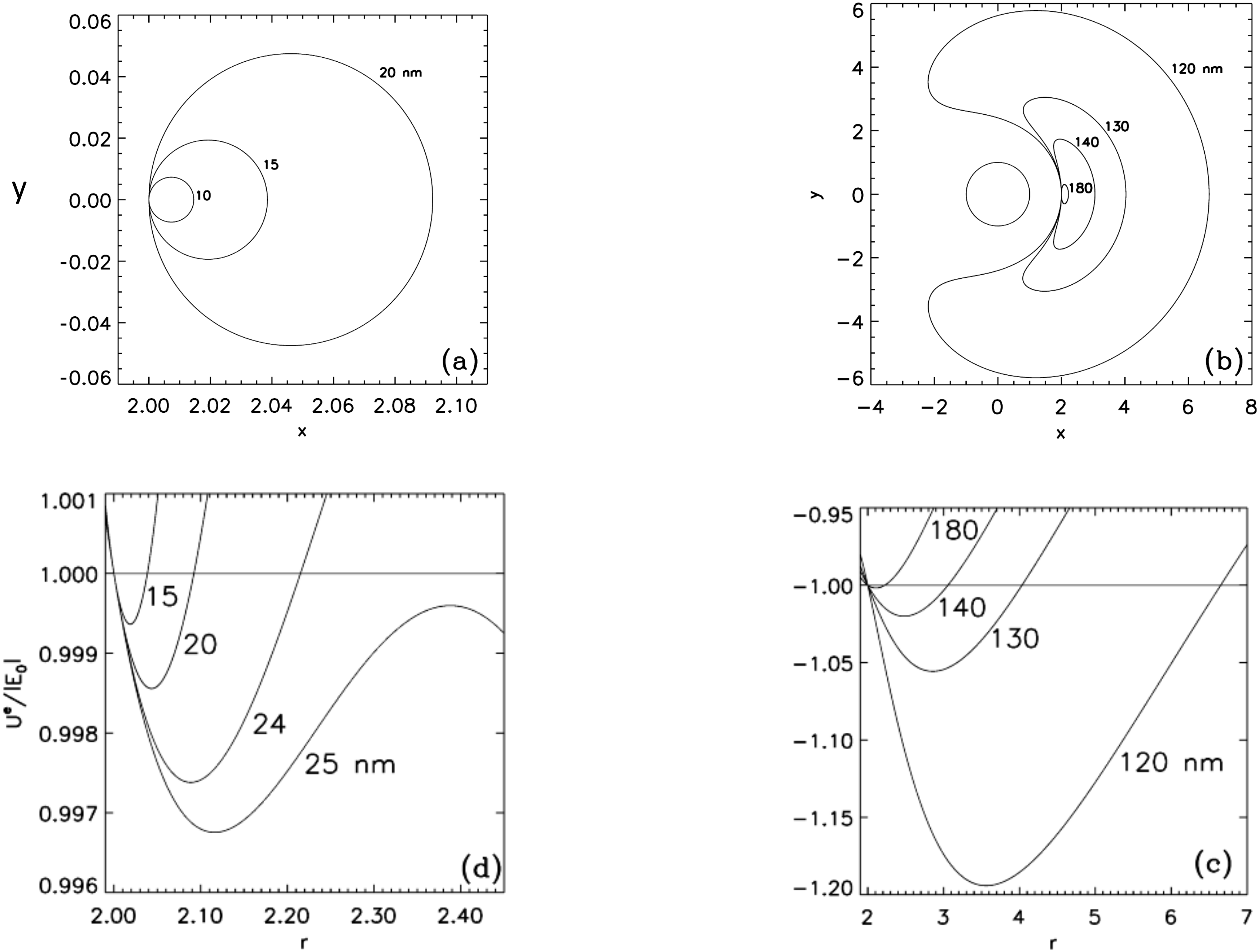

$\phi = +10$ V Kepler start, outside synchronous radius

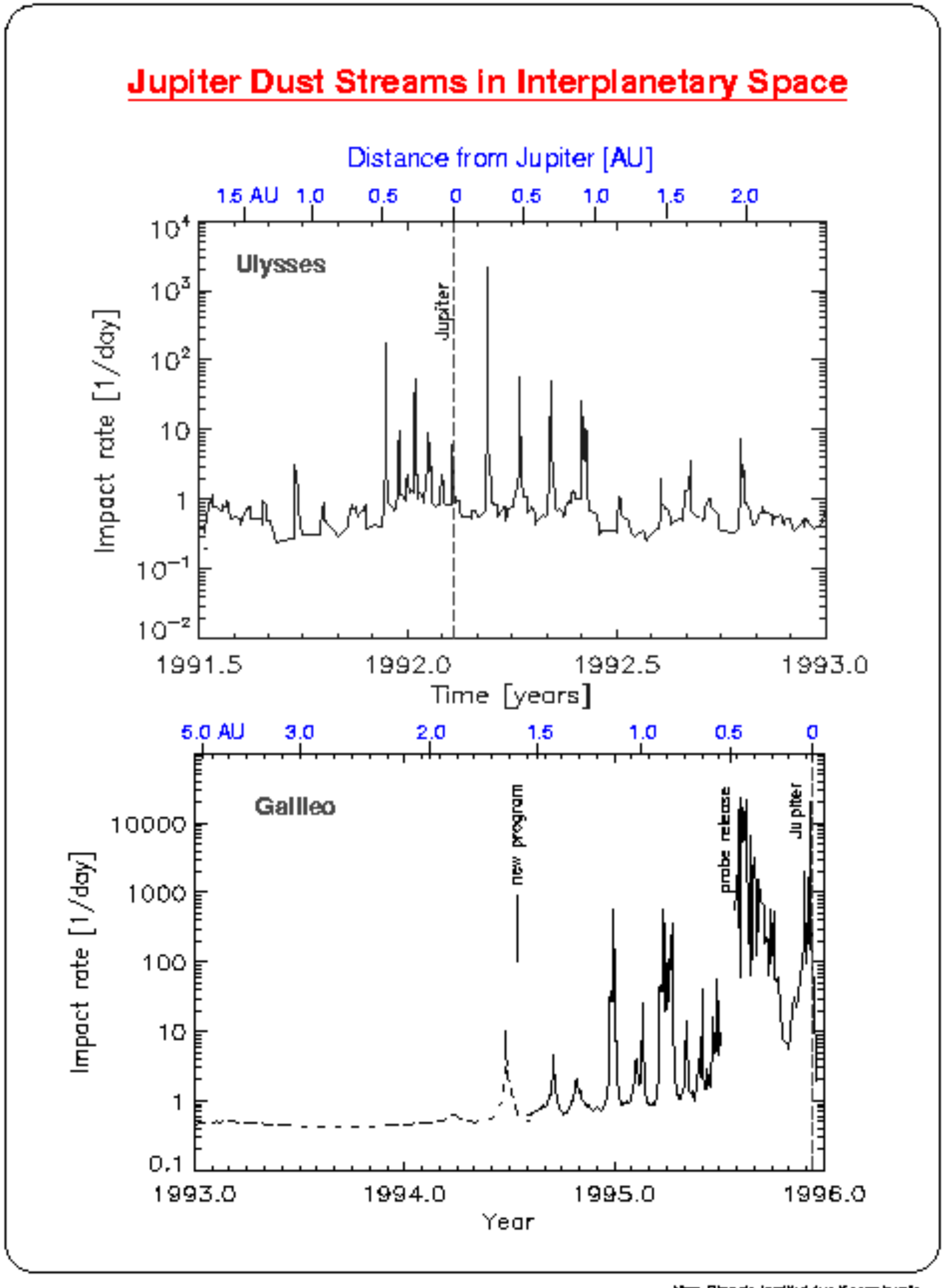
Jupiter Dust Streams in Interplanetary Space
Distance from Jupiter [AU]
1.5 AU 1.0 0.5 0 0.5 1.0 1.5 2.0
Ulysses
Jupiter
Impact rate [1/day]
10^4 10^3 10^2 10 1 10^{-1} 10^{-2}
1991.5 1992.0 1992.5 1993.0
Time [years]
5.0 AU 3.0 2.0 1.5 1.0 0.5 0
Galileo
new program
probe release
Jupiter
Impact rate [1/day]
10000 1000 100 10 1 0.1
1993.0 1994.0 1995.0 1996.0
Year
Max-Planck-Institut fur Kernphysik

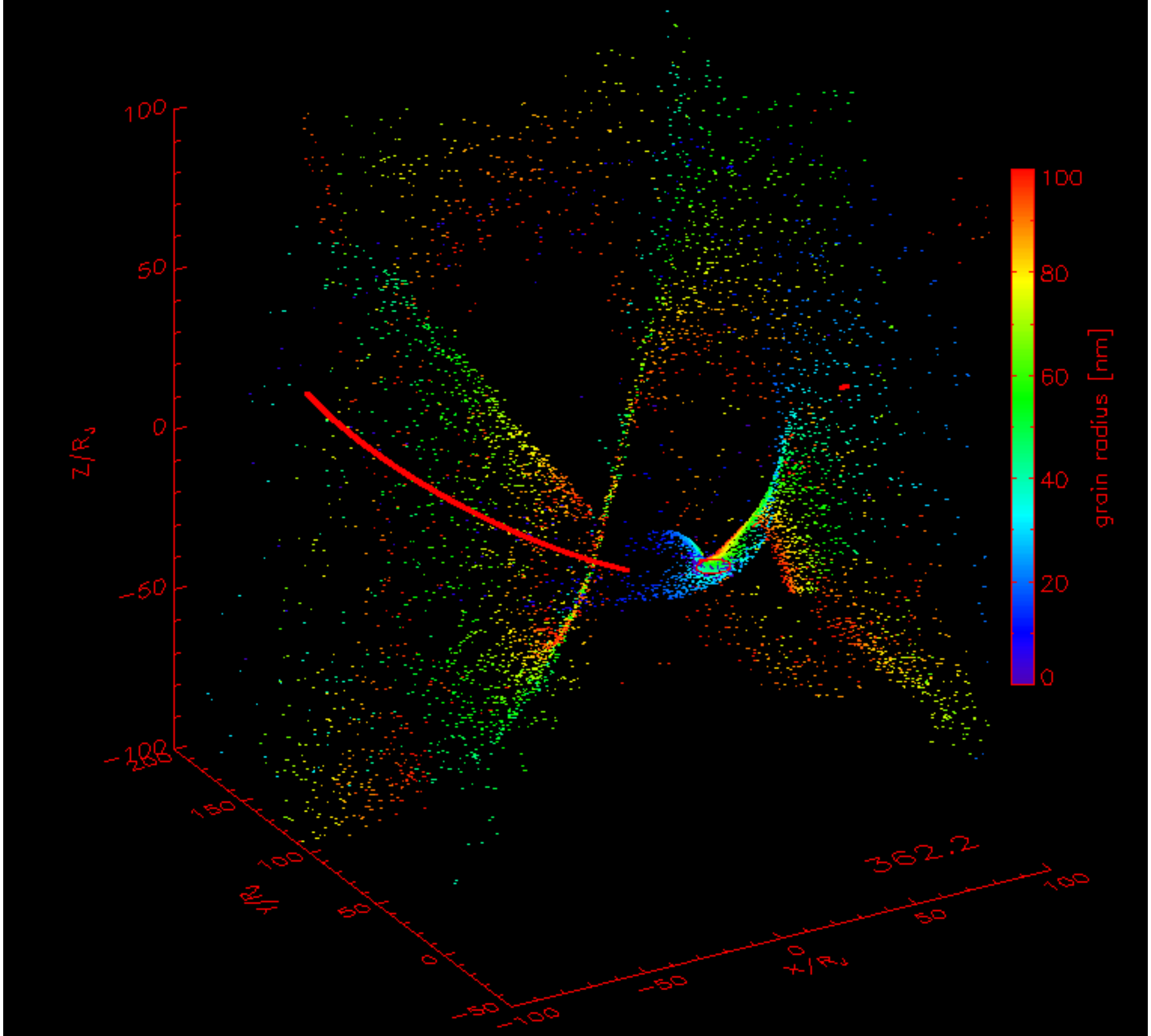

100
50
0
-50
-100
Z/R$_J$
200
150
100
50
0
-50
Y/R$_J$
-100
-50
0
50
100
X/R$_J$
362.2
100
80
60
40
20
0
grain radius [nm]

Long-Time Monitoring of Jovian Dust Streams with Galileo

6 years of Galileo dust measurements (1996 to 2002)
Dust fluxes colour-coded superimposed upon Galileo trajectory

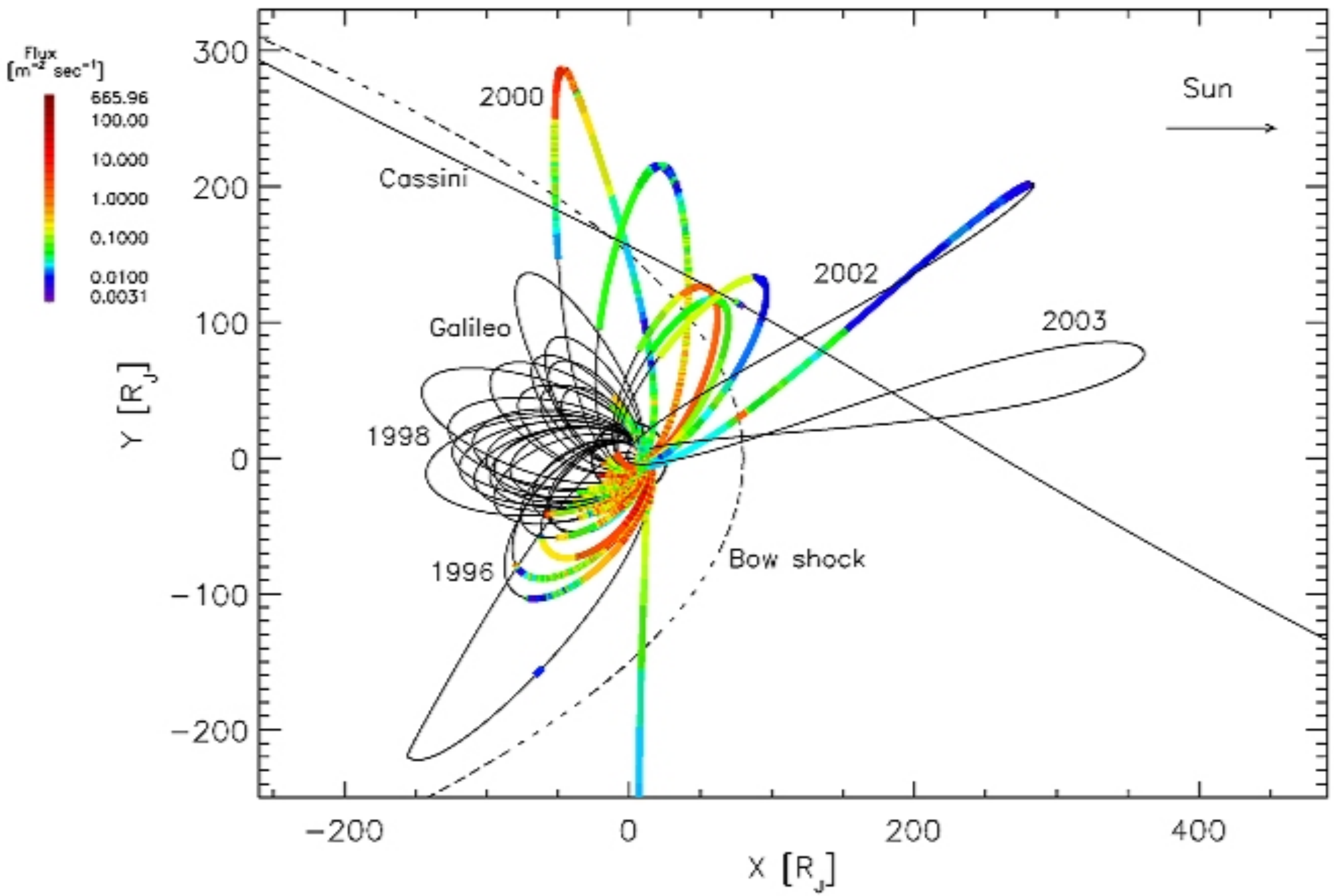

Calculated average emission pattern (GRL, 1997)

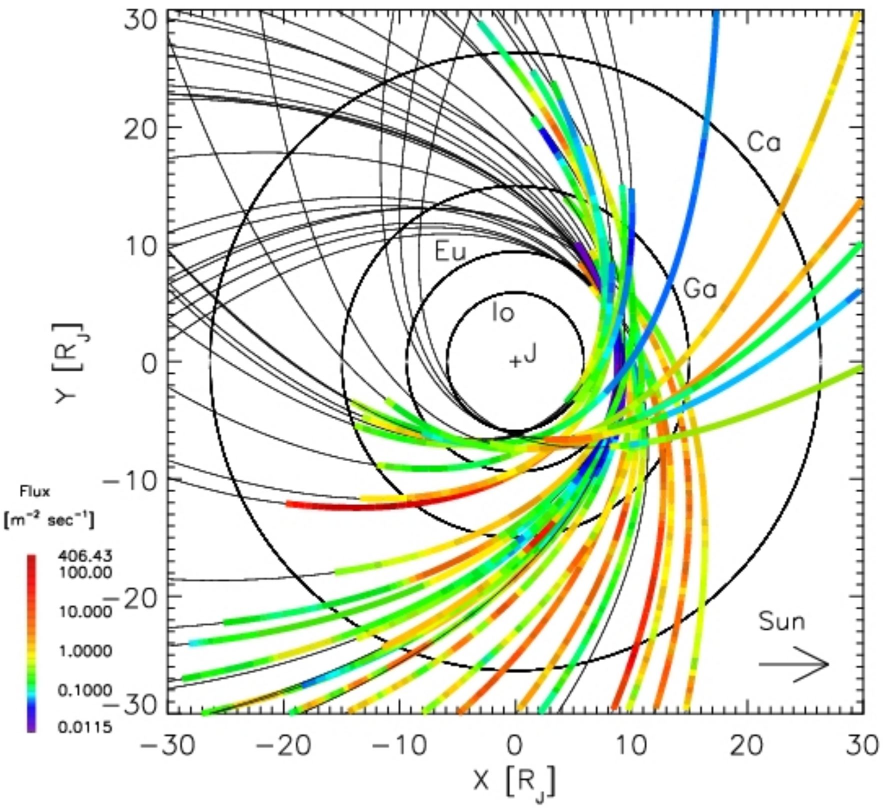

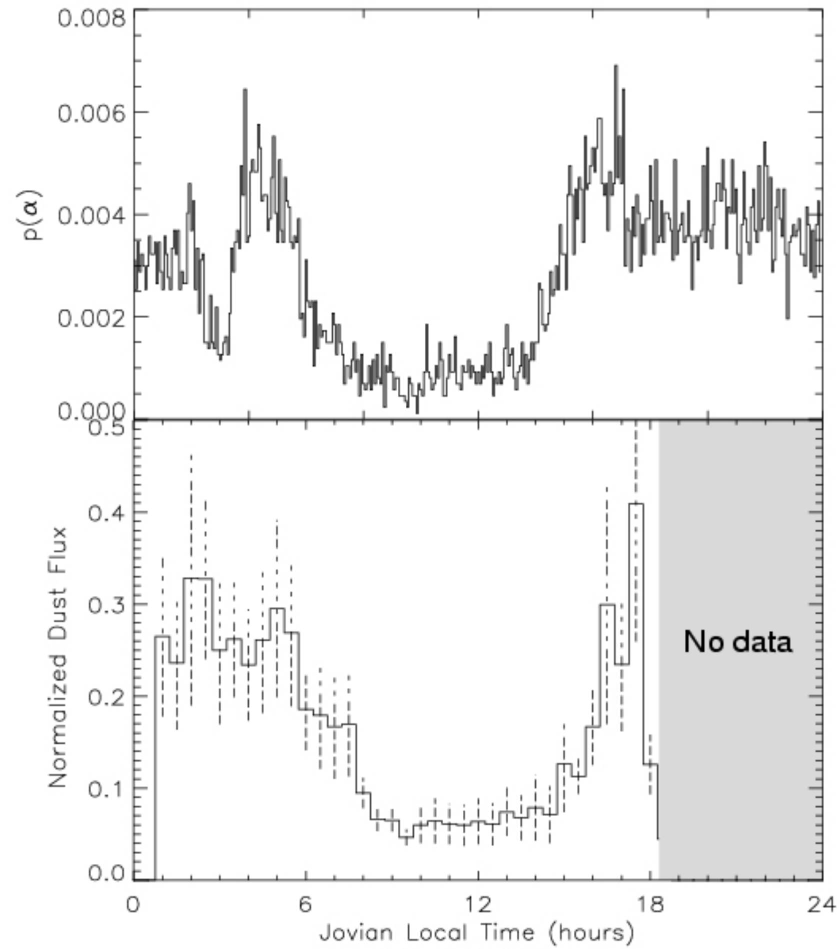

Measured average emission pattern (Kruger *et al.*, 2002)

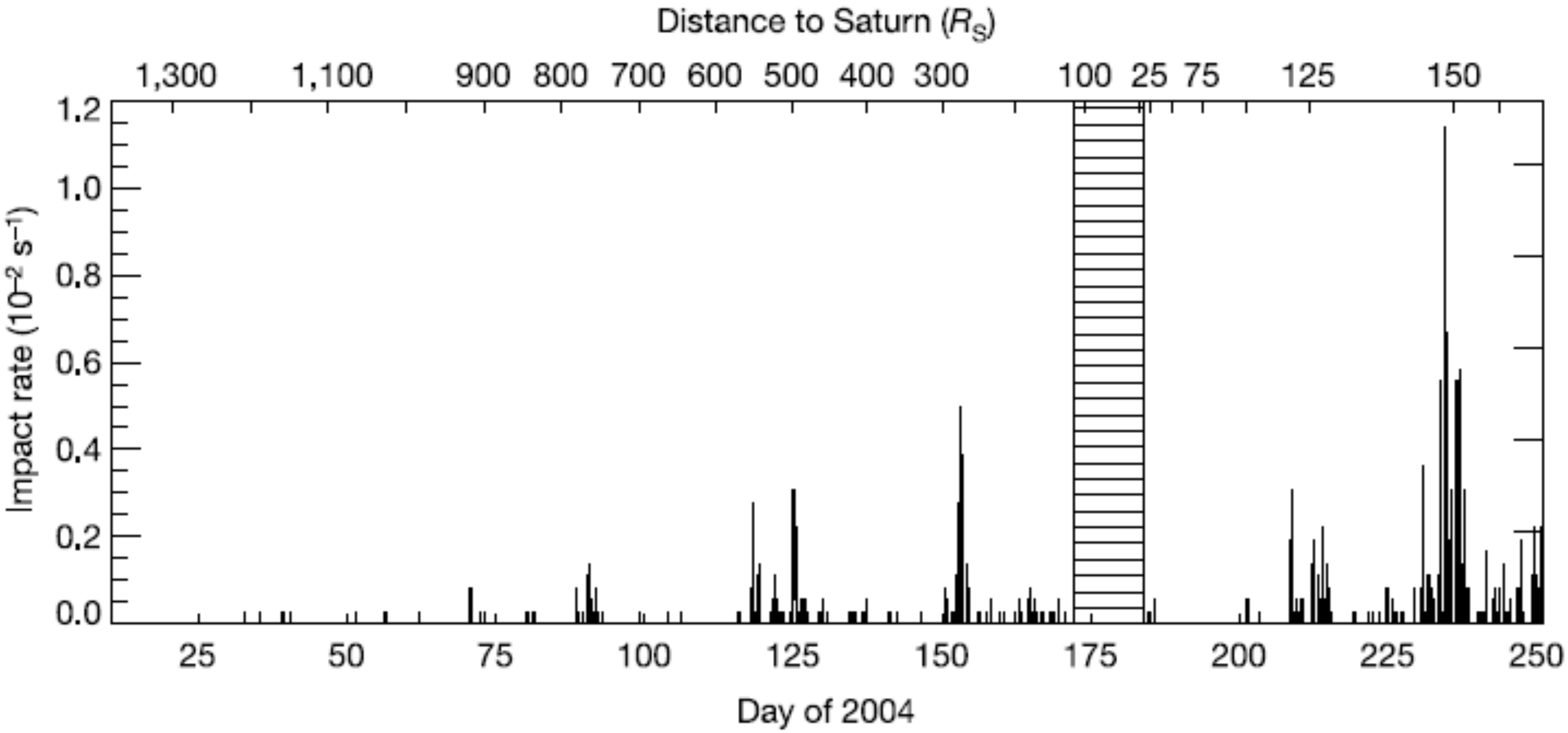

Srama et al., 2005

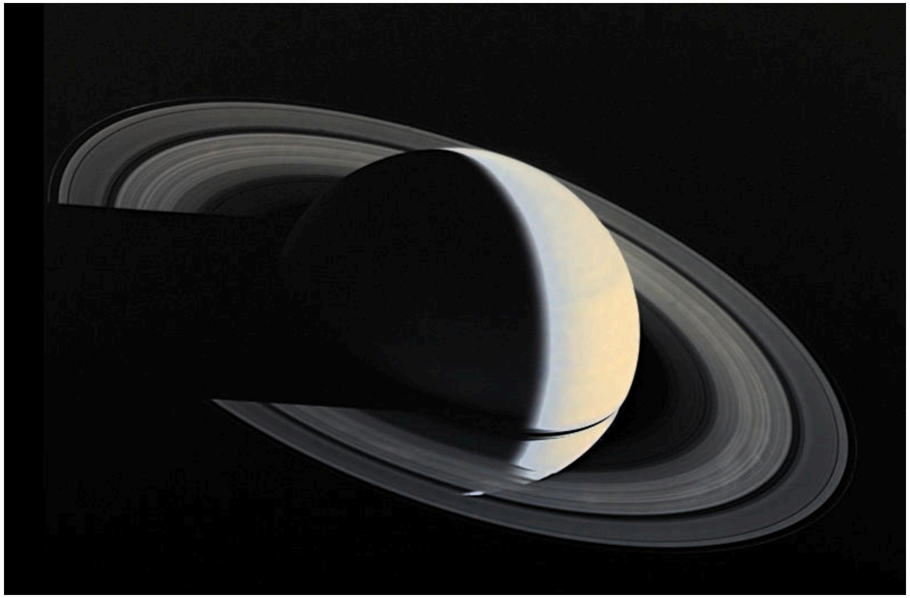

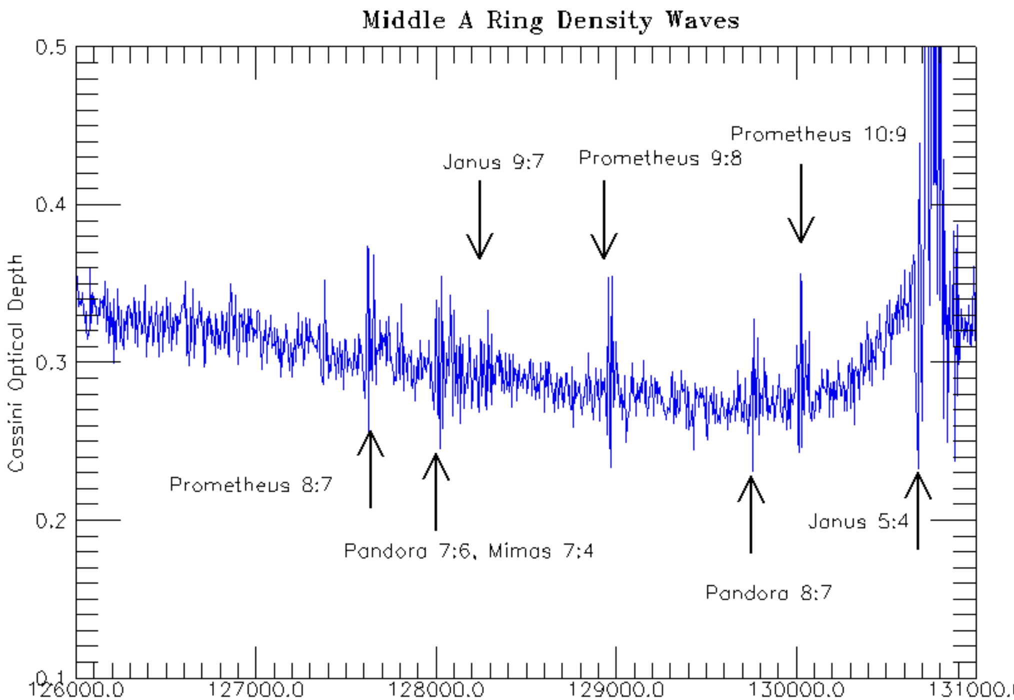

Middle A Ring Density Waves
Cassini Optical Depth
0.5
0.4
0.3
0.2
0.1
126000.0
127000.0
128000.0
129000.0
130000.0
131000.0
Janus 9:7
Prometheus 9:8
Prometheus 10:9
Prometheus 8:7
Pandora 7:6, Mimas 7:4
Pandora 8:7
Janus 5:4

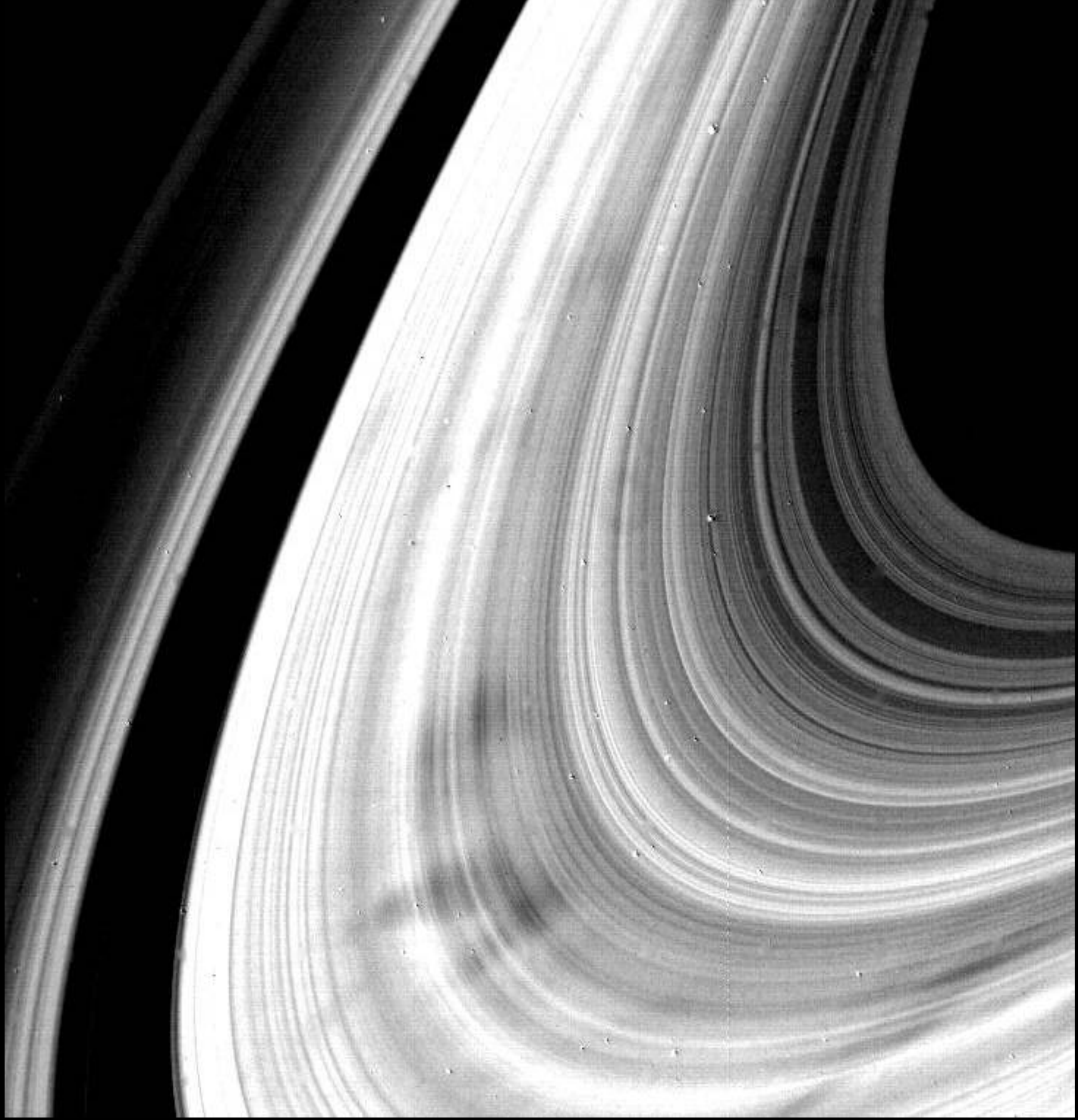

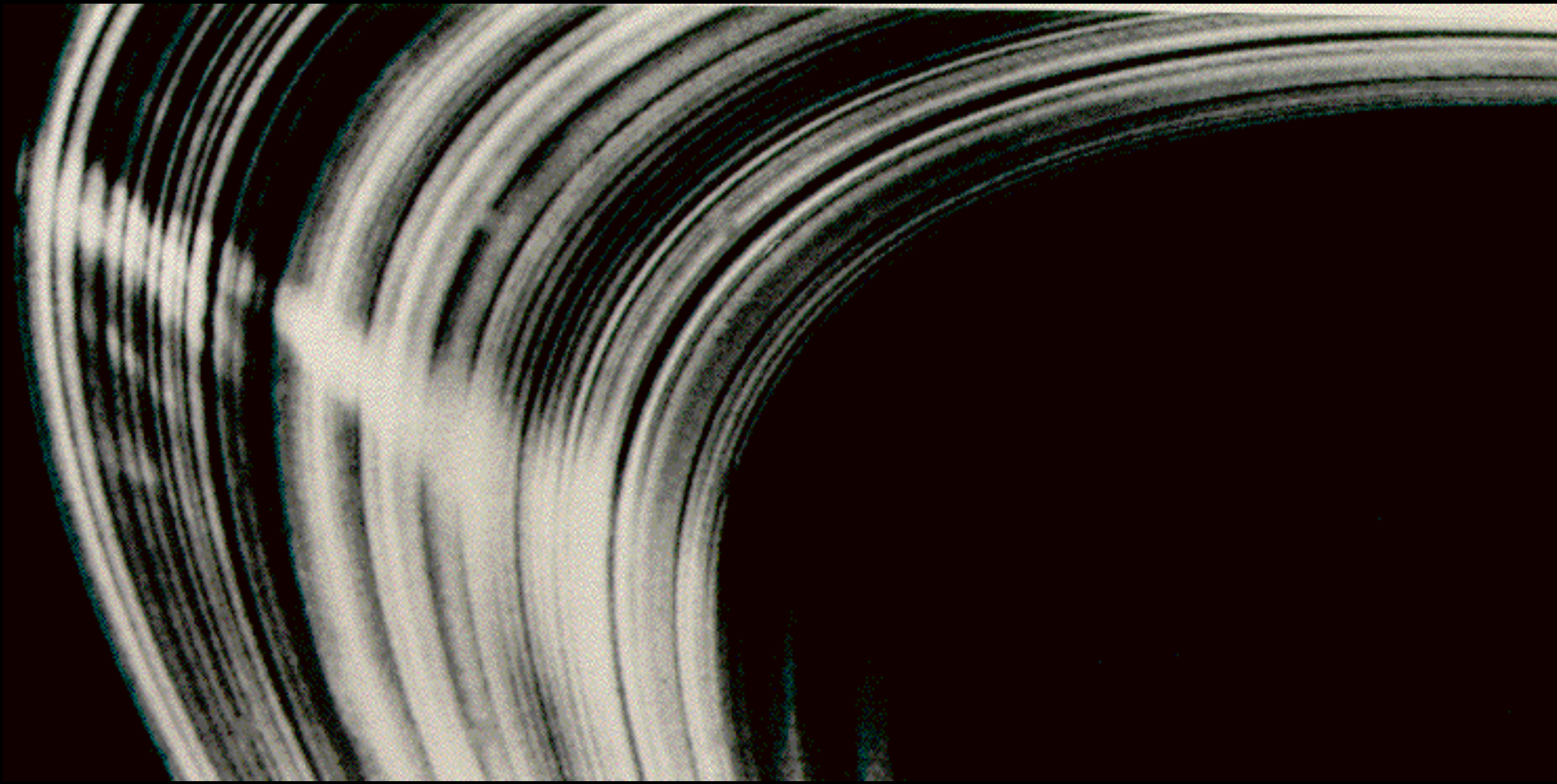

``… cannot be explained with the known laws of physics ! ” (JPL 1980)

``….. there is a difference between the known laws of physics and the laws of physics known to you ! ”

Hannes Alfven

(1980)

Properties from visual inspection:

intermittent, 0.1-10 % contrast, l: 10^4 km & w: 2000 km, close to R_S,
appear in < 5 min, seem radially aligned in the "morning" and shear away,
typical grain size <1 μm, dust cloud height < 80 km

Questions:

Are grains lifted off the ring-plane or just rearranged in plane?
What is the plasma density and temperature near the rings ?
How can thin radially aligned structures be produced ?
Why is the morning side of the rings preferred ?
What determines the frequency of occurrence?

Ideas:

Static : alignment of charged grains (E or B)

Dynamic : single particle trajectories (external or internal trigger)

Collective : dusty plasma waves (instability, solitons)

Evolution of a Spoke's real estate

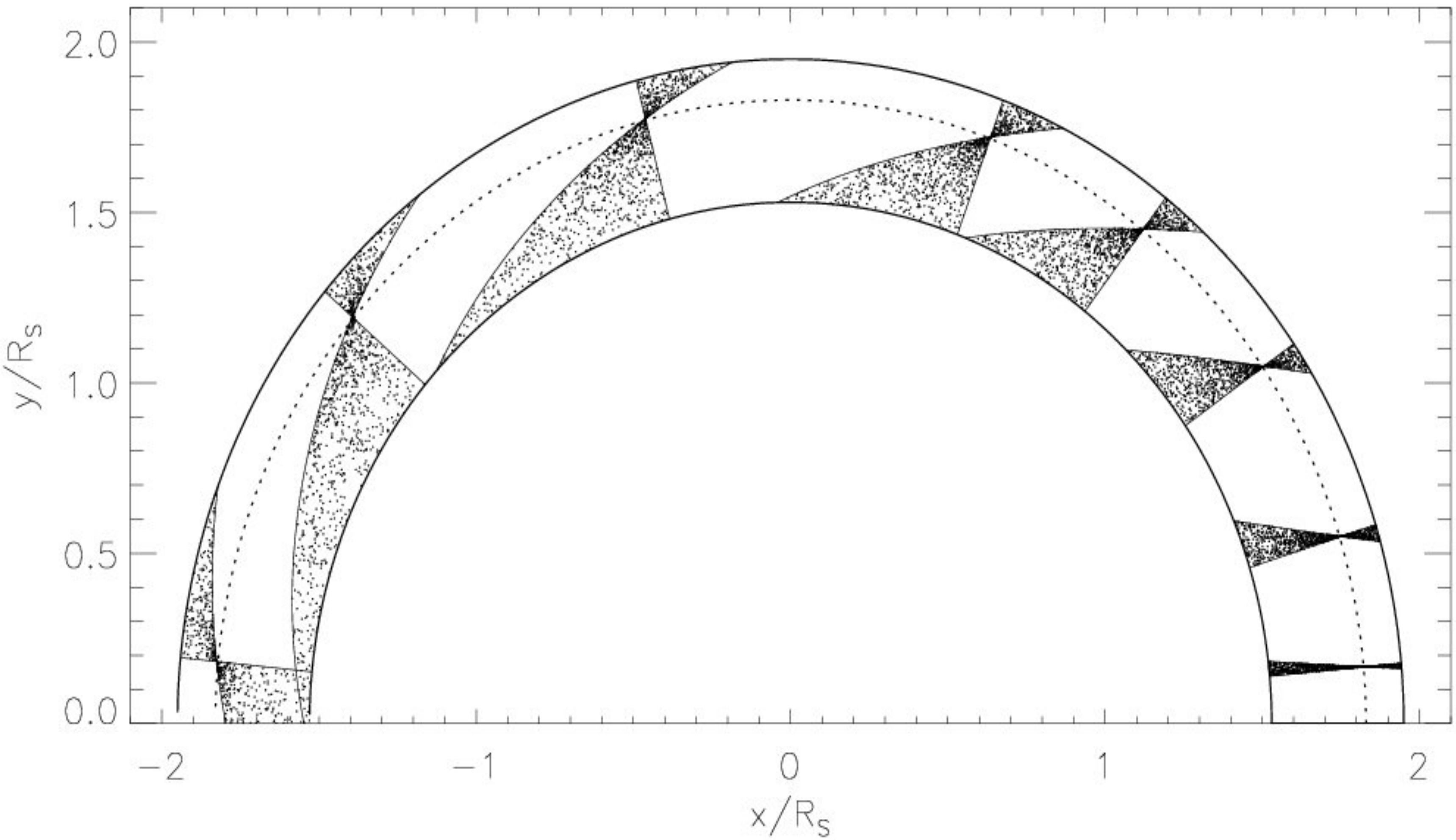

Dust lift-off from a surface in plasma

Surface charge density

$$\sigma_e = \frac{E_\perp}{4\pi e} \simeq \frac{1}{4\pi e \lambda_D} \frac{\phi_S^V}{300} = 750\ \phi_S^V \left(\frac{n_e}{T_e}\right)^{0.5}$$

Dust charge on the surface $\longrightarrow$ Probability to have an e $\ll 1$

$$Q_S^e \simeq \pi a^2 \sigma_e \ll 1 \qquad \longrightarrow \qquad P_e = 2.4 \times 10^{-5} a_\mu^2 \phi_S^V \left(\frac{n_e}{T_e}\right)^{1/2}$$

Dust charge in free space

$$Q_F^e \simeq 700 a_\mu \phi_D^V \gg Q_S^e$$

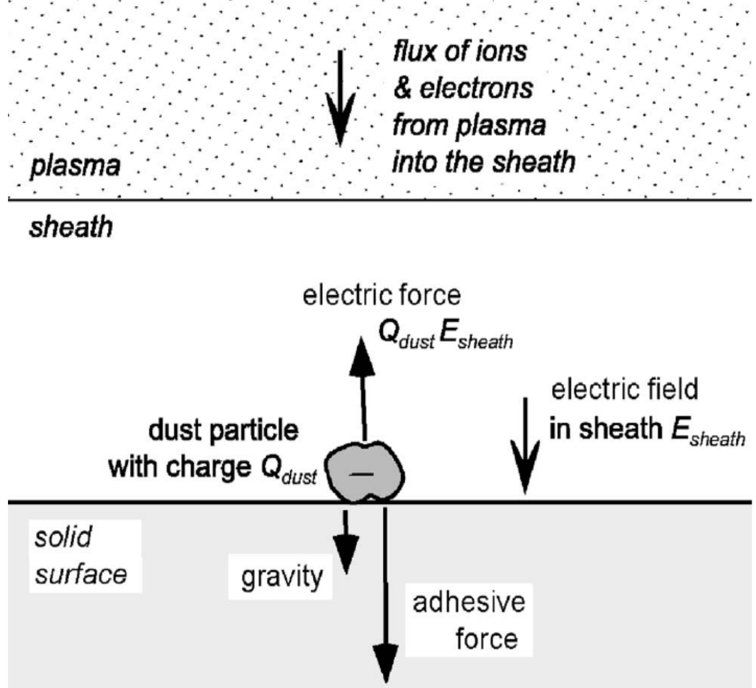

1) lift-off (1 e !) $P_e \sim a^2$

2) transit through the sheath $t_D \sim a^{-3/2}$

3) (dis)charging time $t_C \sim a^{-2}$

$P_{escape} = P_e \exp(-t_D/t_C) \sim a^2$ for small a and $\sim \exp(a^{-3.5})$ for large a

Photoelectron flux	Γ_0	$\mathrm{cm}^{-2}\mathrm{s}^{-1}$	2.5×10^7
Plasma temperature	T_P	eV	2
Plasma density	n_p	cm^{-3}	0.1 - 1
Debye length	λ_D	cm	$1 - 3 \times 10^3$
Surface potential	Φ_S	V	$\pm$ 5
Surface charge density	σ_e	cm^{-2}	$1 - 3 \times 10^3$
Surface electric field	E_s	V/m	< 0.5
Probability of 1 e charge	P_e		$10^{-4} a_\mu^2$

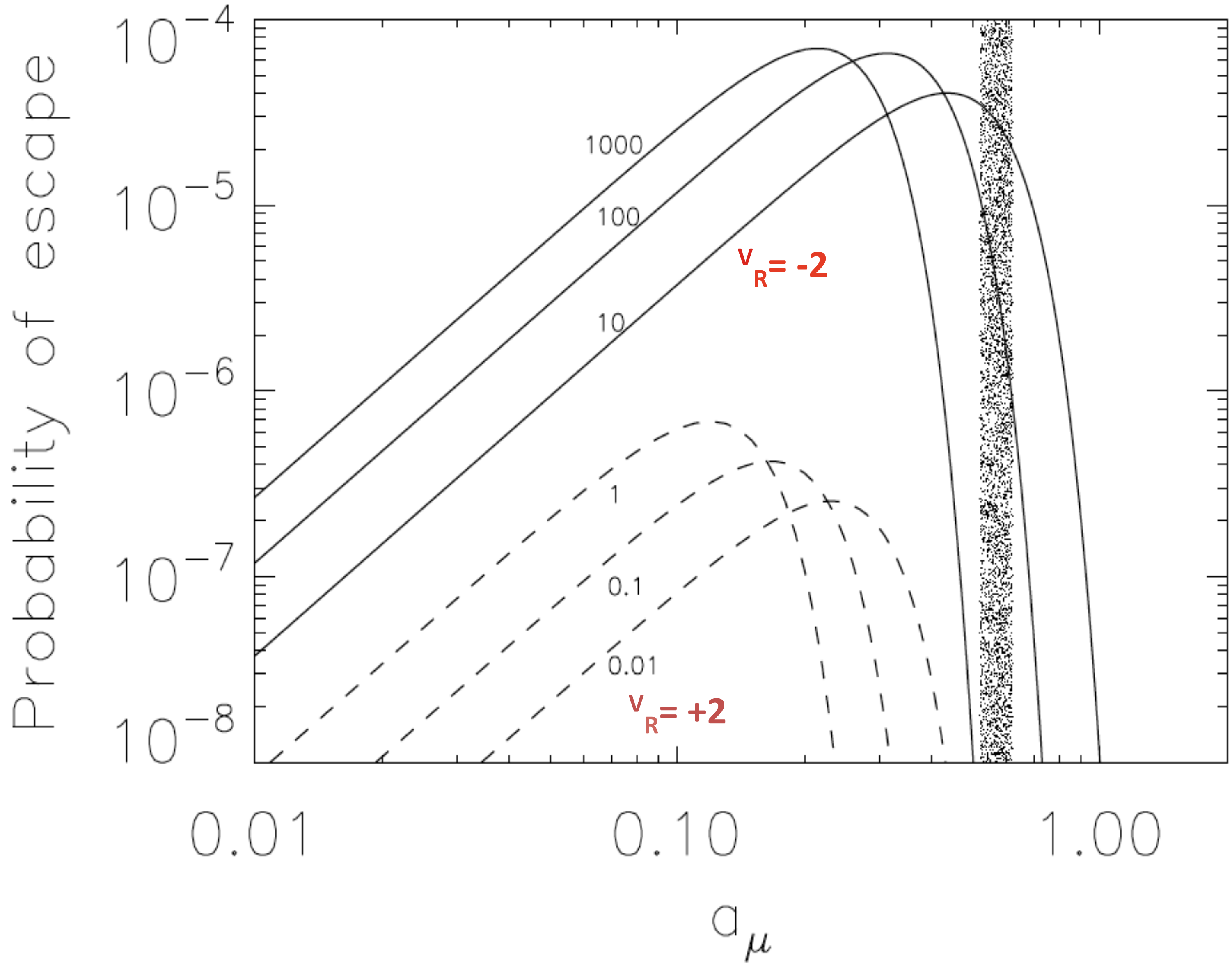
Probability of escape
10^{-4}
10^{-5}
10^{-6}
10^{-7}
10^{-8}
1000
100
10
1
0.1
0.01
V_R= -2
V_R= +2
0.01
0.10
1.00
a_μ

Meteorite impact model

Need higher than `normal' plasma density for dust lift-off !

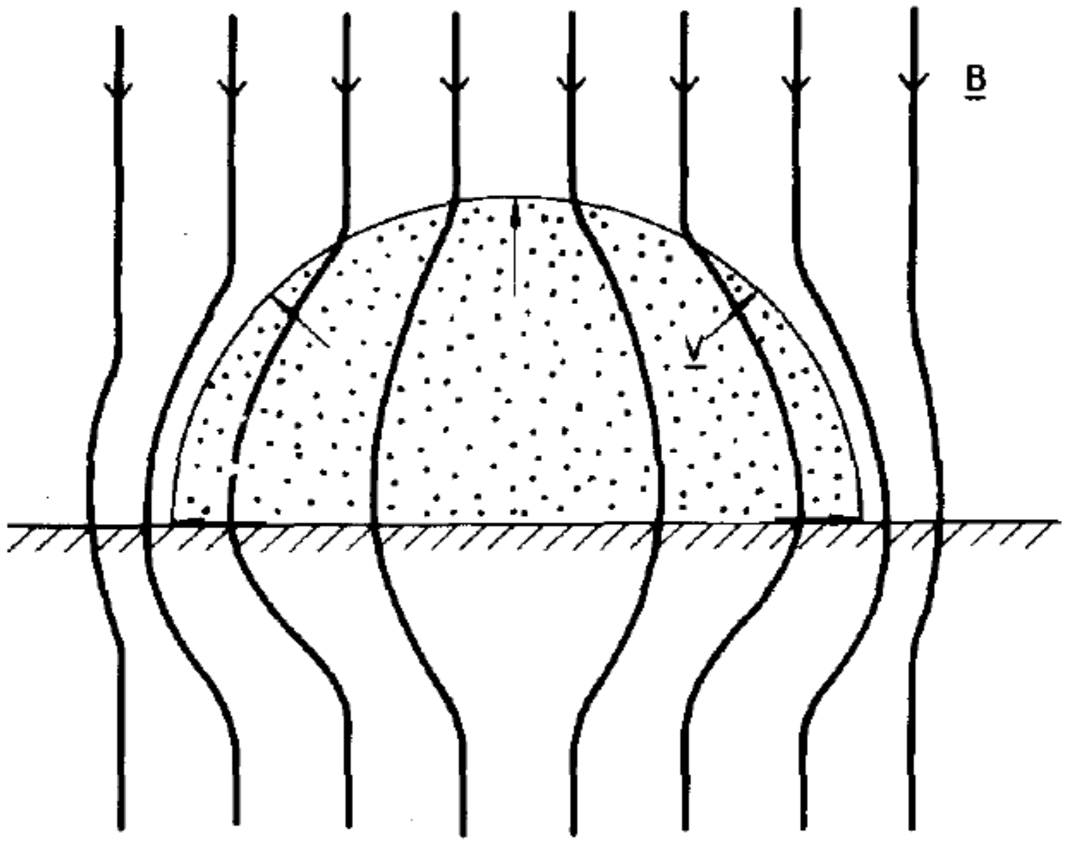

FIG. 2. Schematic diagram of the hemispherical expansion ($v_d = 0$) of a plasma cloud just at the ring surface, treated as a flat plate.

Morfill and Goertz, 1983

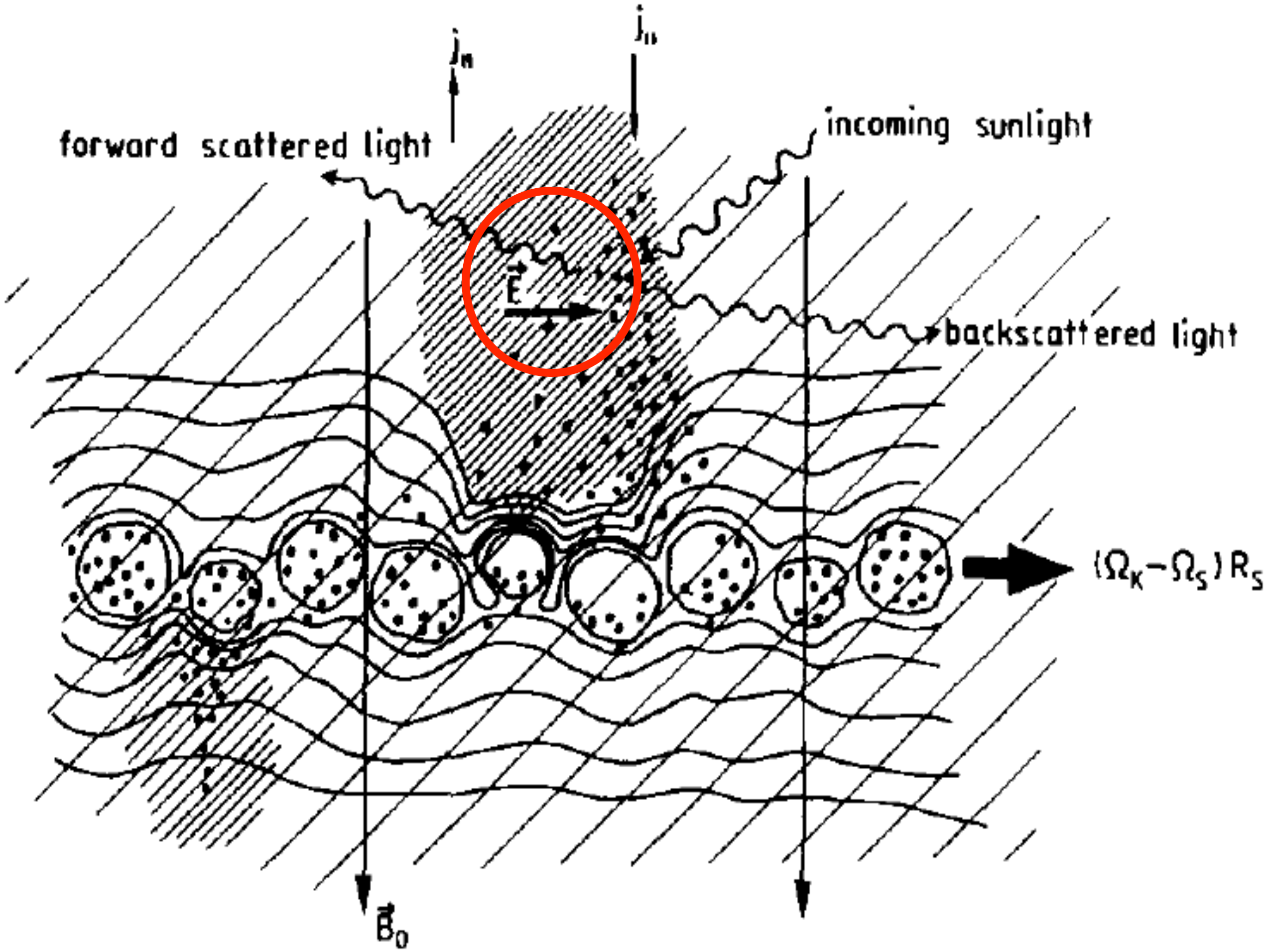

FIG. 2. A schematic view of the model for formation of spokes. Underneath a dense plasma column (indicated by heavy shading) the equipotential contours are compressed and a large surface electric field exists. Dust particles are lifted off the rings and drift through the cloud, which polarizes. A pair of field-aligned currents closes the current.

Goertz and Morfill, 1983

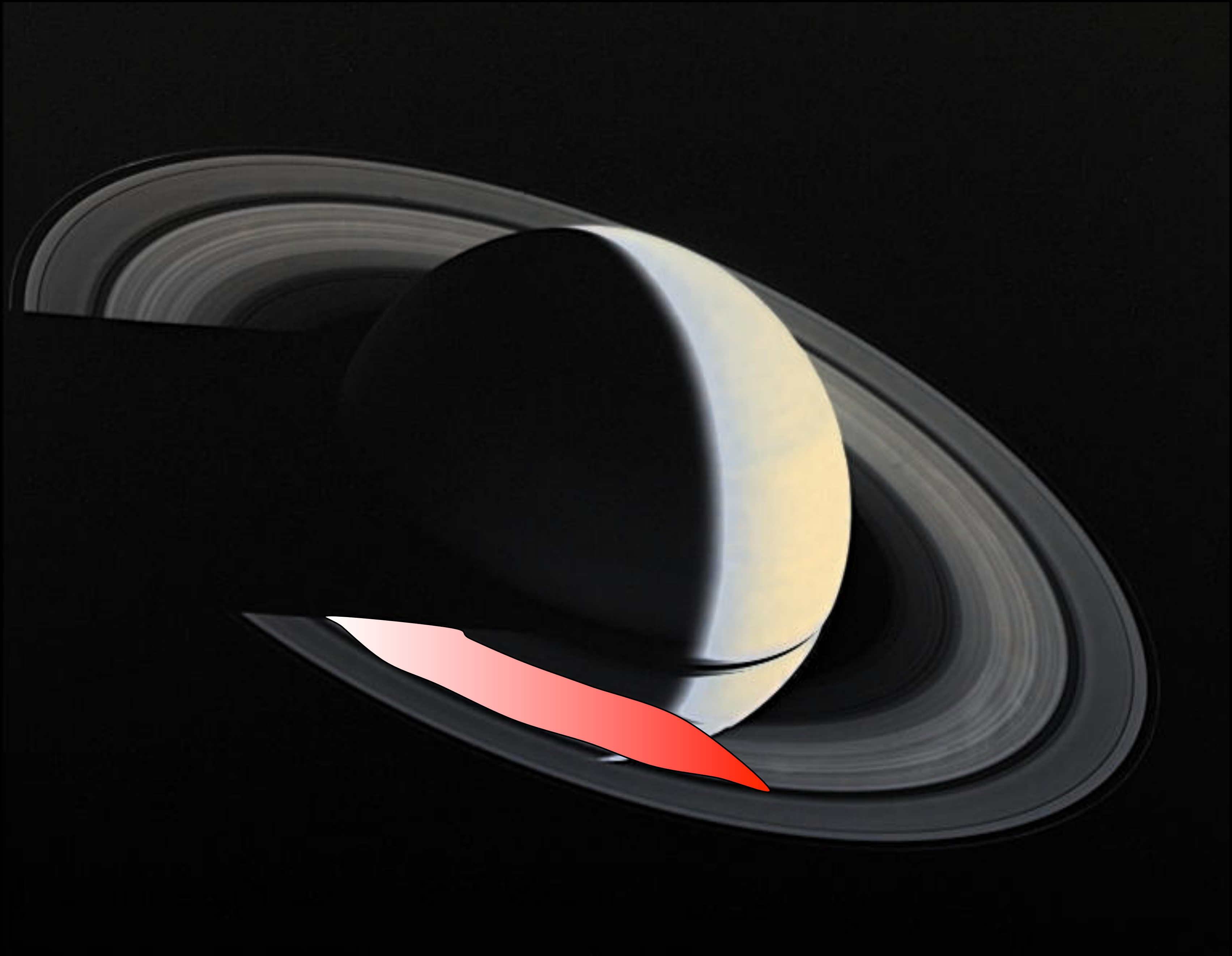

Saturn

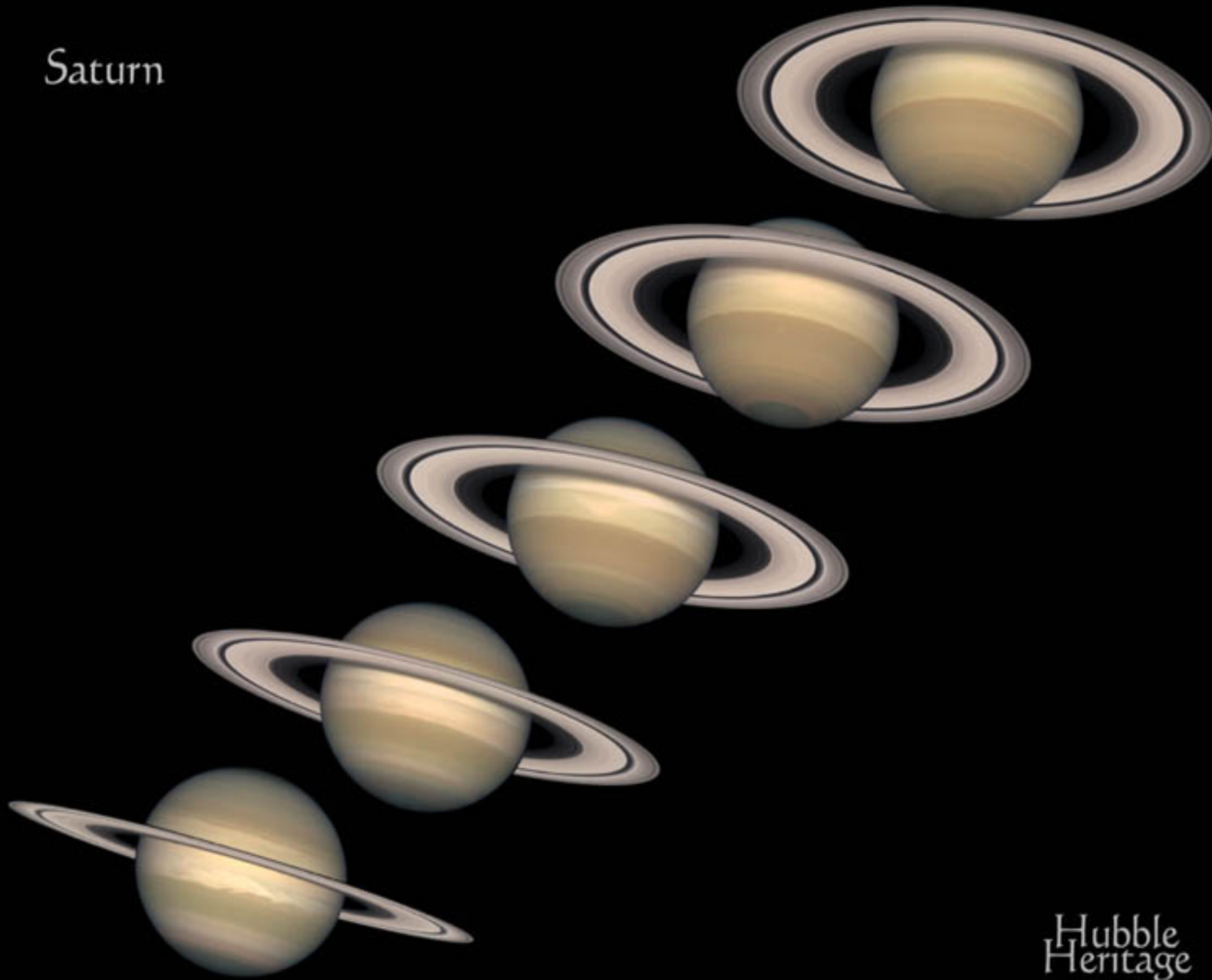

NASA and The Hubble Heritage Team (STScI/AURA) • Hubble Space Telescope WFPC2 • STScI-PRC01-15

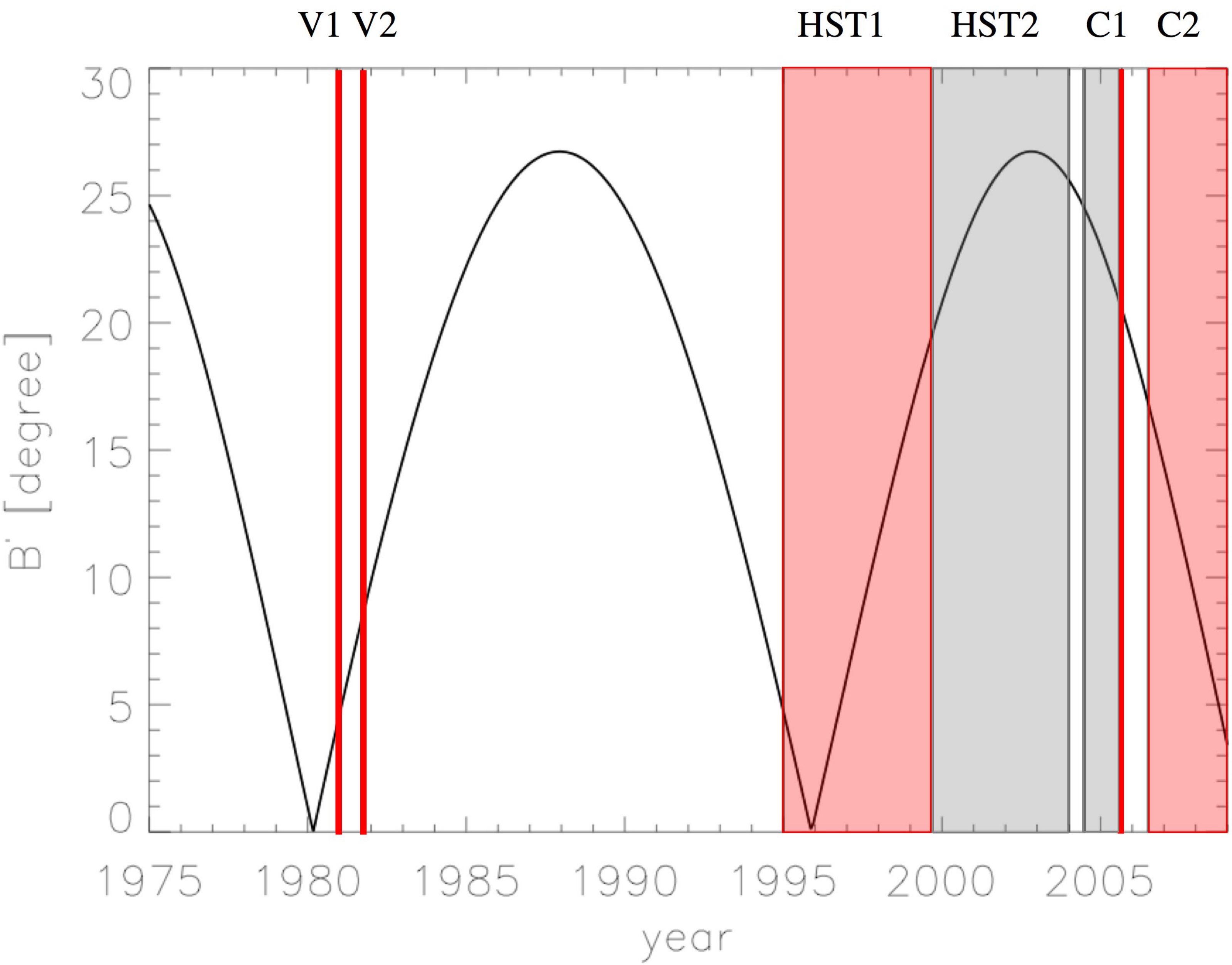

V1 V2
HST1
HST2
C1
C2
30
25
20
15
10
5
0
B' [degree]
1975
1980
1985
1990
1995
2000
2005
year

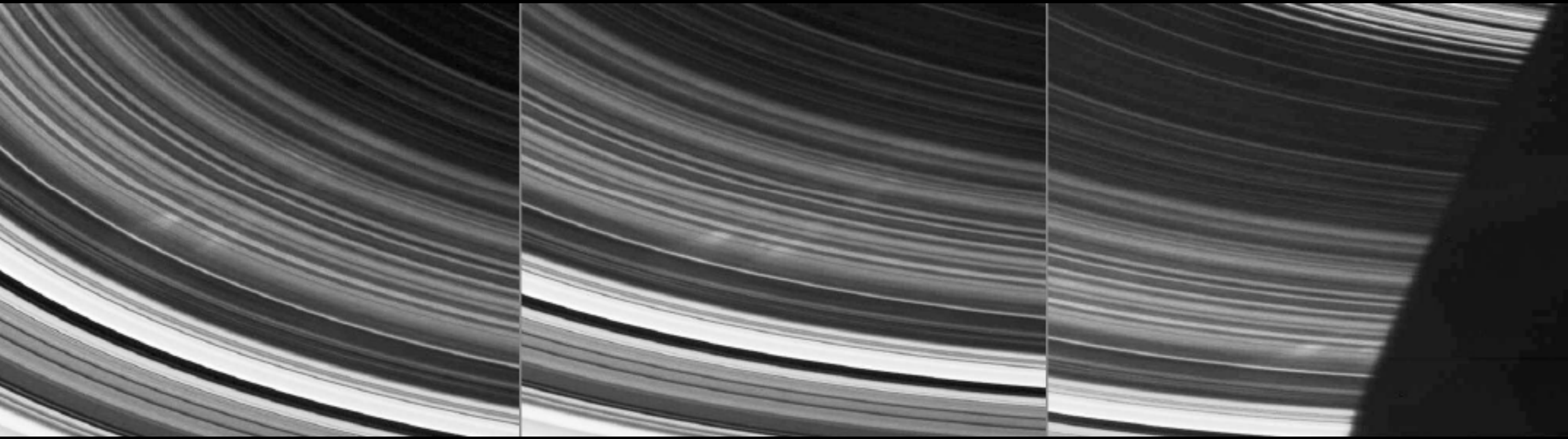

4) Dusty plasmas on the surfaces of airless bodies

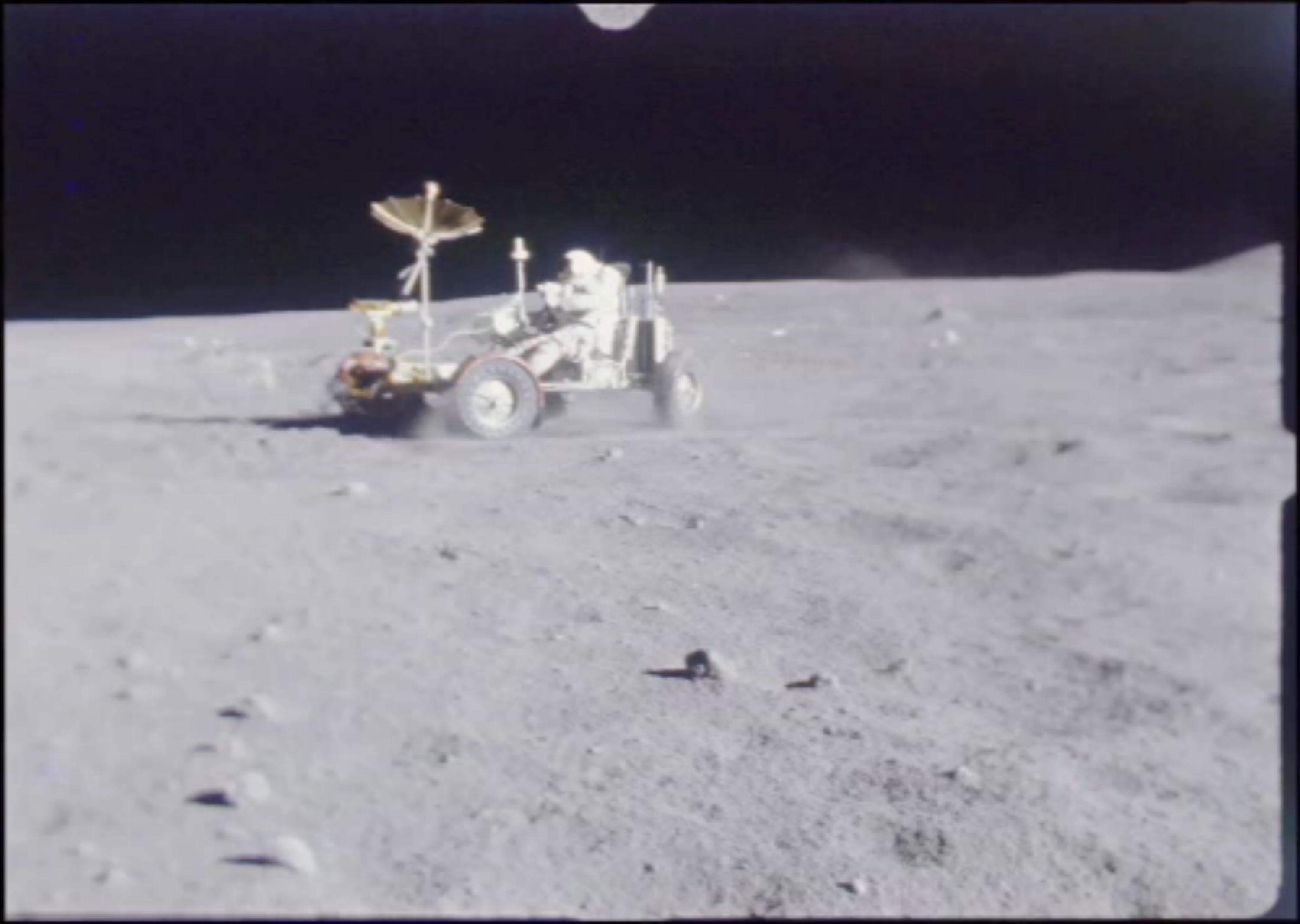

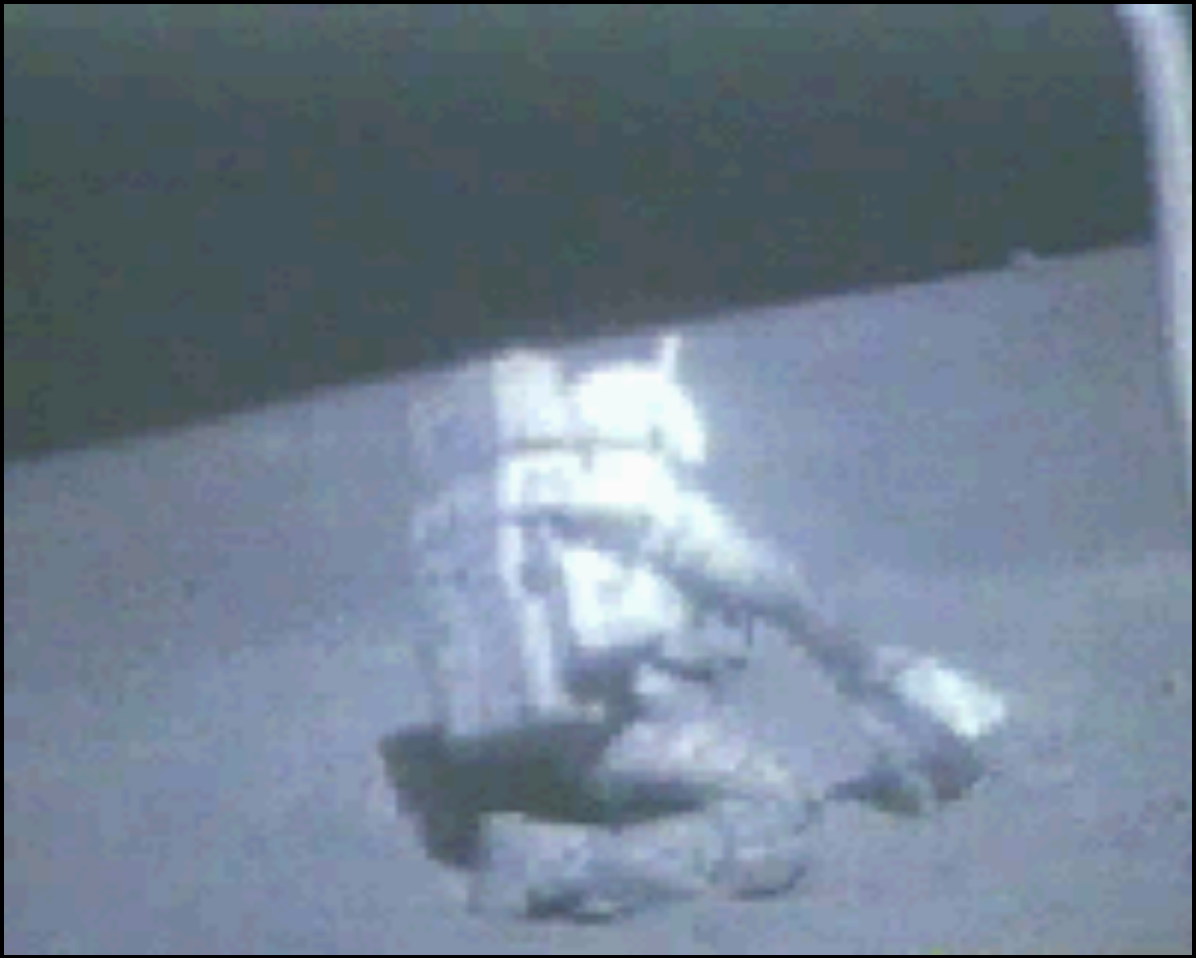

LUNAR DUST, PLASMA, AND UV ENVIRONMENT

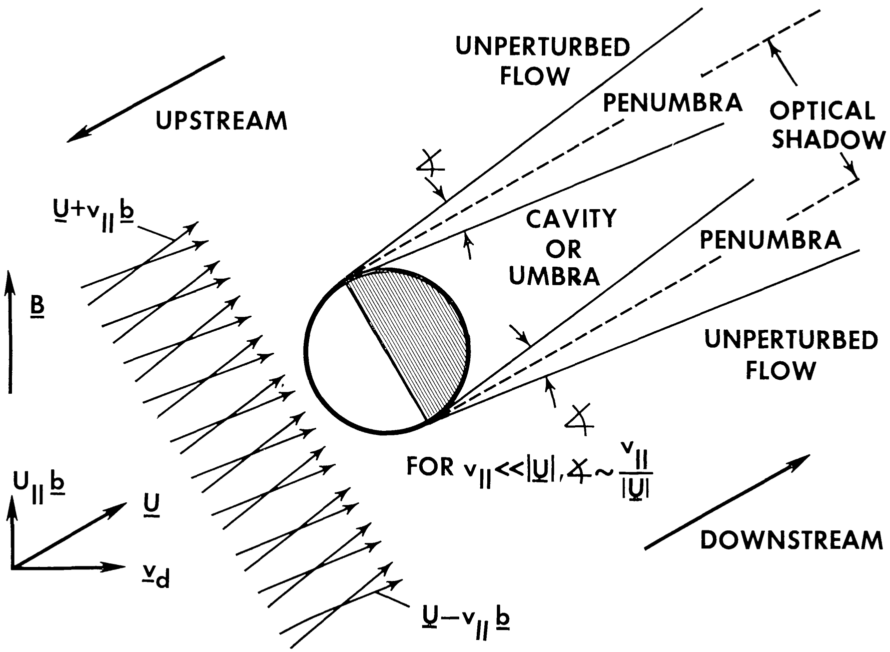

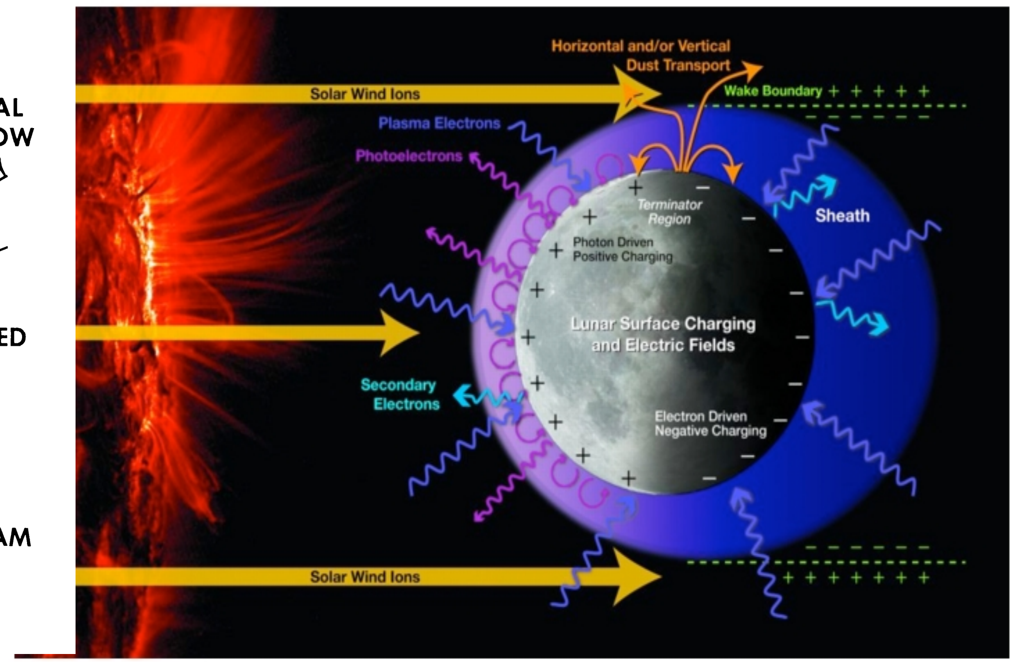

NIGHTSIDE CHARGING

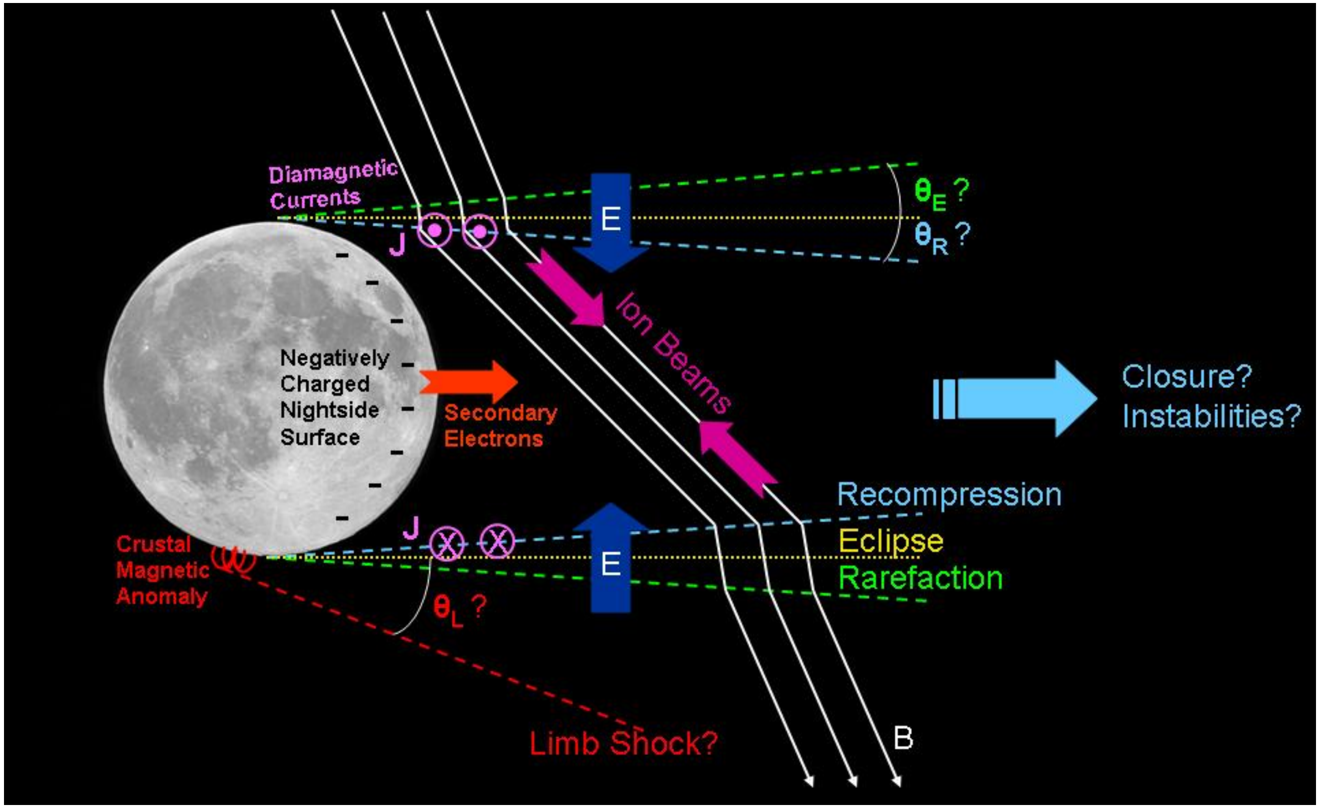

$$kT_e \approx m_p v_{sw}^2 / 2$$

Halekas, 2010

$$\phi \approx -m_p v_{sw}^2 / (2e)$$

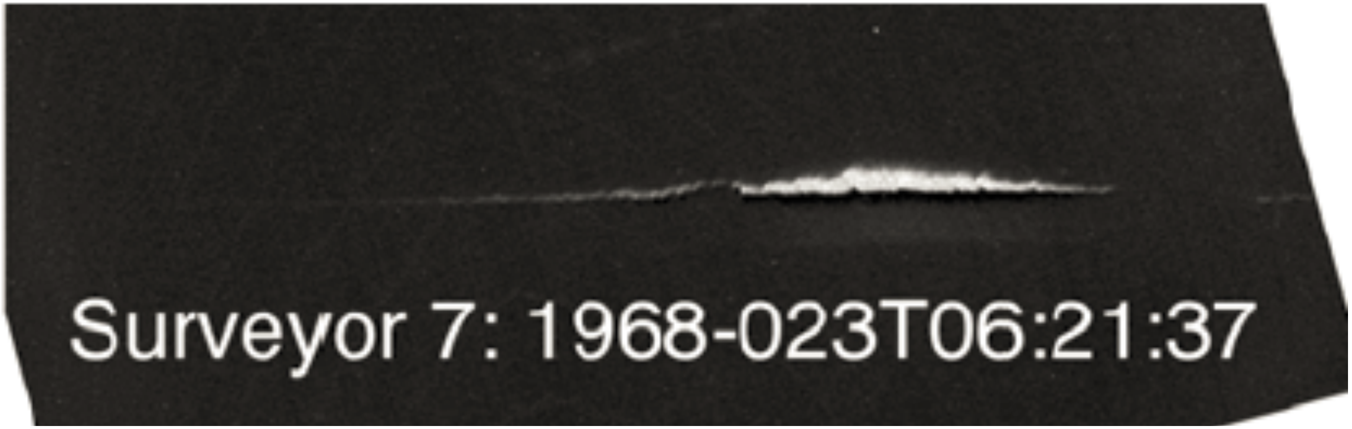
Surveyor 7: 1968-023T06:21:37

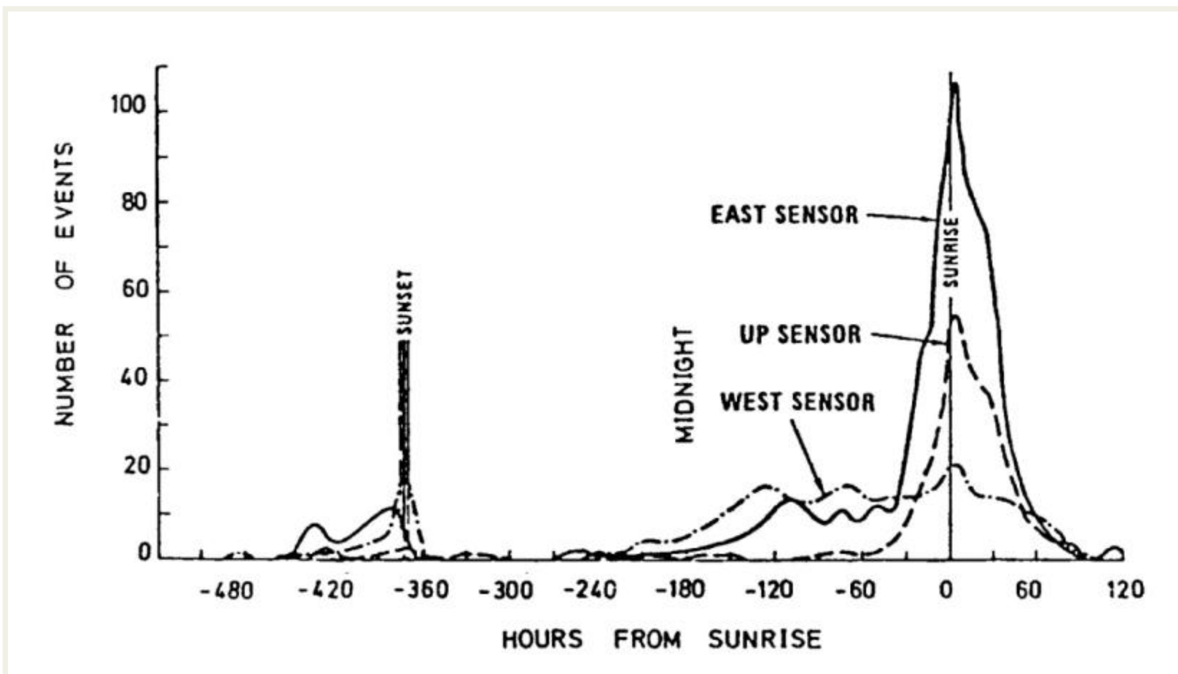
NUMBER OF EVENTS
100
80
60
40
20
0
SUNSET
MIDNIGHT
EAST SENSOR
UP SENSOR
WEST SENSOR
SUNRISE
-480
-420
-360
-300
-240
-180
-120
-60
0
60
120
HOURS FROM SUNRISE

APOLLO ERA UNRESOLVED OBSERVATIONS

Gene Cernan sketches from Apollo Command Module

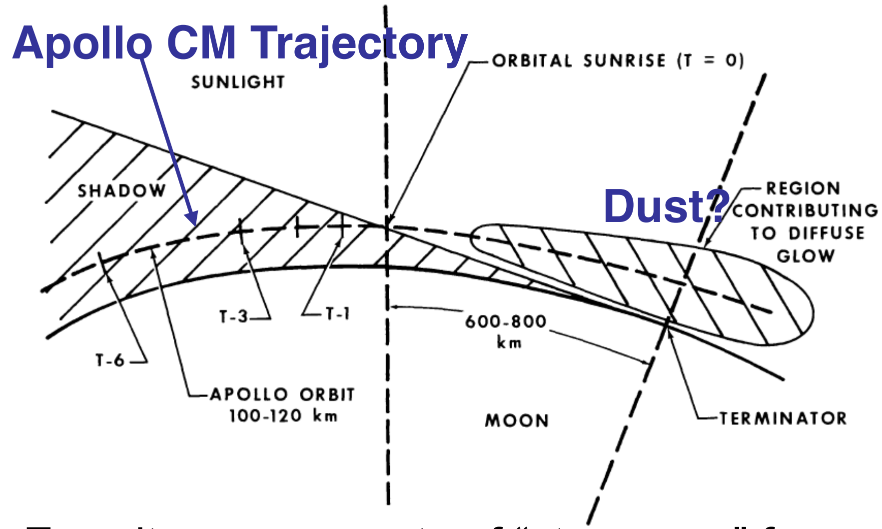

McCoy and Criswell, 1974

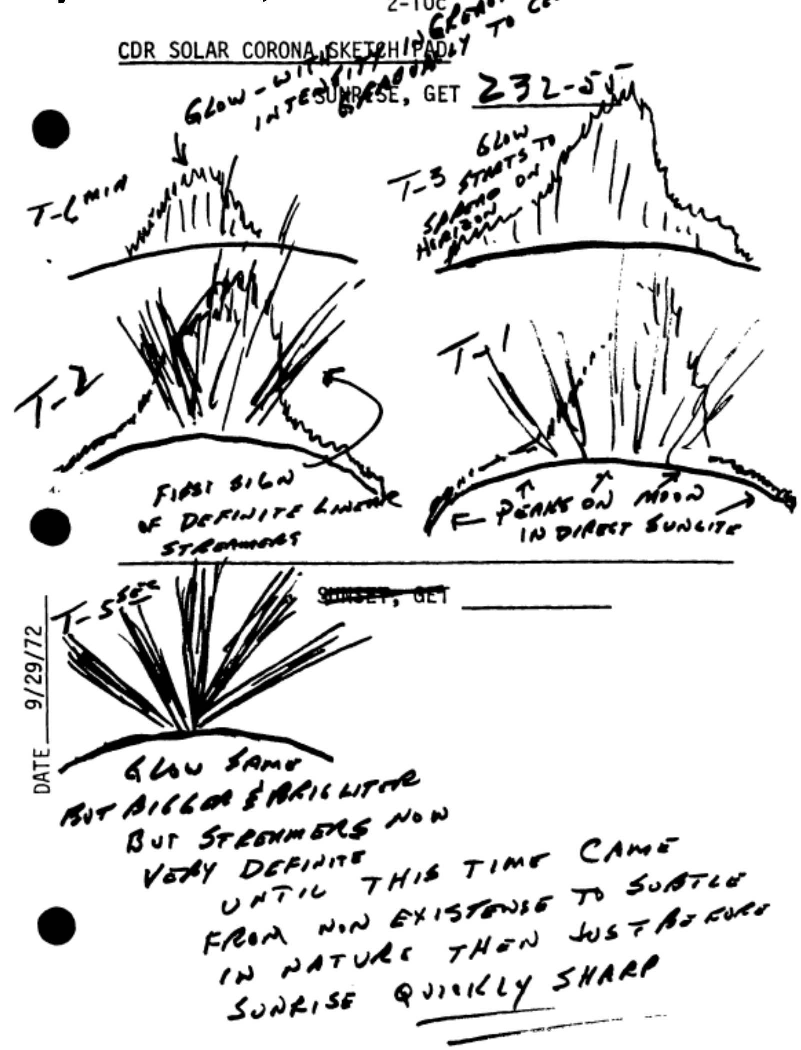

- Eyewitness accounts of “streamers” from Apollo command module
- Too bright to be meteoritic ejecta
- Exosphere and/or high altitude (50 km) dust is one possibility
- Key goal if LADEE is to help resolve this open question

UV CHARGING (DAYSIDE)

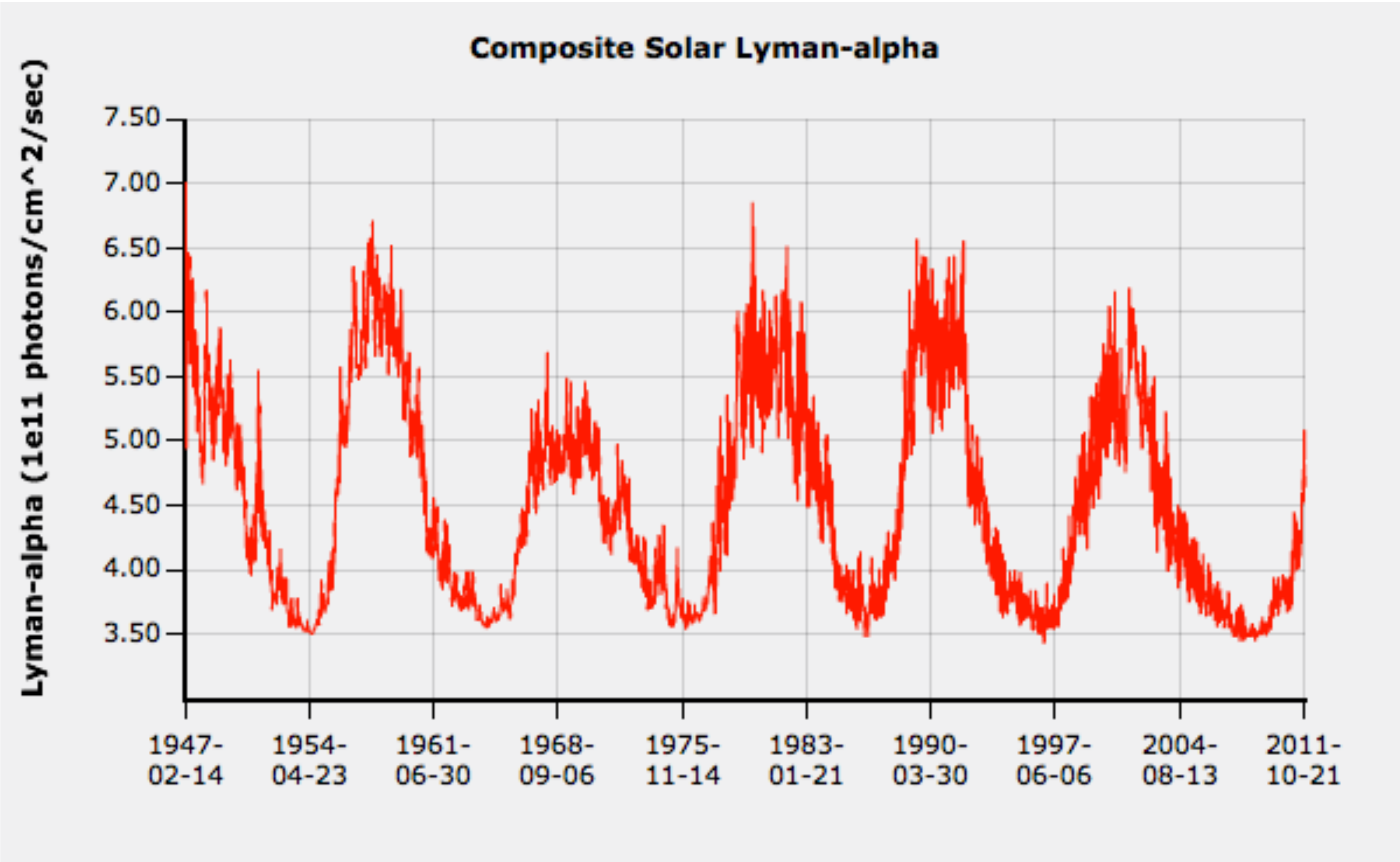

UV CHARGING (DAYSIDE)

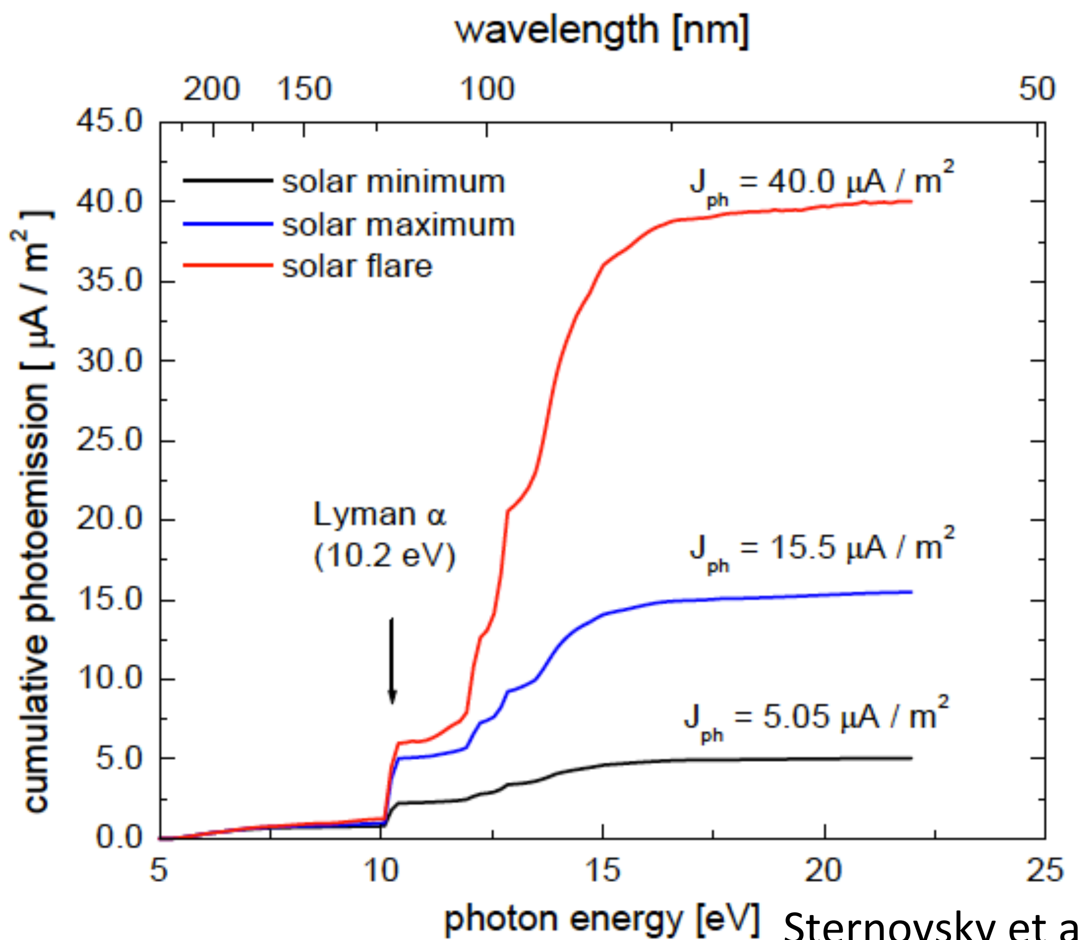

Sternovsky et al., 2008

•0.6 m^3, 60-cm diameter vacuum chamber

•10^{-6} Torr operating vacuum

•Collector and grid aid in obtaining clean measurements

•Xe-excimer UV lamps peak emission at 172 nm (7.21 eV)

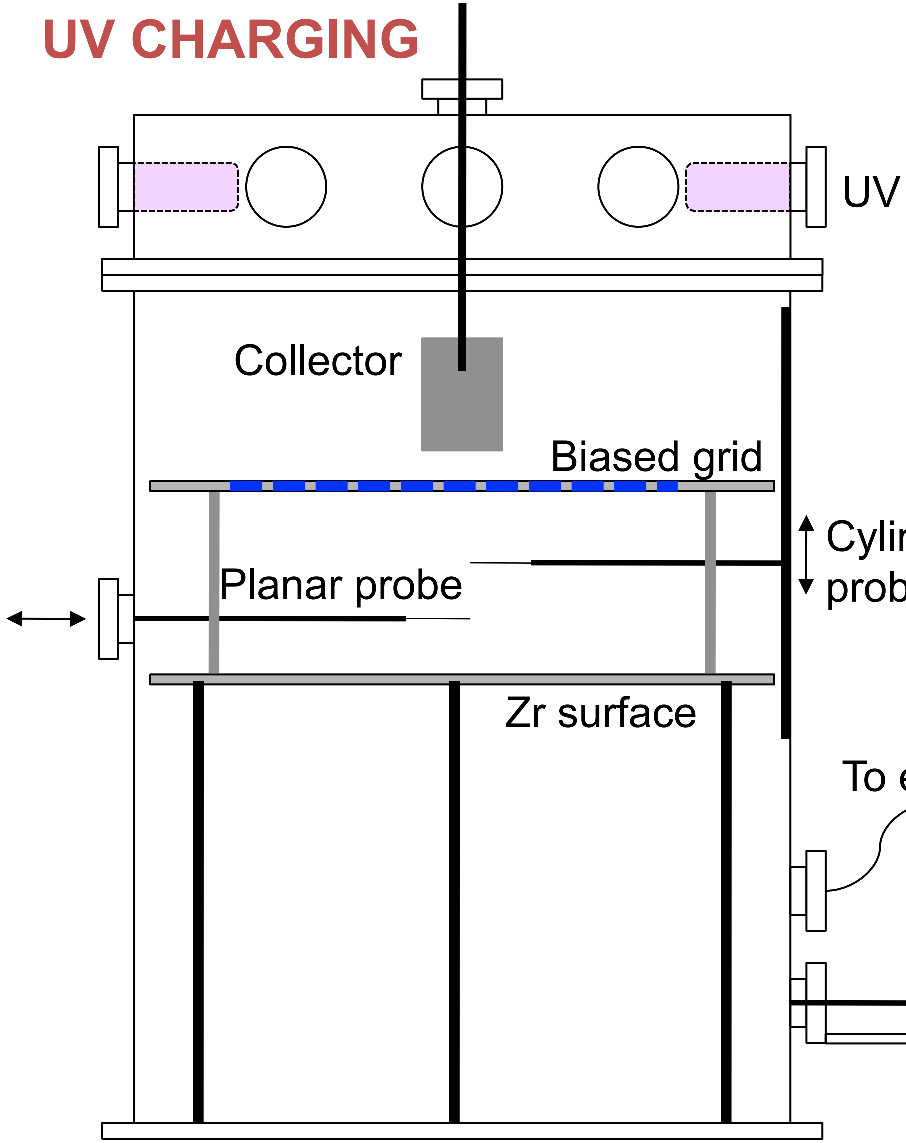

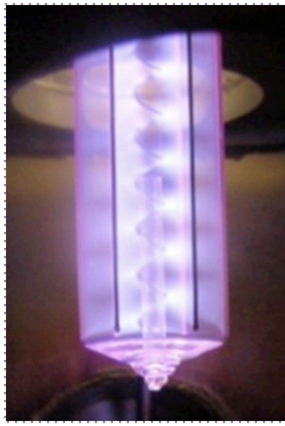

UV CHARGING (Cerium-Oxide)

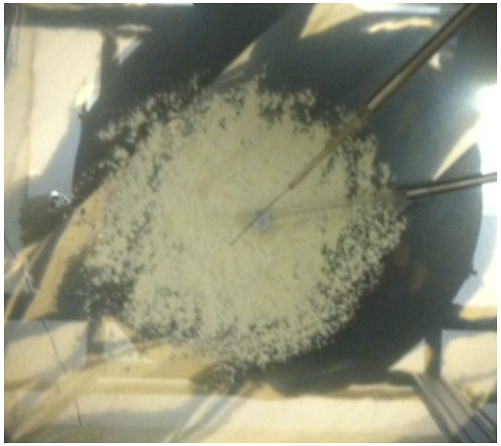

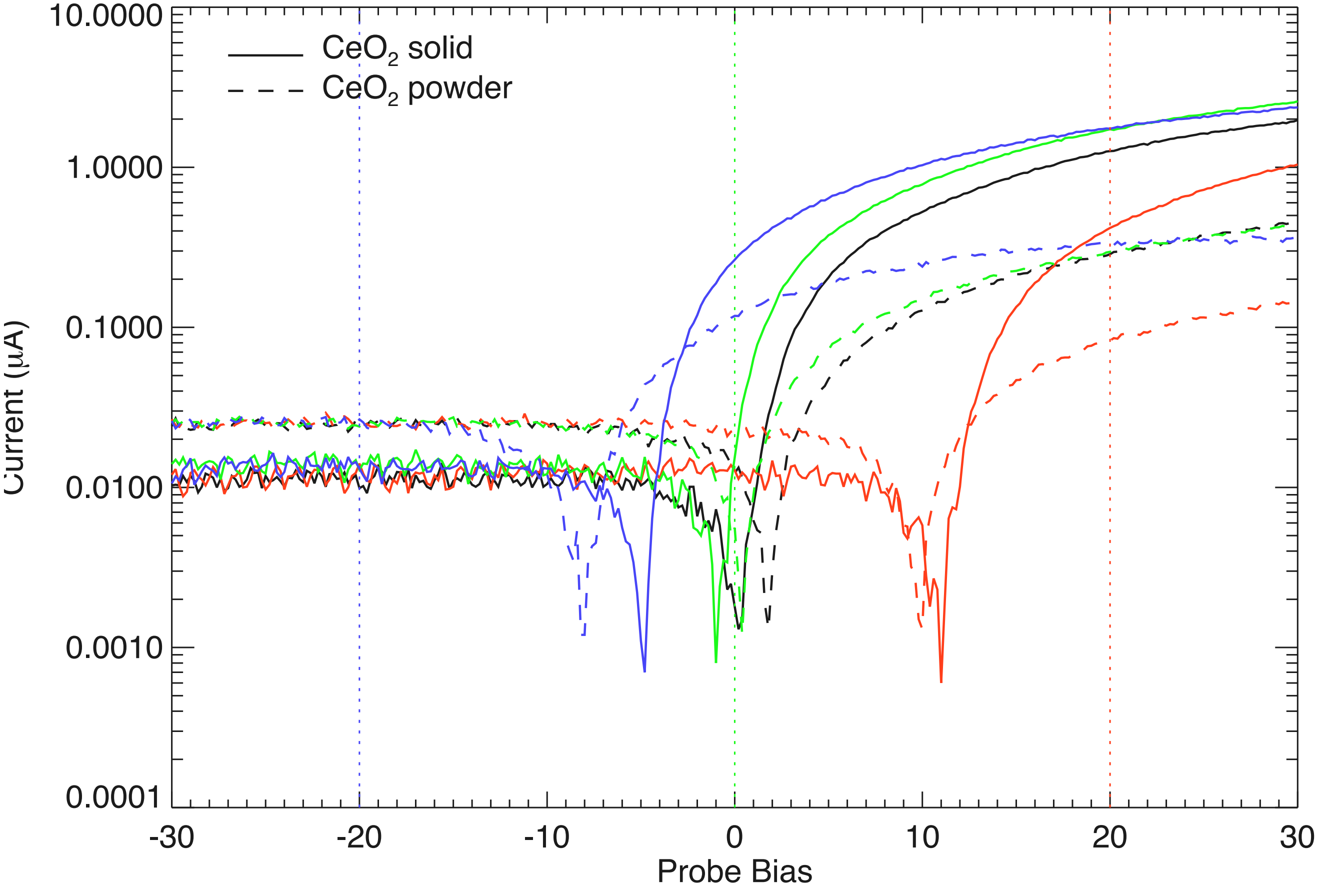

Dove et al., 2011, 2012

UV CHARGING

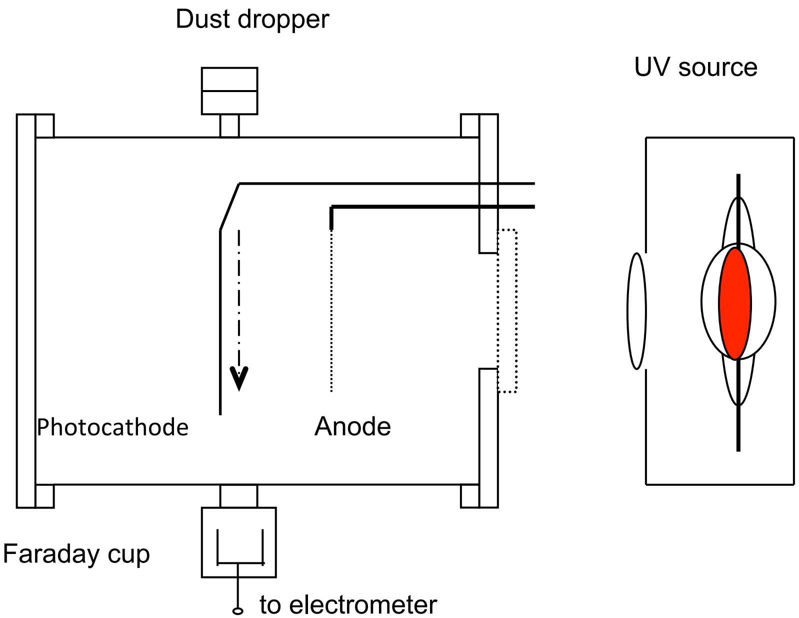

Dust dropper
UV source
Photocathode
Anode
Faraday cup
to electrometer

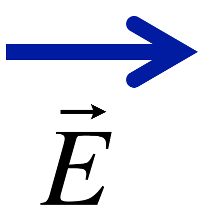

$\vec{E}$

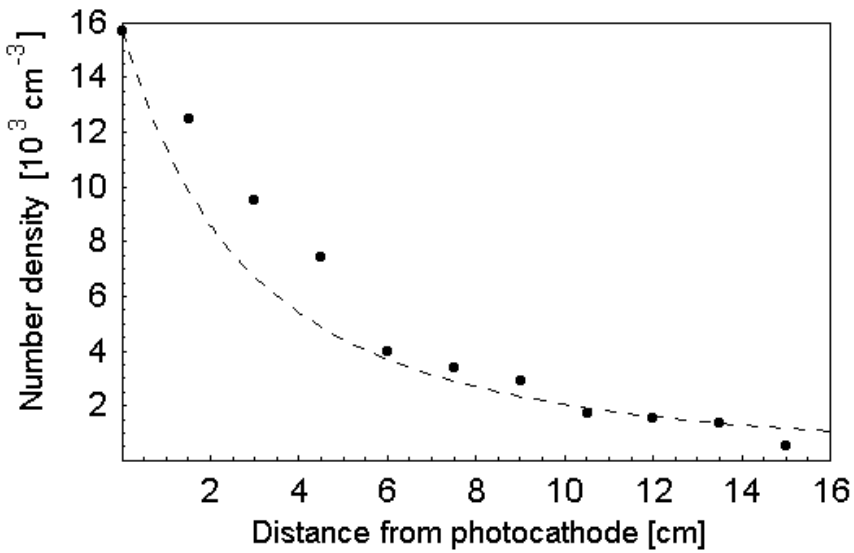

Number density [10^3 cm^{-3}]
16
14
12
10
8
6
4
2
2 4 6 8 10 12 14 16
Distance from photocathode [cm]

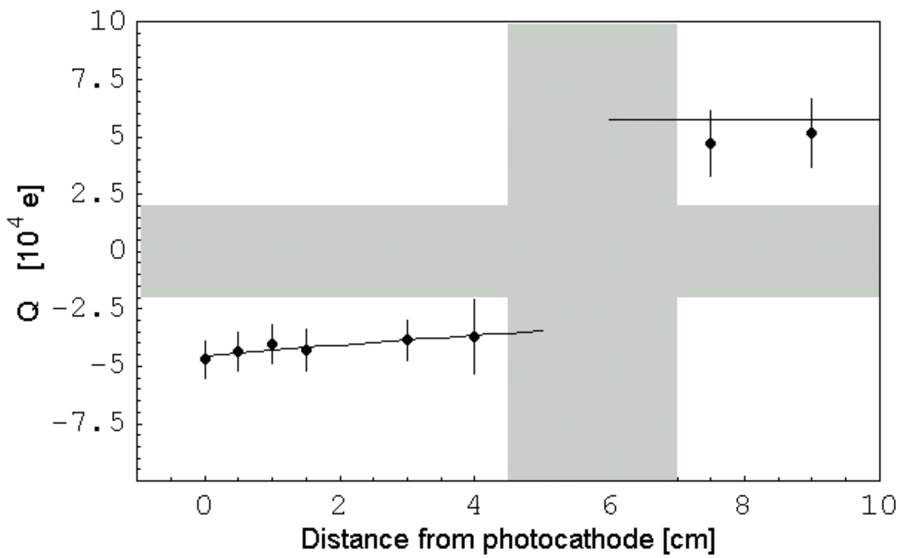

Q [10^4 e]
10
7.5
5
2.5
0
-2.5
-5
-7.5
0 2 4 6 8 10
Distance from photocathode [cm]

LEVITATING DUST

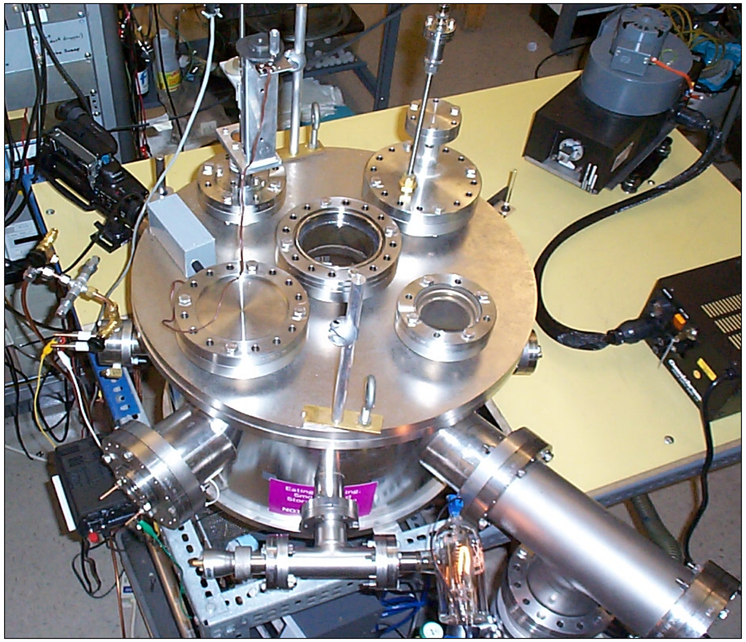

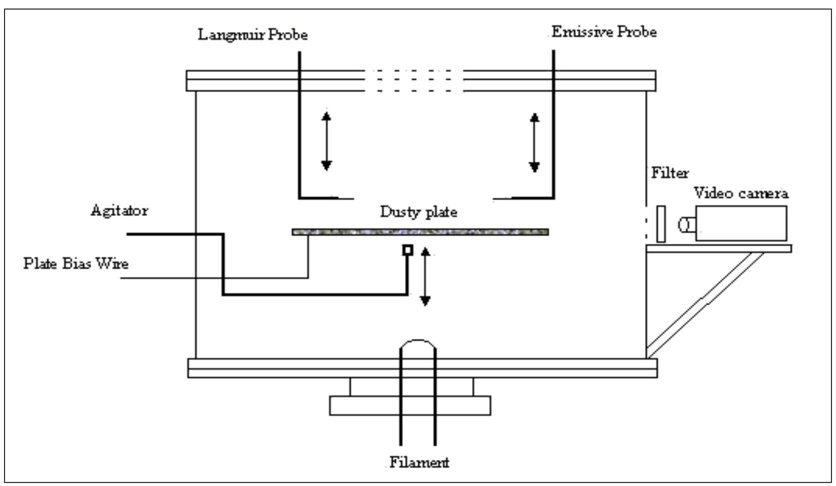

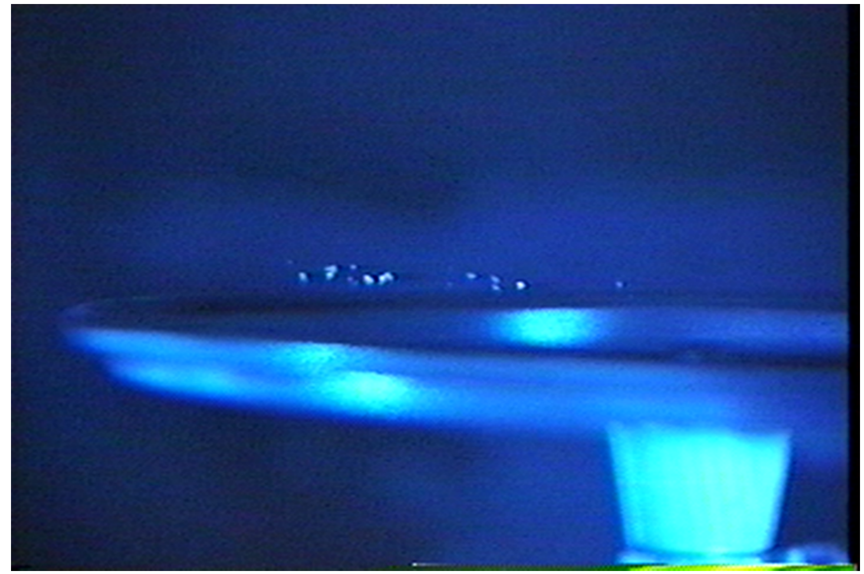

Sickafoose et al., 2002

SWIRLS

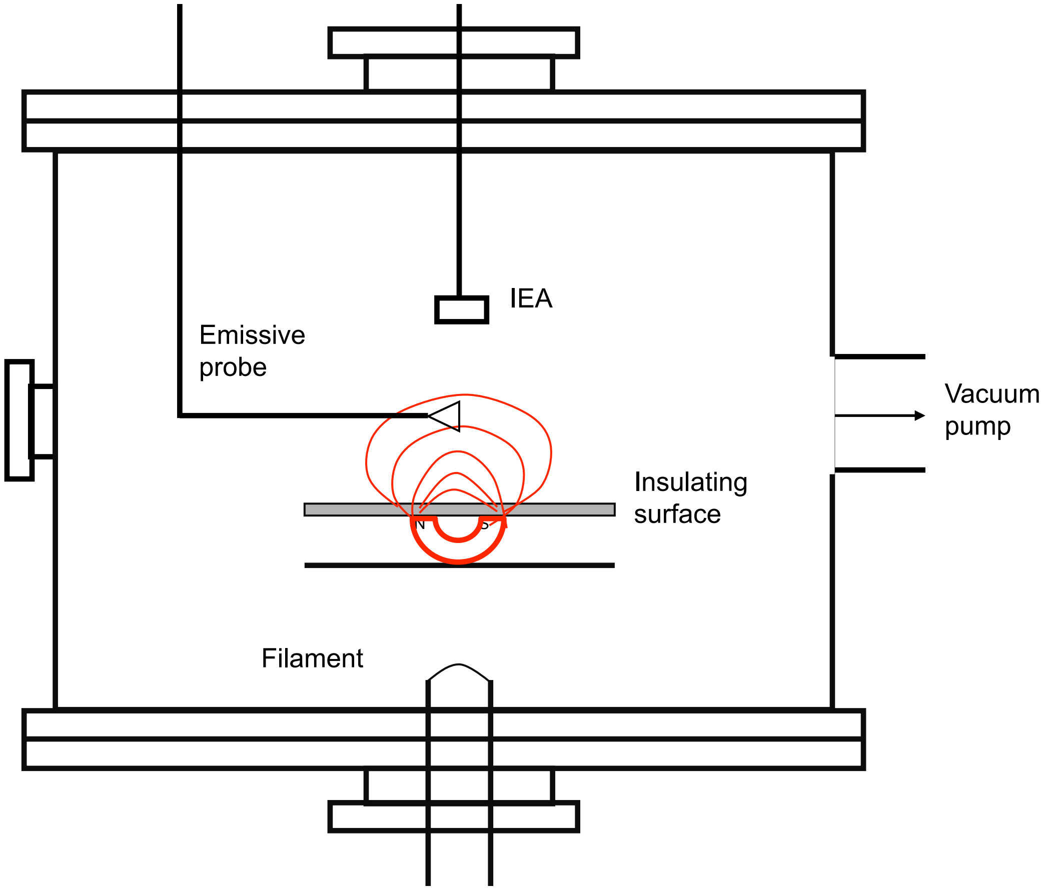
IEA
Emissive probe
Vacuum pump
Insulating surface
Filament

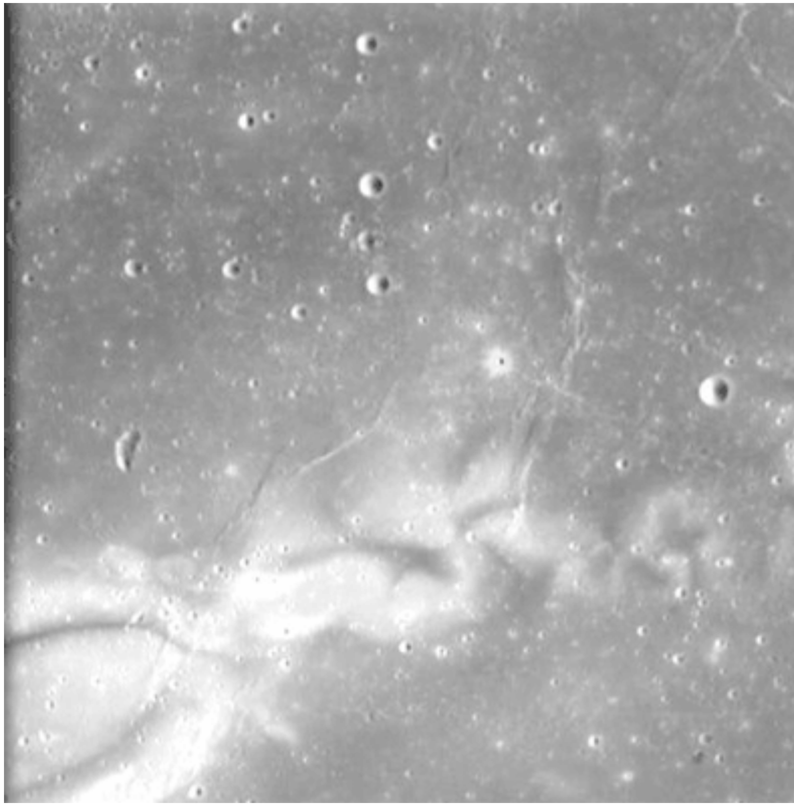

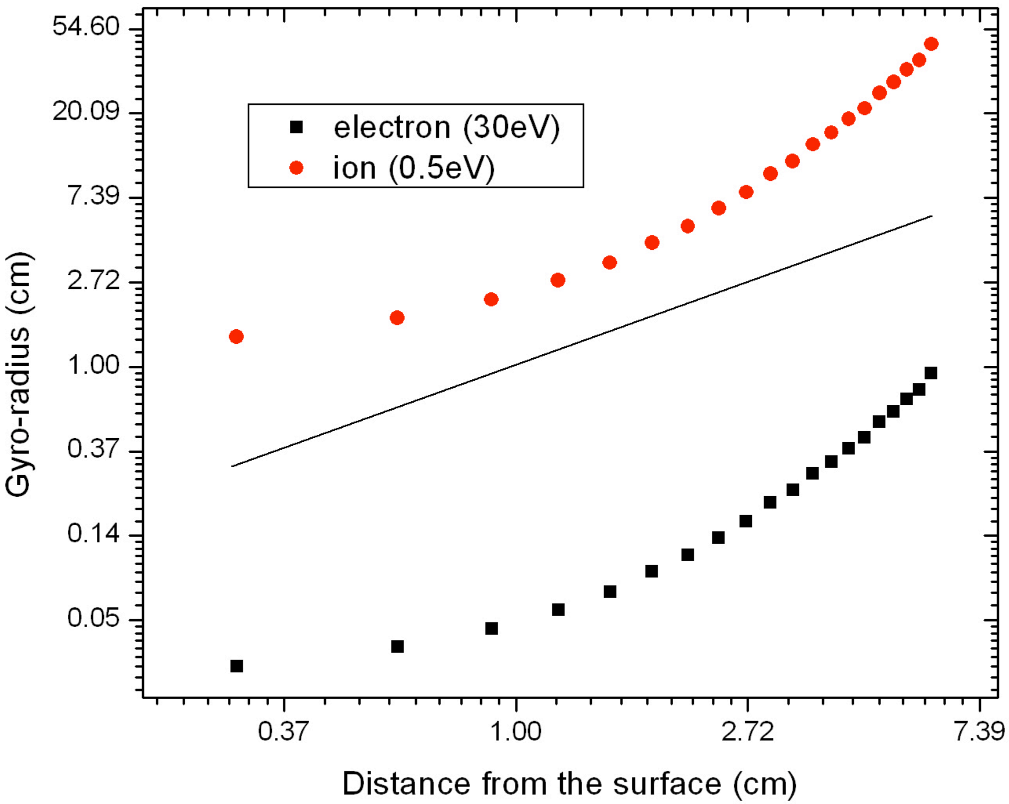

Electrons : magnetized ($r_e < d$)
Ions : unmagnetized ($r_i > d$)

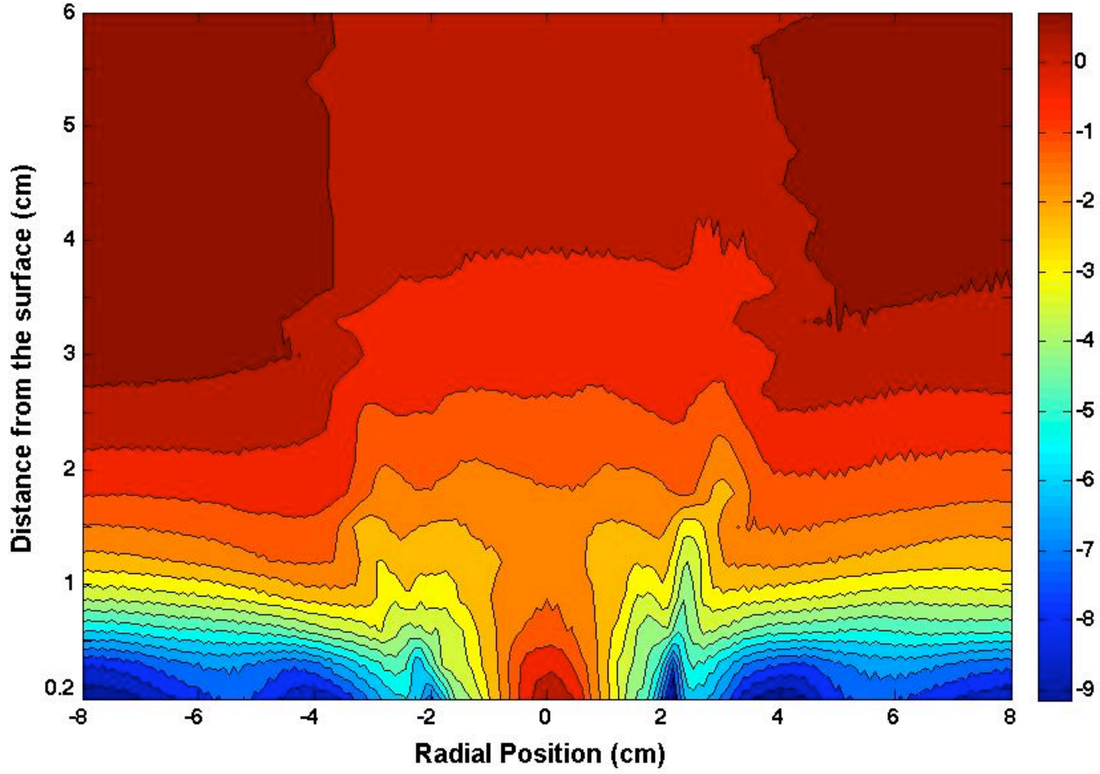

Non-monotonic sheath

- More positive surface potential than the bulk to reflect the ions back into the plasma.
- Potential minimum due to collisions and magnetic-mirror-trapping.

Xu Wang et al., 2012

Horizontal fluctuations

Topography effects everything.

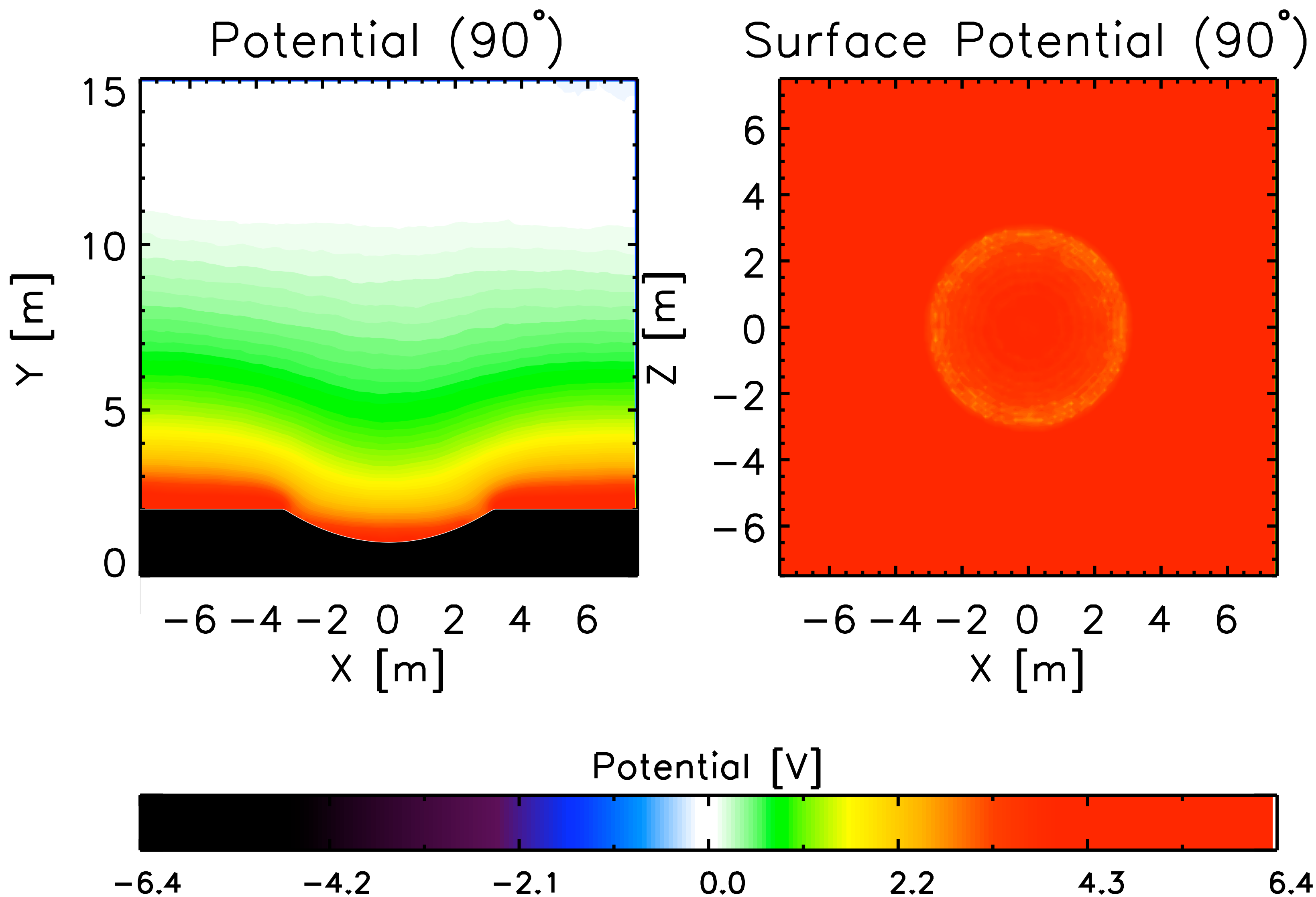

Topography effects everything.

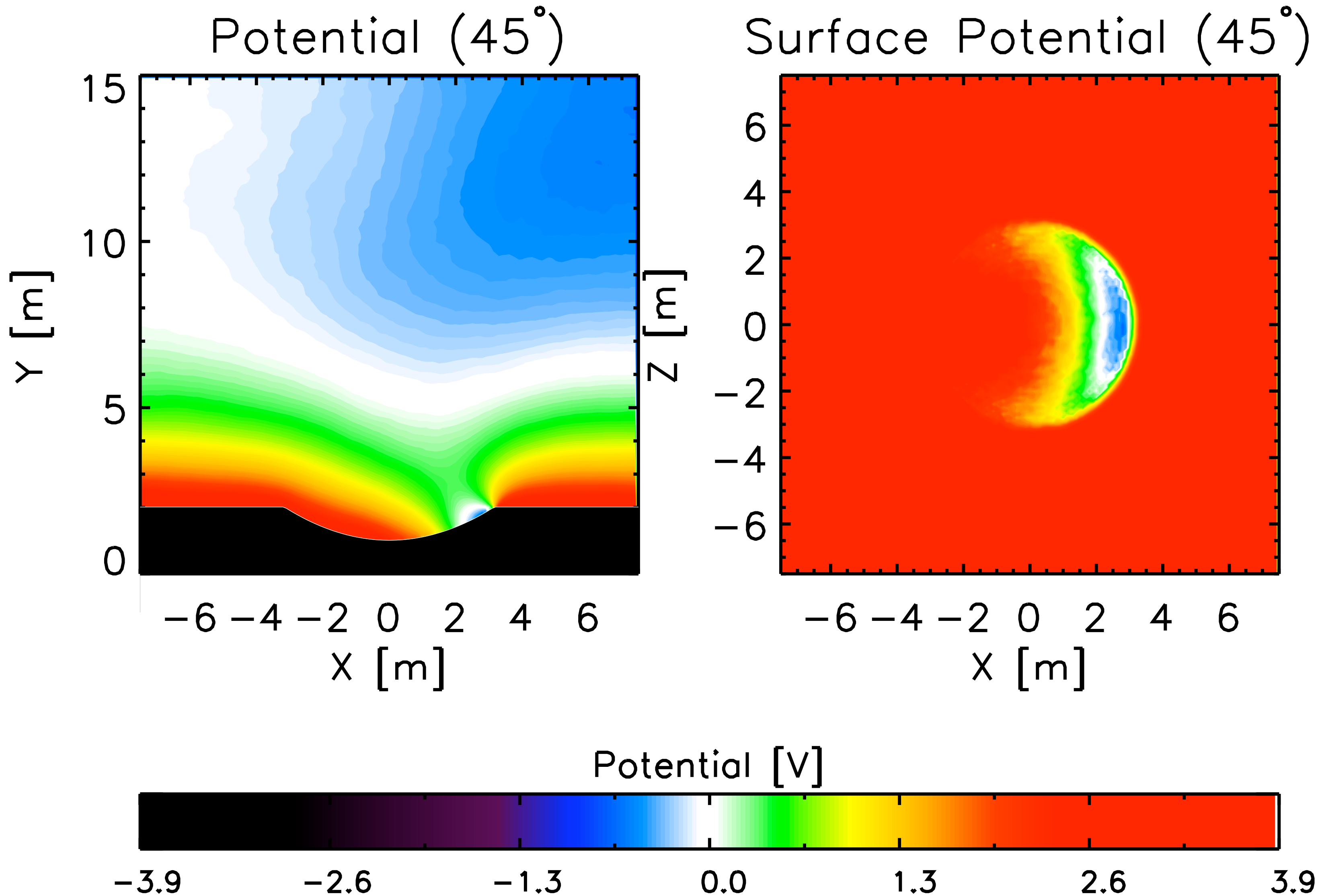

A spacecraft alters its environment.

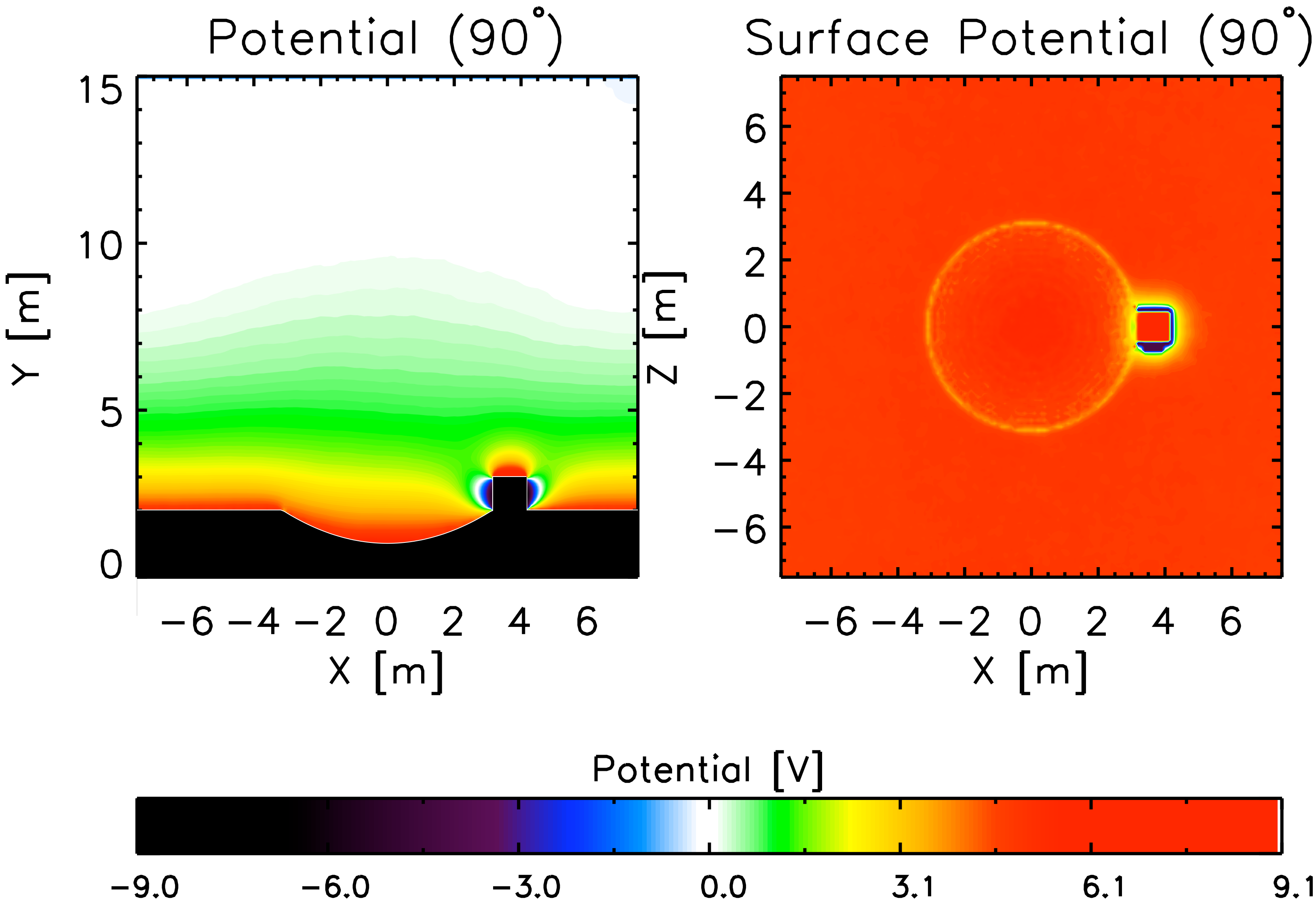

Topography effects everything.

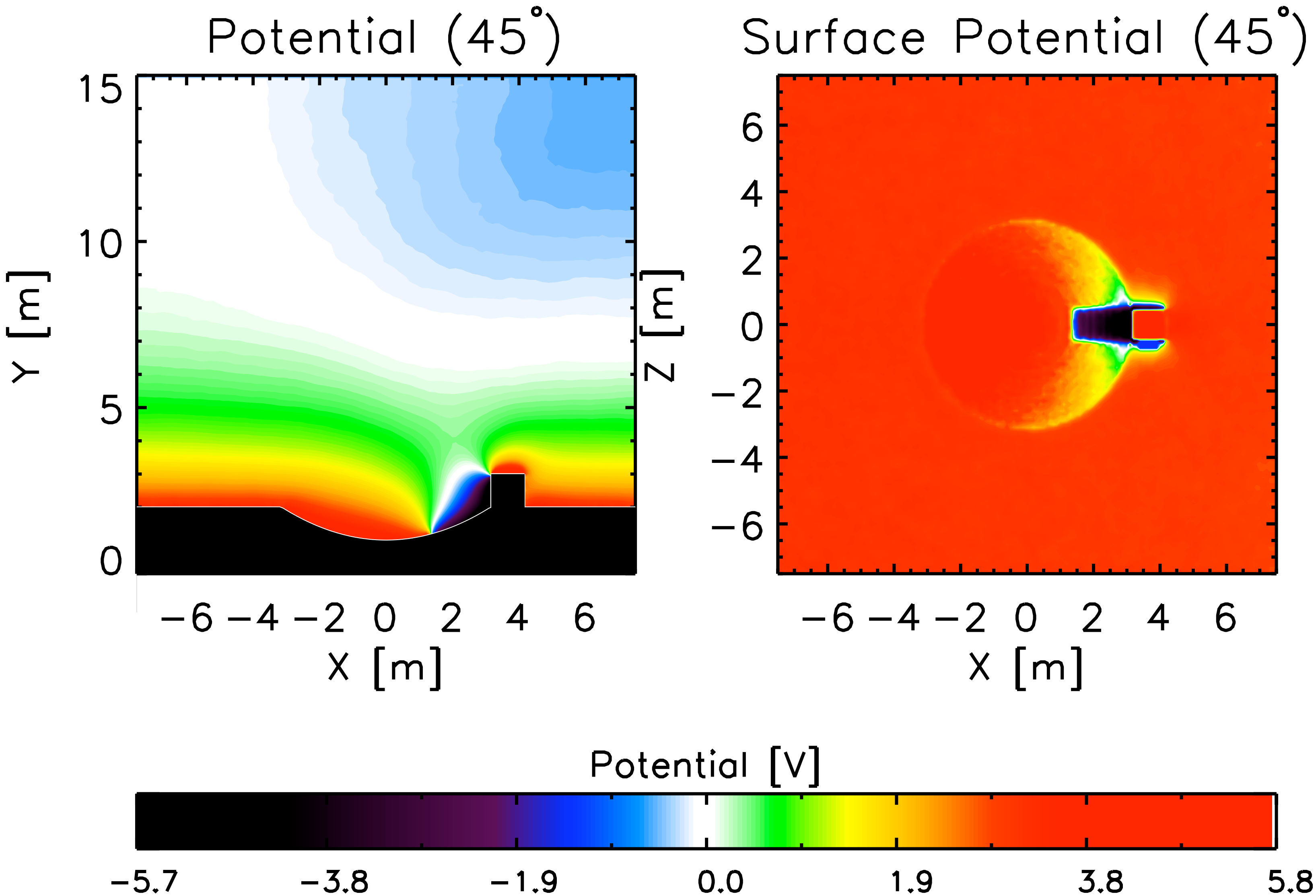

Dust moves around the surface.

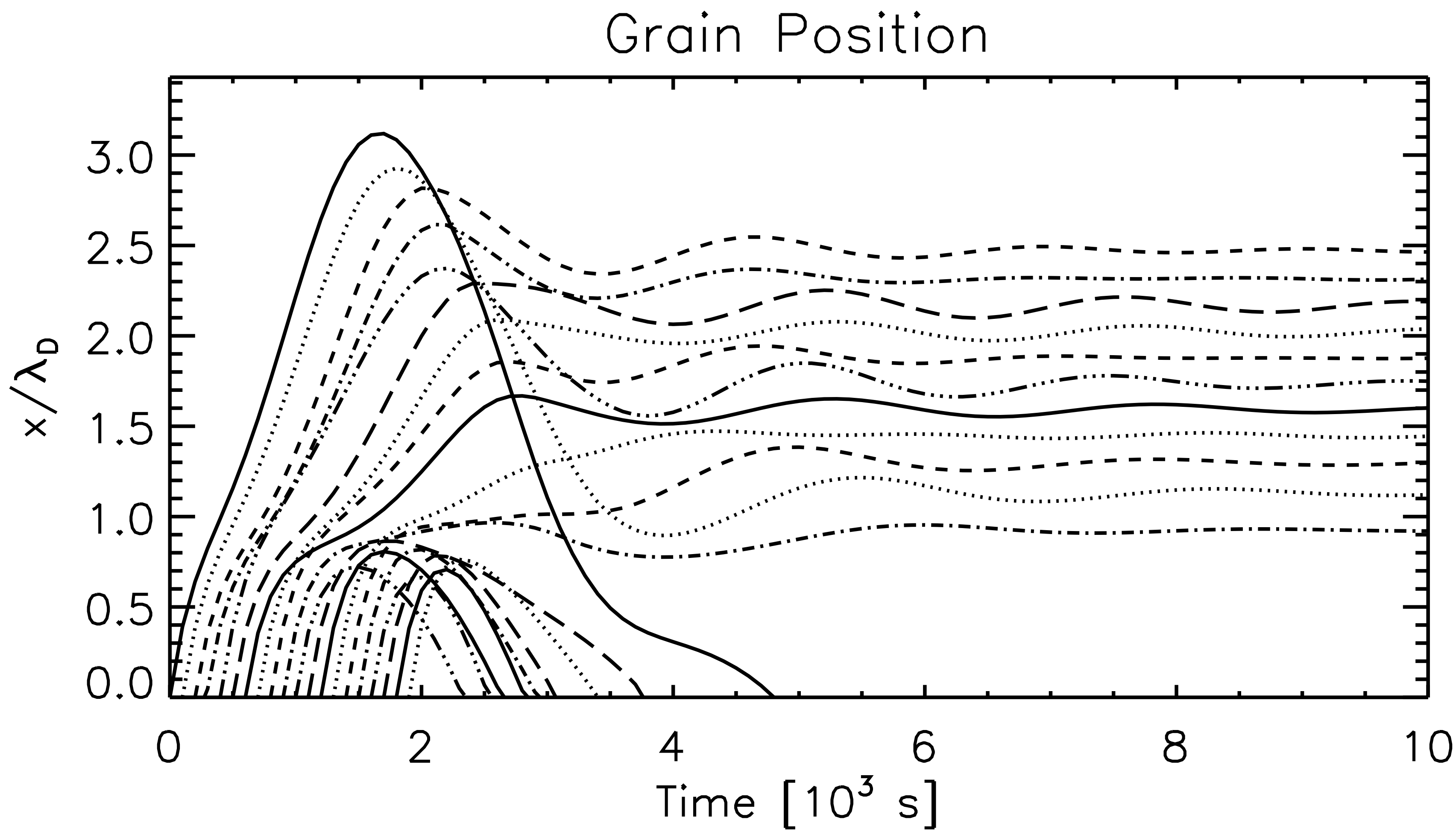

Szalay et al., 2012

Dust accumulates in craters.

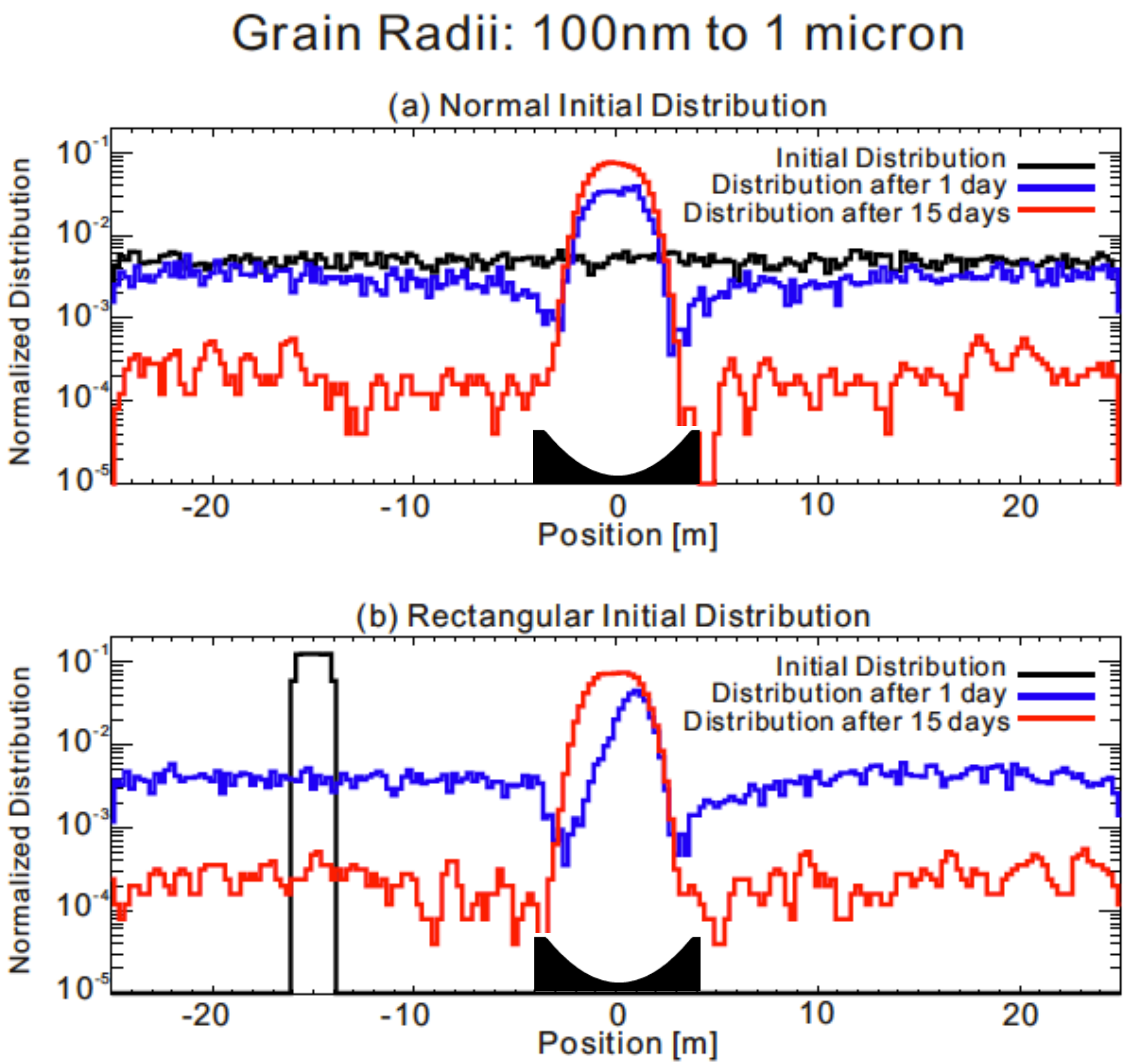

Poppe et al., 2012

Dust ponds can form.

Classification:
C - Carbonaceous
S - Silicaceous
M - Metallic

"Ponding" on Eros

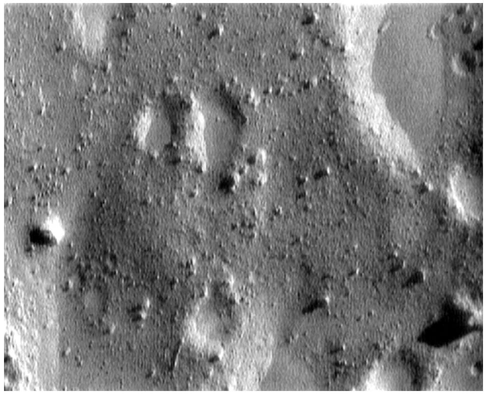

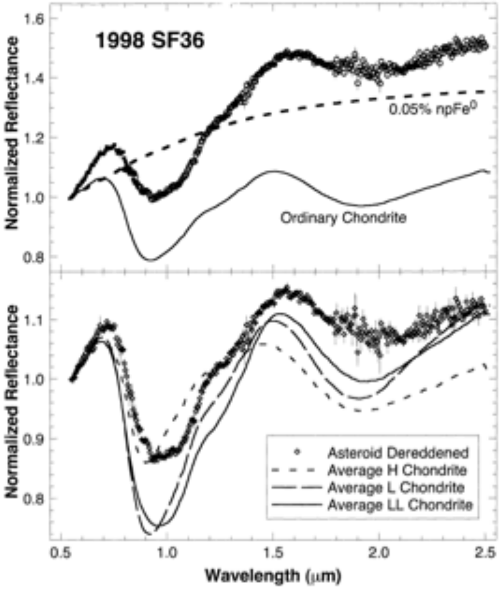

LRO - LAMP

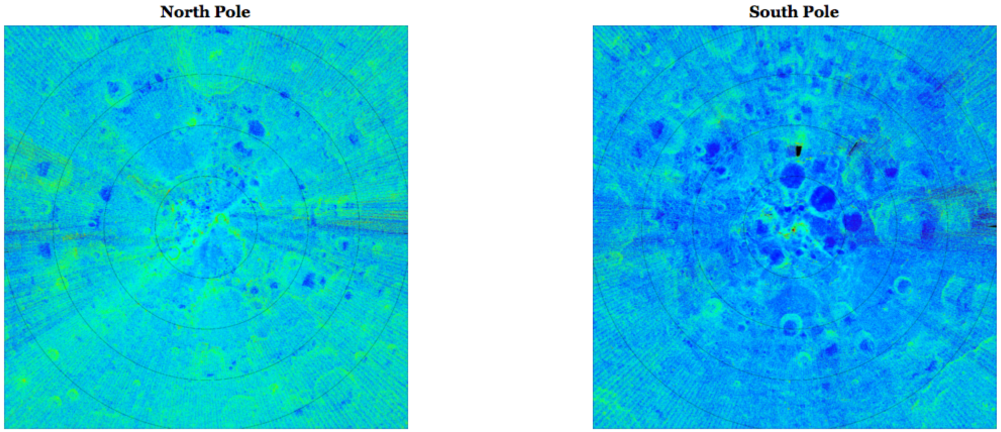

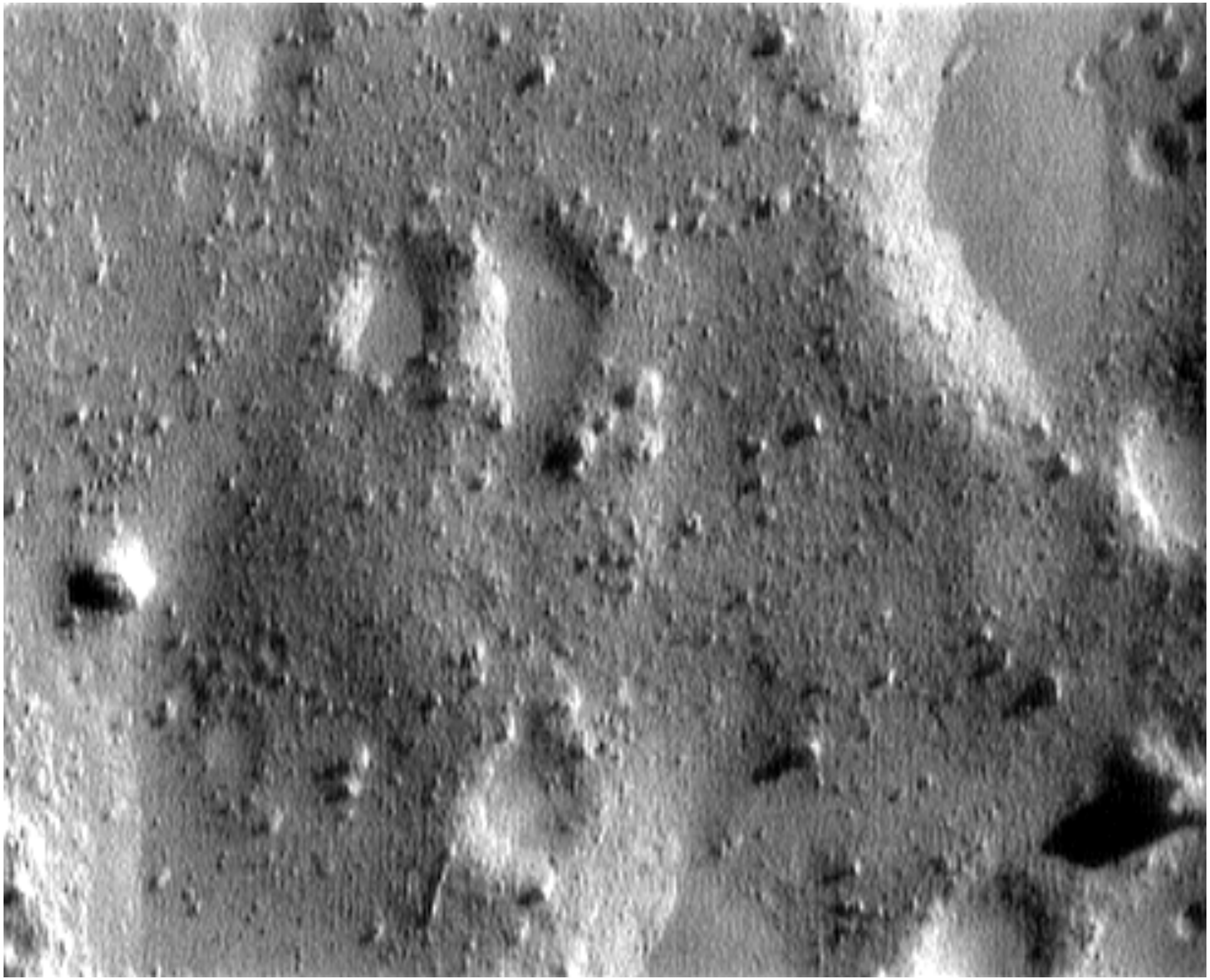

5) Dusty plasmas in comets

CHANGING COMETARY PLASMA ENVIRONMENT

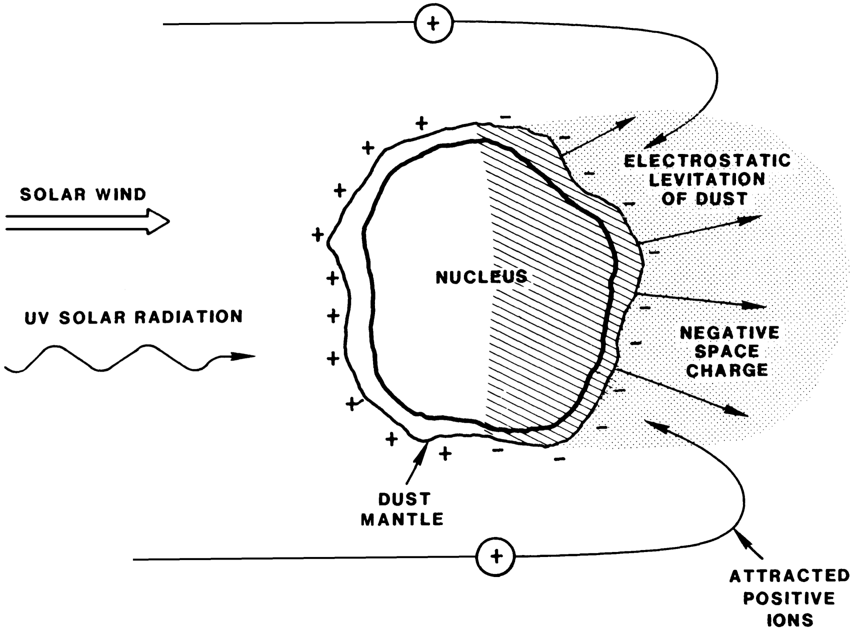

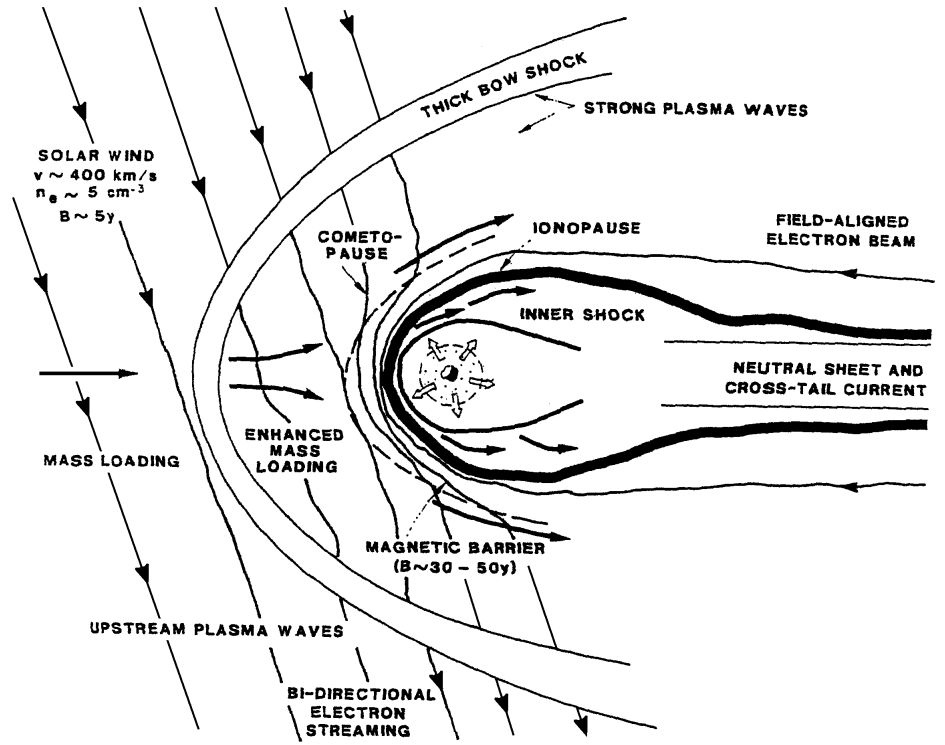

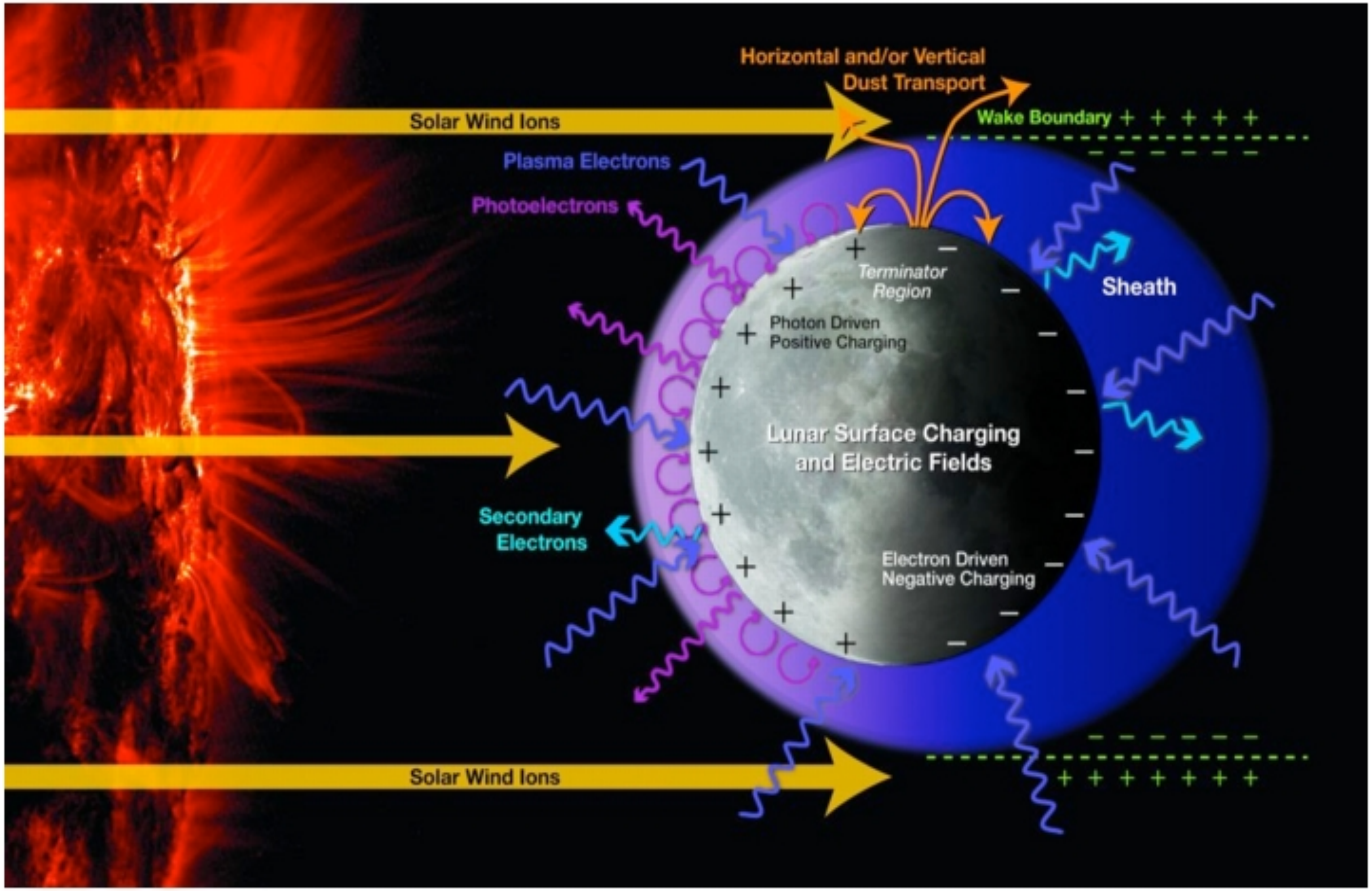
Horizontal and/or Vertical
Dust Transport
Solar Wind Ions
Wake Boundary
Plasma Electrons
Photoelectrons
Terminator
Region
Sheath
Photon Driven
Positive Charging
Lunar Surface Charging
and Electric Fields
Secondary
Electrons
Electron Driven
Negative Charging
Solar Wind Ions

THE TILTED UMBRELLA

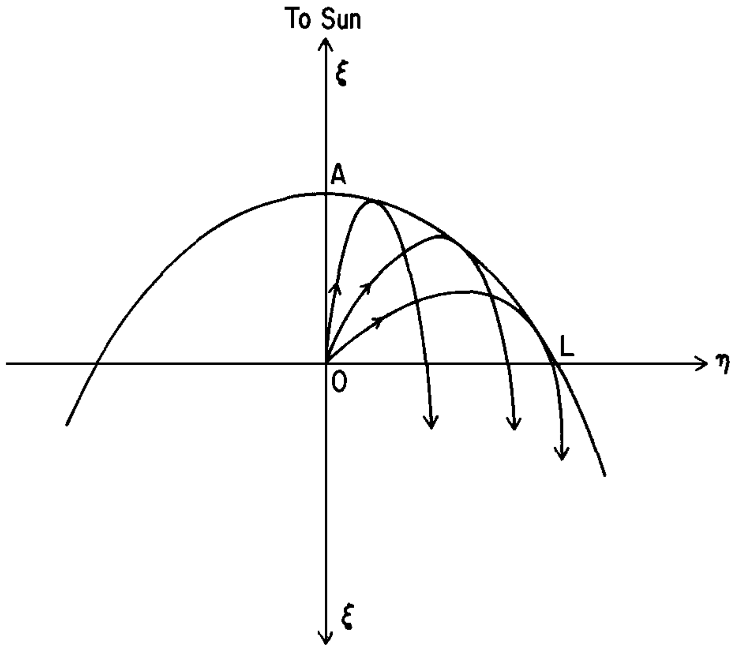

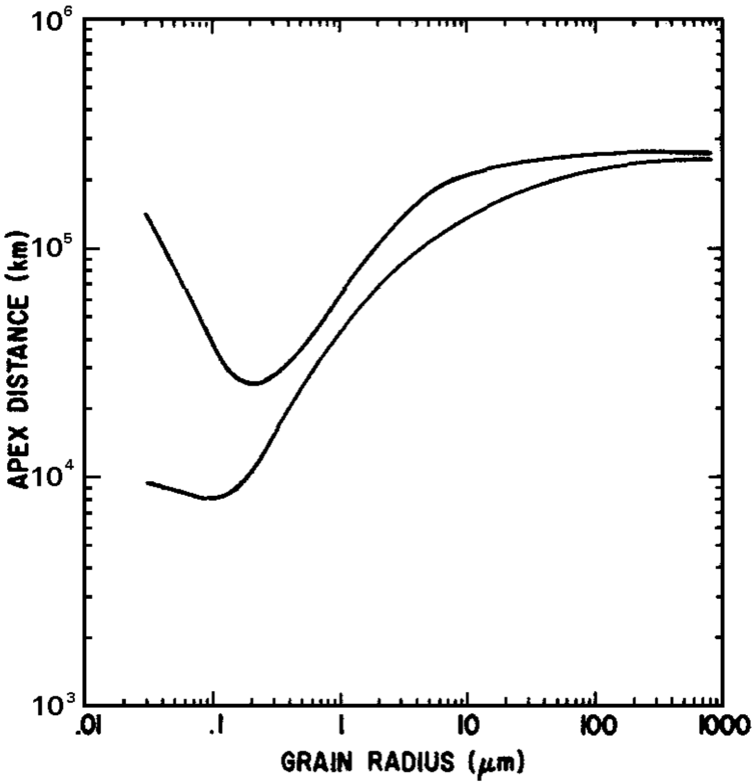

$$\beta = \frac{F_{rad}}{F_{grav}} \approx \frac{6 \times 10^{-5} Q_{pr}(a)}{a\rho},$$

Eddington, 1910

THE FOLDED/TILTED UMBRELLA

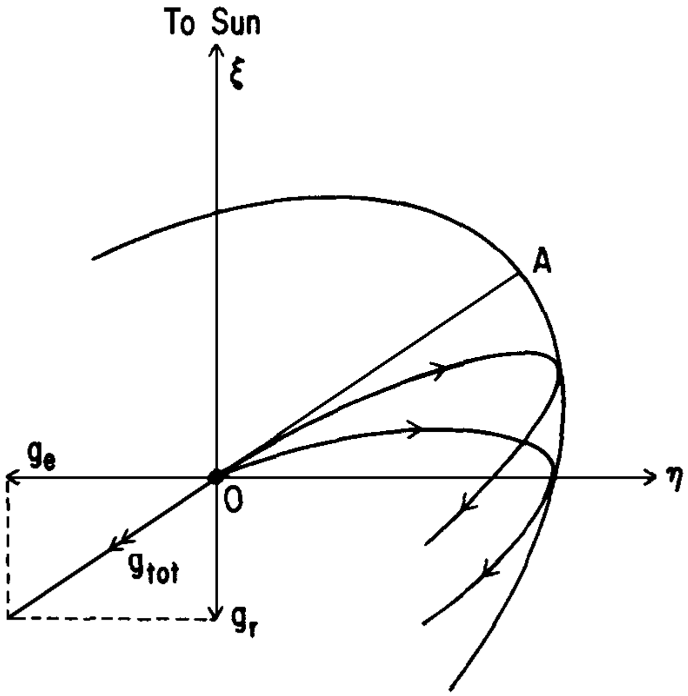

$$\kappa = \frac{|g_e|}{|g_r|} = 10^{-2} \frac{|\phi(\mathrm{V})|}{Q_{pr} a(\mu)}.$$

Wallis and Hasan, 1983

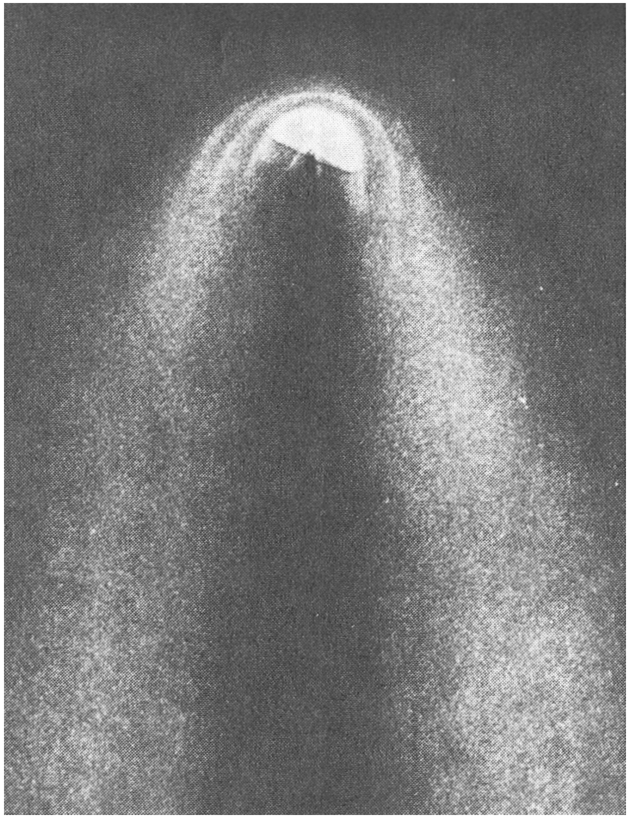

Comet Donati (1858), drawing by (G.P. Bond)

THE FOLDED/TILETED/WRINKLED UMBRELLA

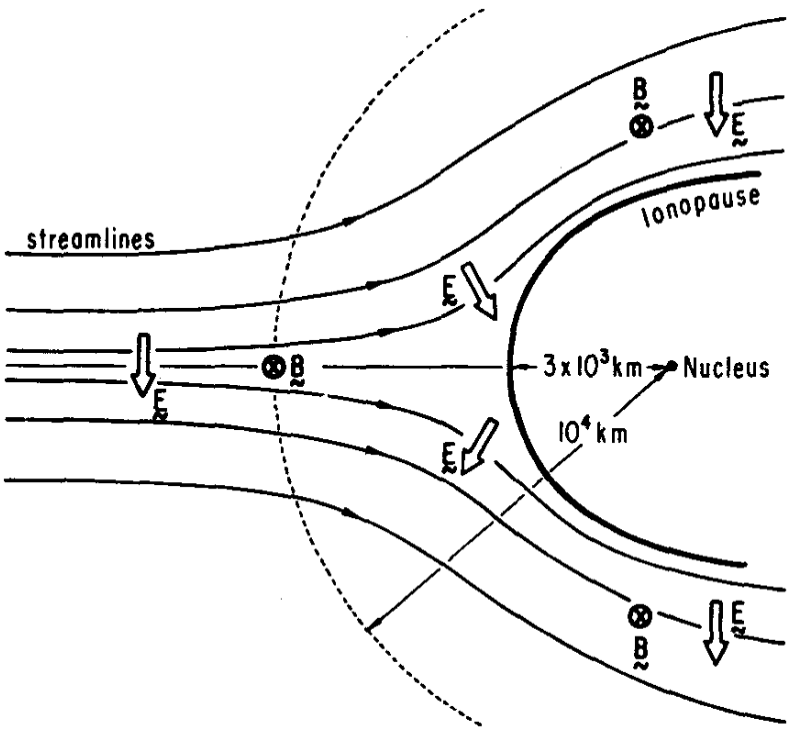

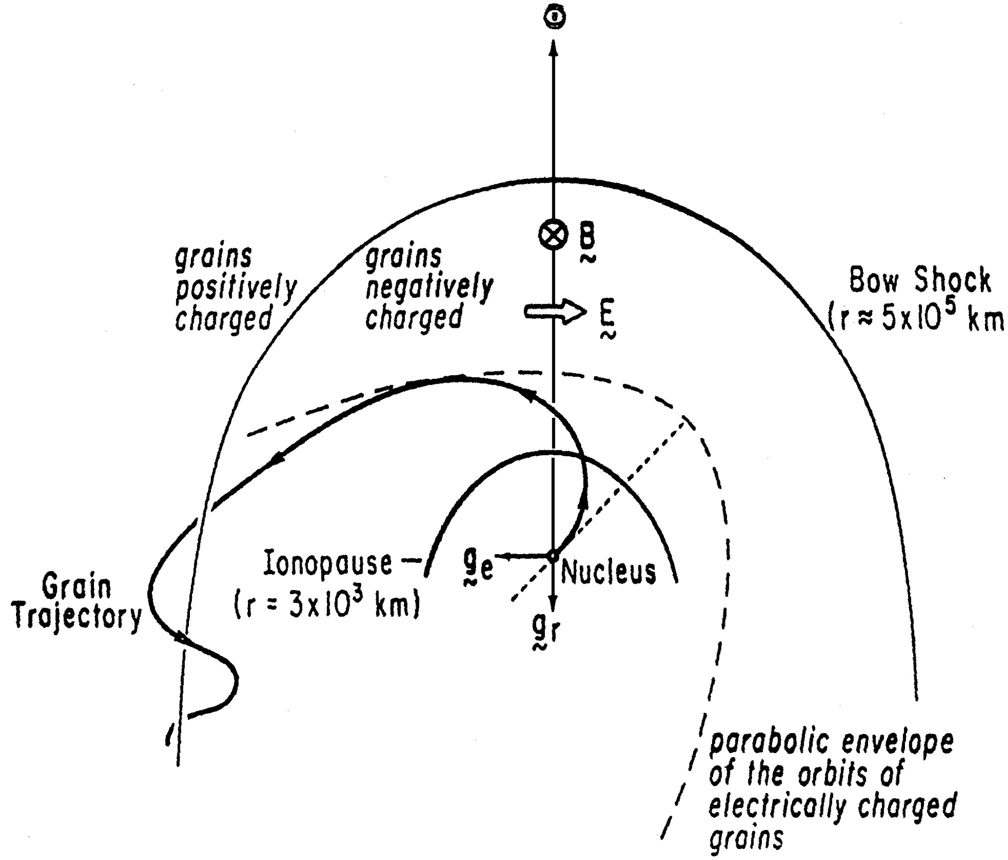

Horanyi and Mendis, 1985

10^4 km behind the nucleus

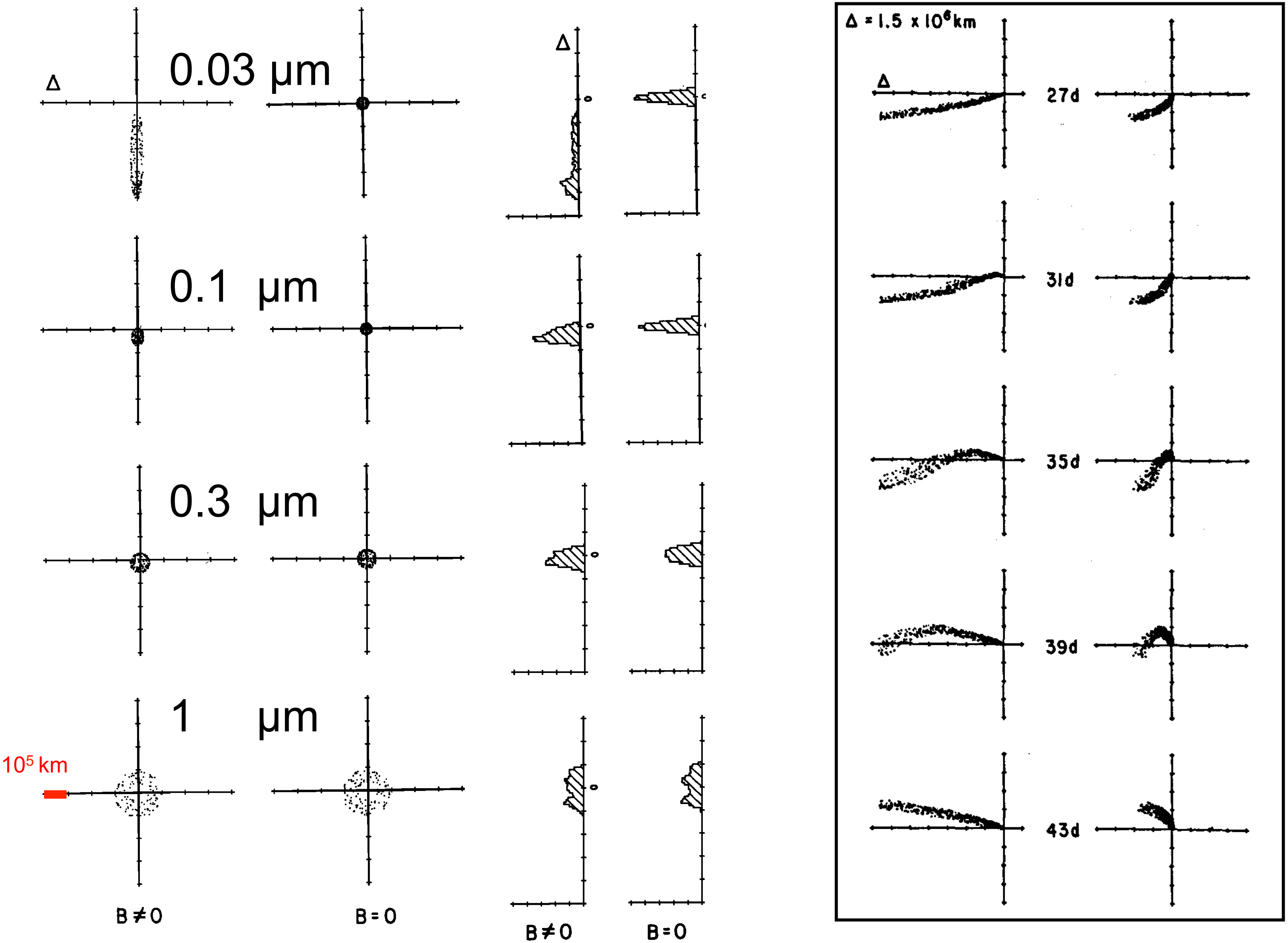

CLUSTERS AND POCKETS OF DUST .....

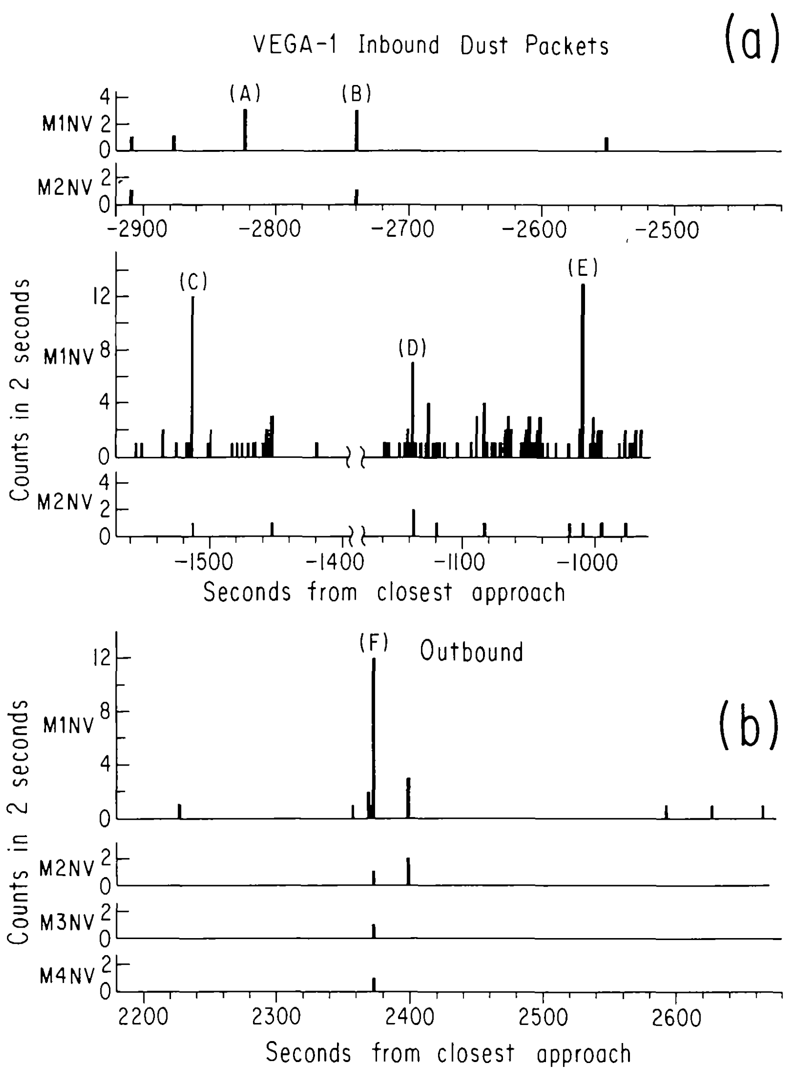

Simpson et al., 1987

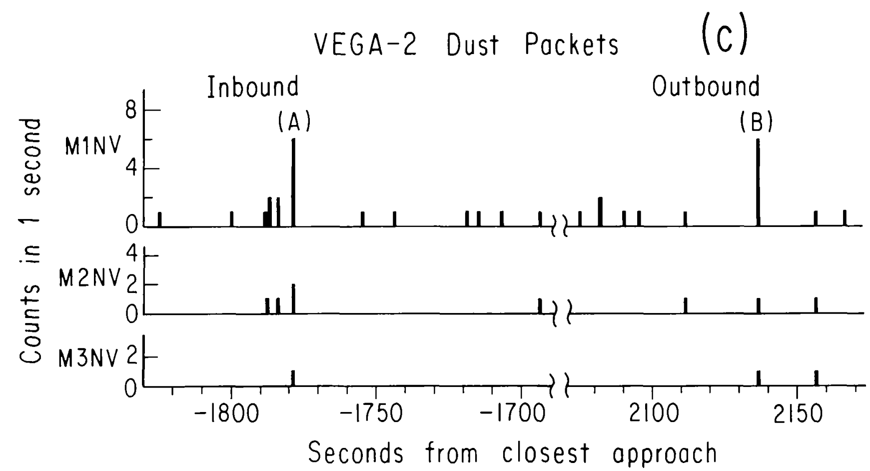

$$a_c(\mu\mathrm{m}) = 6.65 F_t^{-1/2} |\phi(\mathrm{V})|$$

Lord Rayleigh, 1882
Öpik, 1956

ELECTRON 'BITE-OUTS'

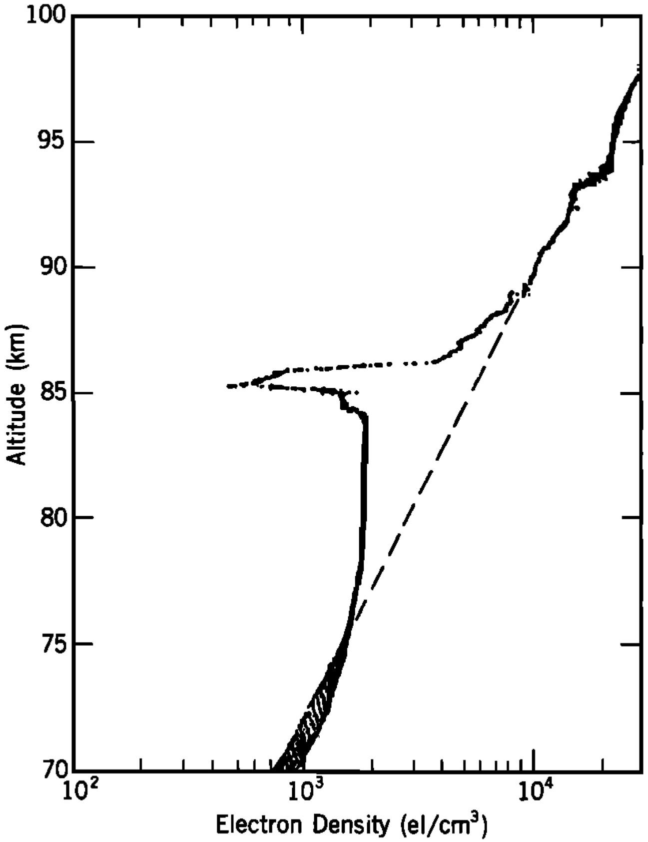

Fig. 1. Electron density profile measured during the STATE 3 rocket flight at Poker Flat, Alaska, on June 17, 1983 [after *Ulwick et al.*, 1988].

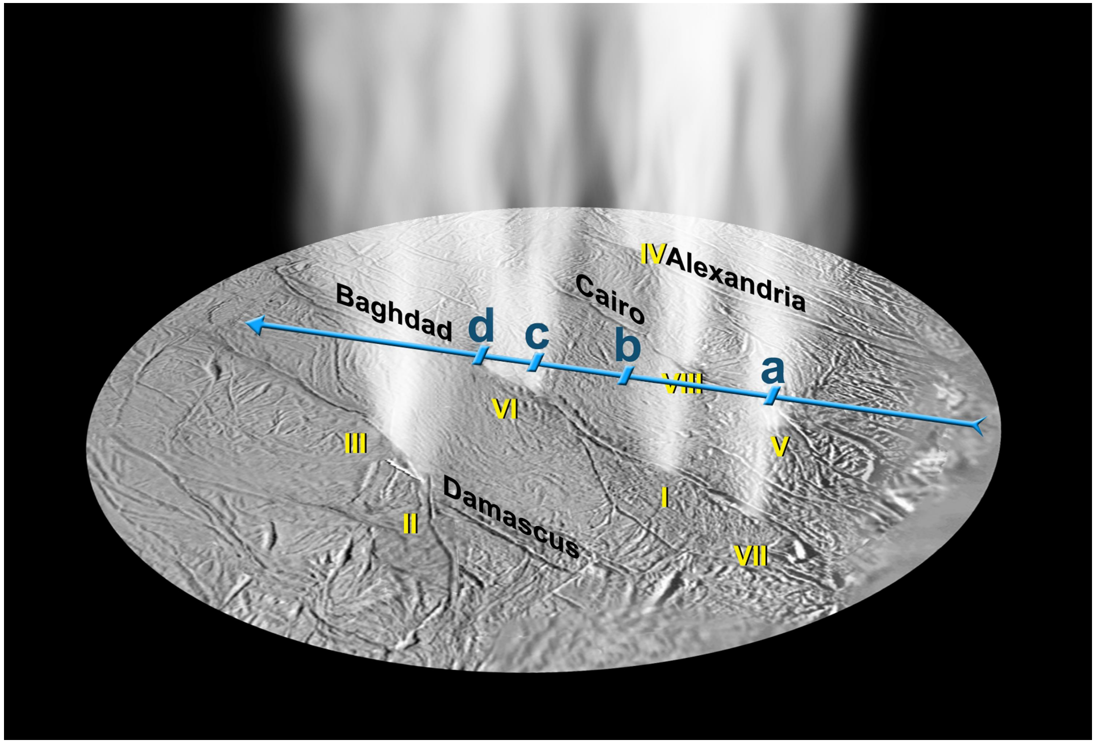

Cassini @ Enceladus

DUSTY PLASMA WAVES

Usual plasma waves are modified due to the presence of dust.

$$n_e - n_i = \int Z(a) n(a)\, da$$

Dust Ion Acoustic Wave (DIA)

Shukla and Silin, 1992

$$\omega^2 = \frac{\delta k^2 c_s^2}{1 + k^2 \lambda_{De}^2} \quad \text{for} \quad k\lambda_{De} \ll 1$$

$$\omega = \delta^{1/2} k c_S$$

$$c_S = \sqrt{k_B T / m} \quad \text{and } \delta = \frac{n_{i0}}{n_{eo}}$$

Dust Acoustic Wave (DA)

$$\omega^2 = Z_d^2 \left(\frac{k_B T_i}{m_d} \right) \left(\frac{n_{d0}}{n_{i0}} \right)$$

DUSTY PLASMA WAVES

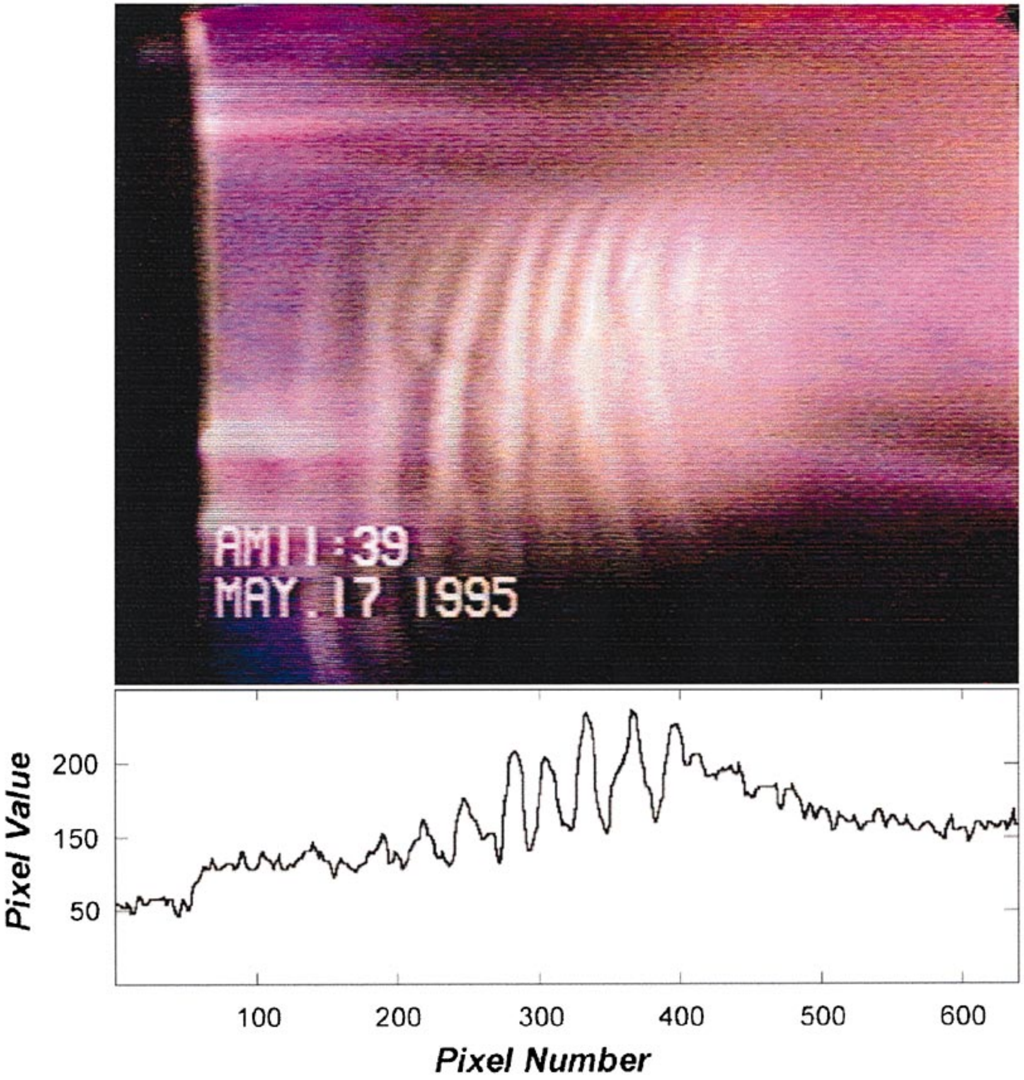

DAW

$$\lambda = 0.6 \text{ cm}$$

$$v_{\varphi} = 9 \text{ cm/s}$$

Rao and Shukla, 1990
Barkan et al., 1995

6) Dust in the heliosphere: interstellar dust, nano-dust

Ulysses Trajectory

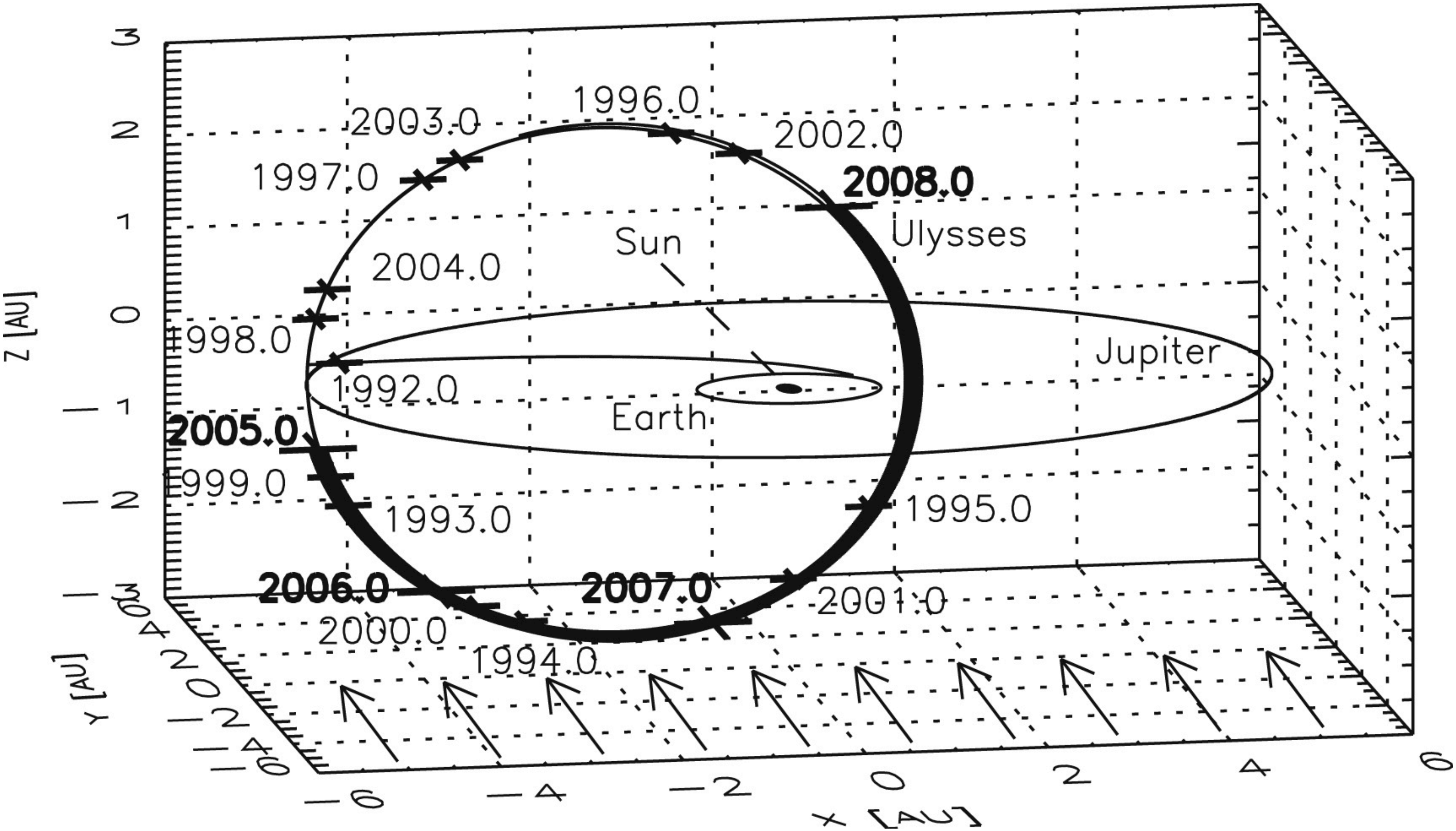

Discovery: ISD in the Solar System

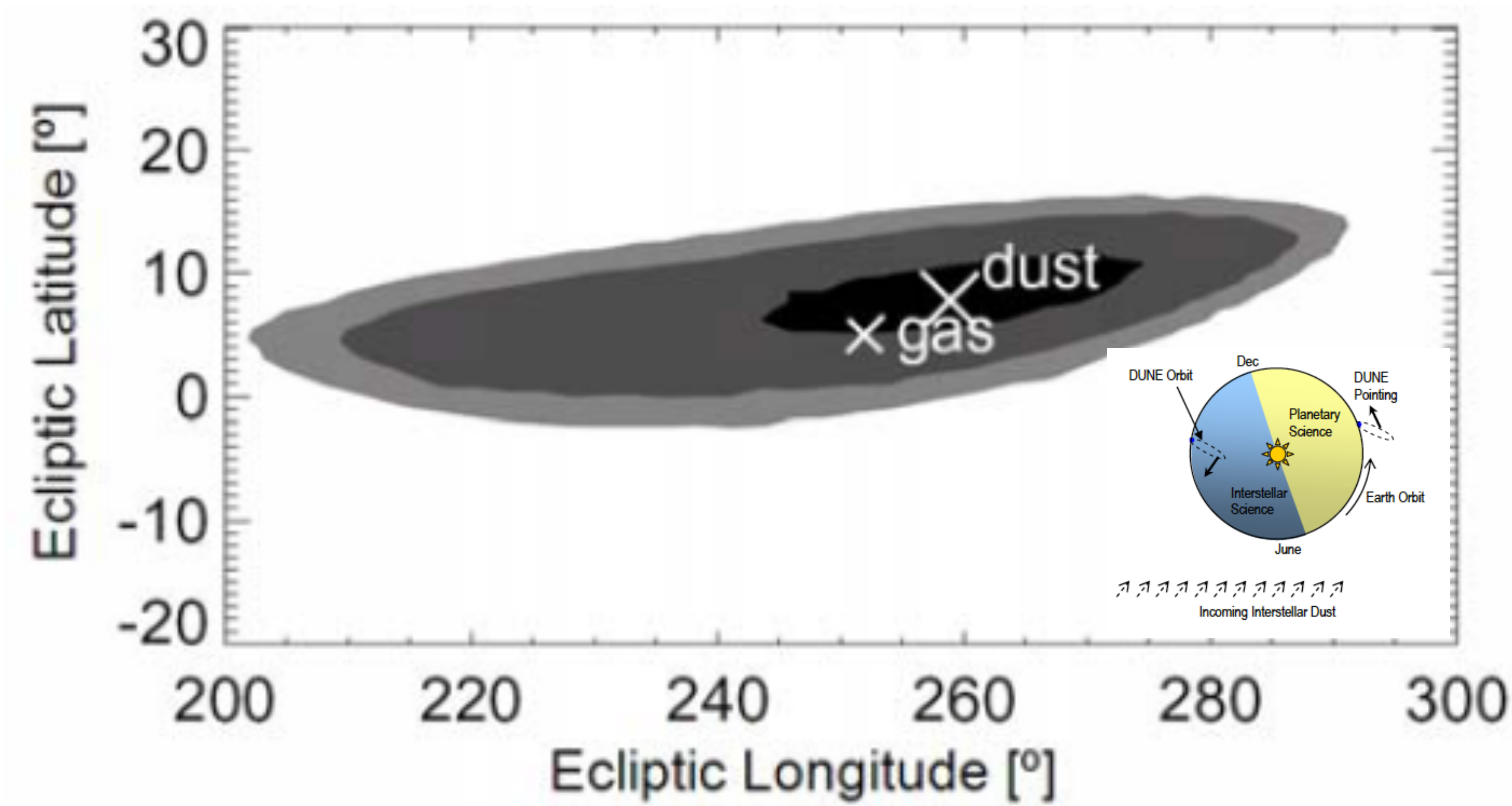

Frisch et al., 1999

Rotation Angle

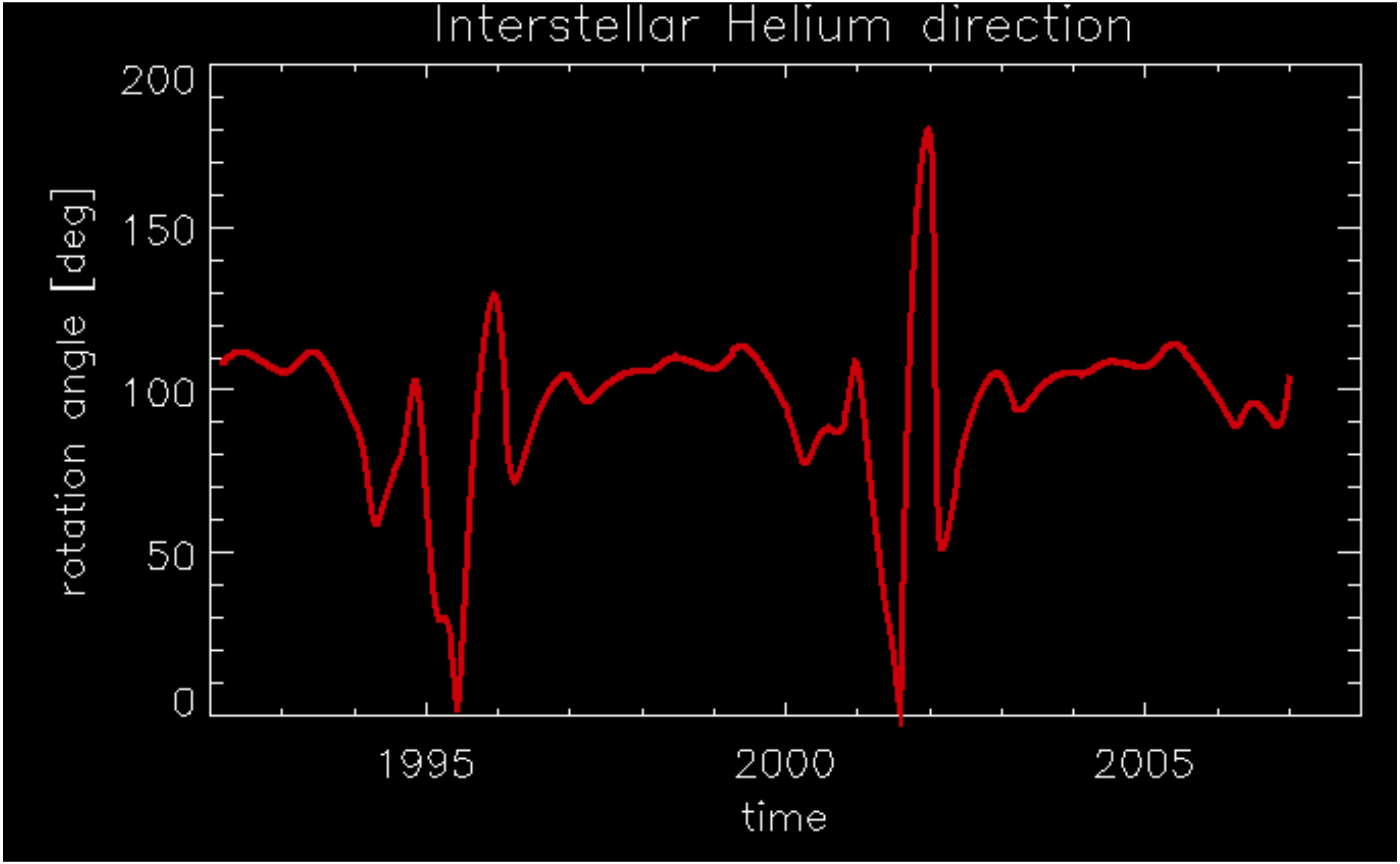

Size Distribution

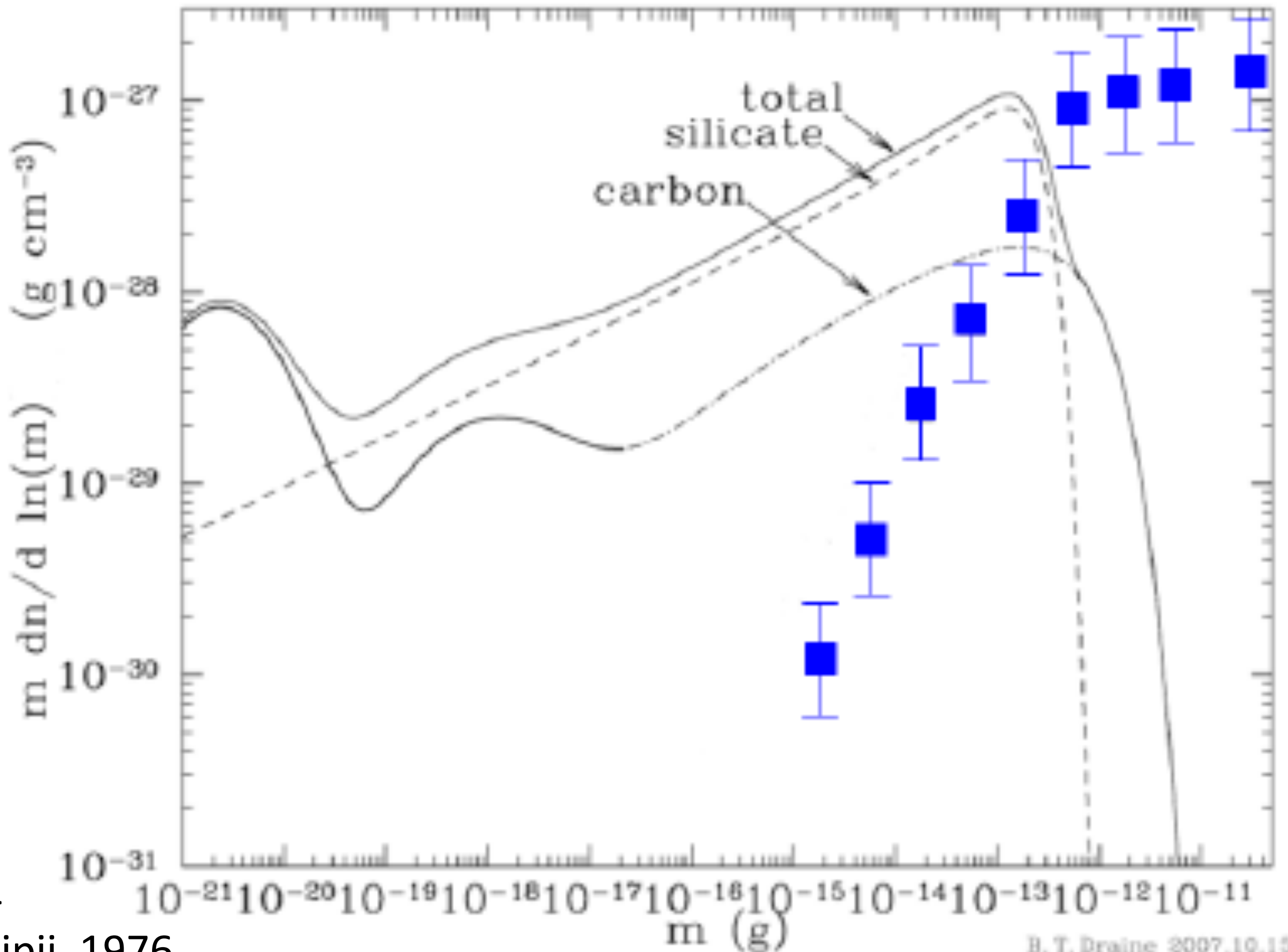

Parker, 1964
Levy and Jokipii, 1976

Time dependent flux

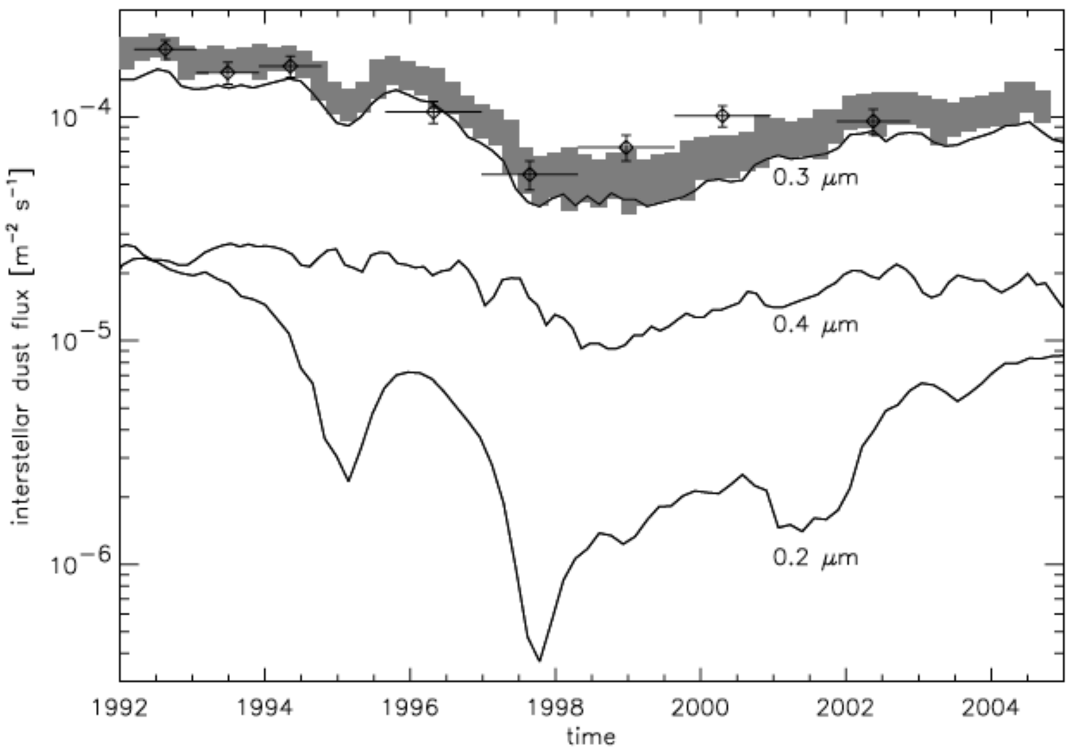

Figure 4. Fit of simulated to measured flux. The fit parameters are the relative contribution of grains of sizes between 0.1 and 0.4 μm (The 0.1 μm curve is not shown, because it did not contribute to the fit). The flux measurements by Ulysses are shown as in Figure 2. The solid lines show the flux profiles of the simulated grains of various sizes, scaled with their best-fit relative contributions. The shaded region indicates the best-fit total predicted flux, with its vertical extent giving the 1σ uncertainty.

Data

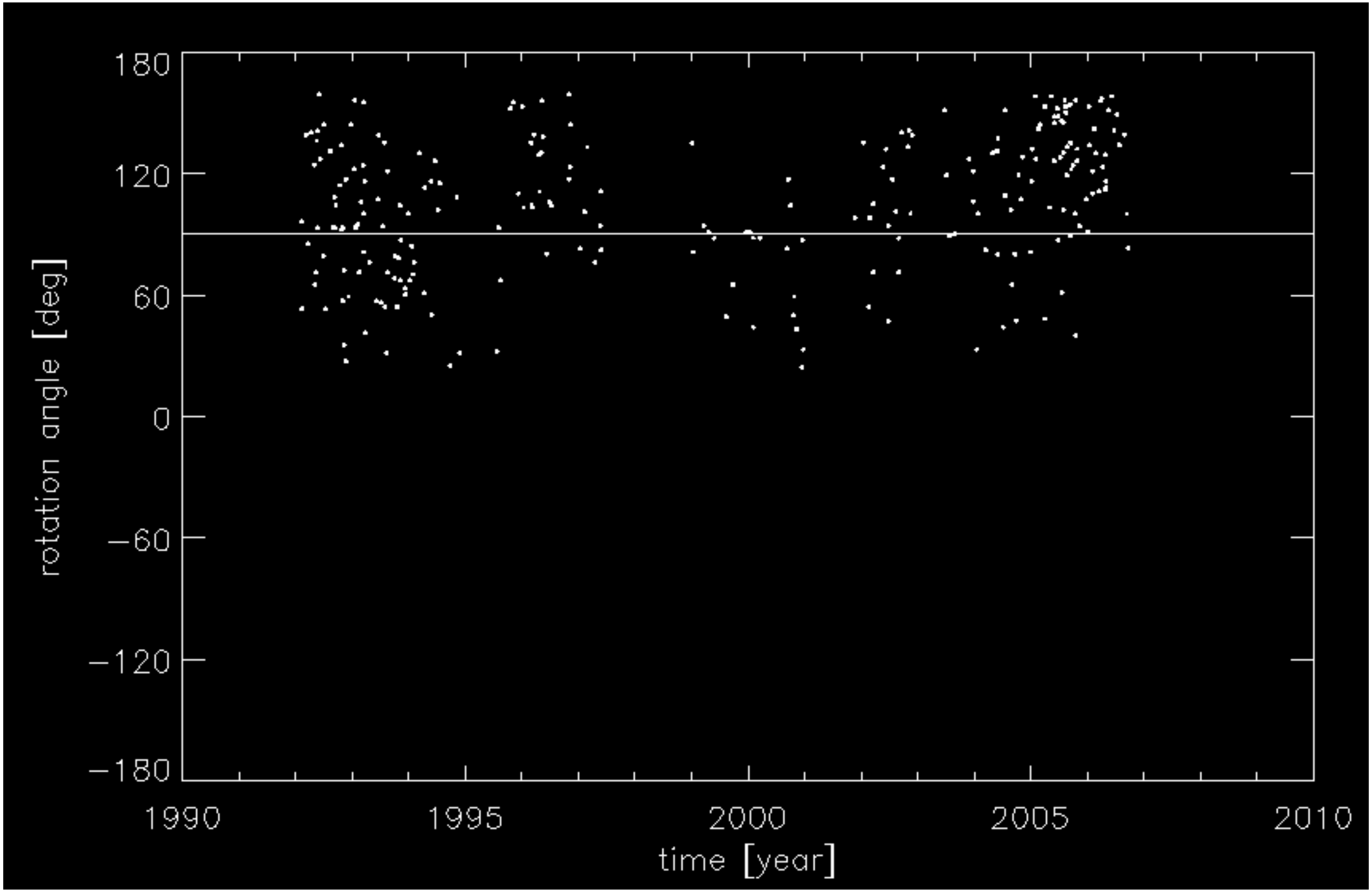

rotation angle [deg]
180
120
60
0
−60
−120
−180
1990
1995
2000
2005
2010
time [year]

Number of Impacts

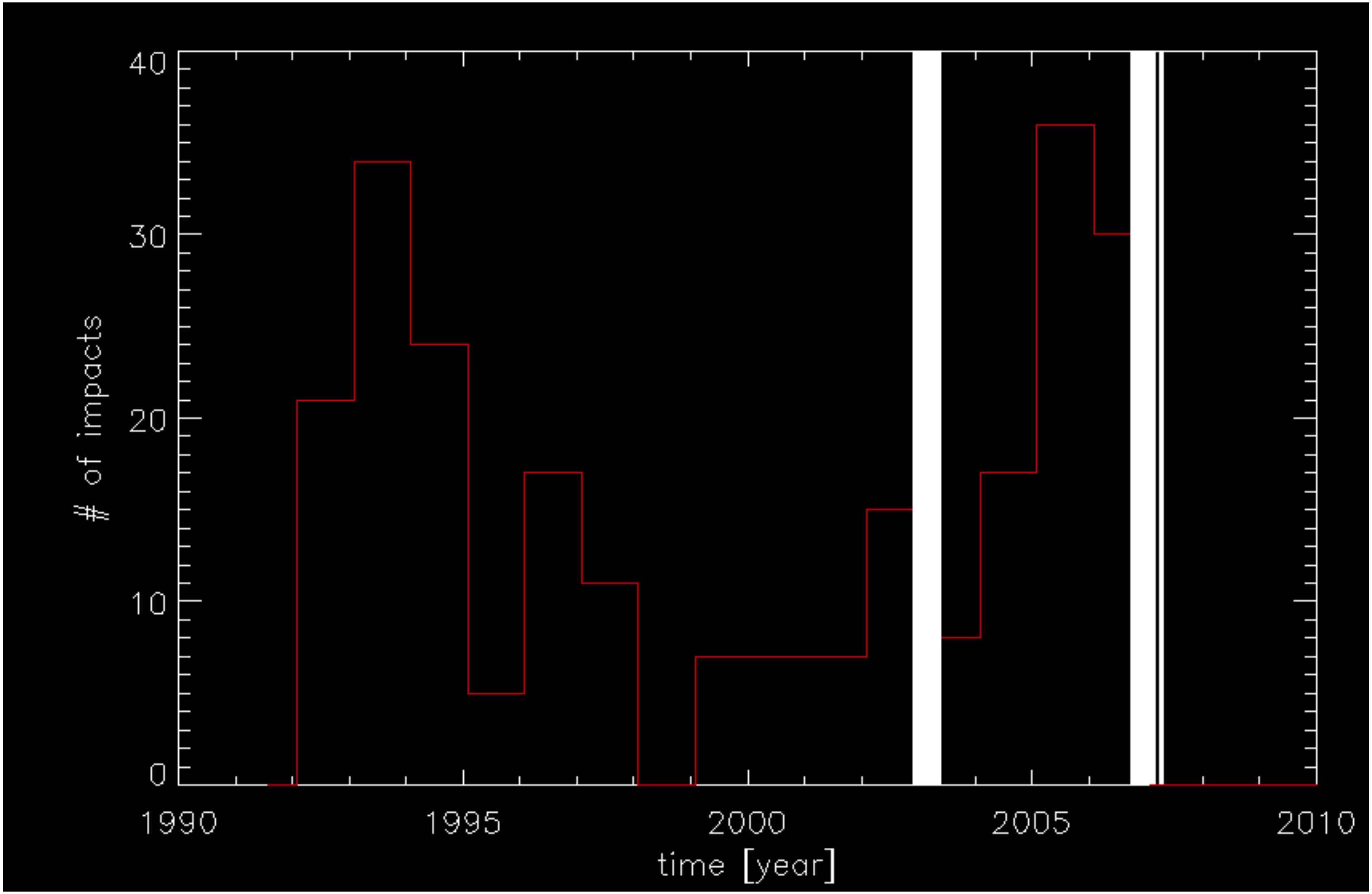

Direction

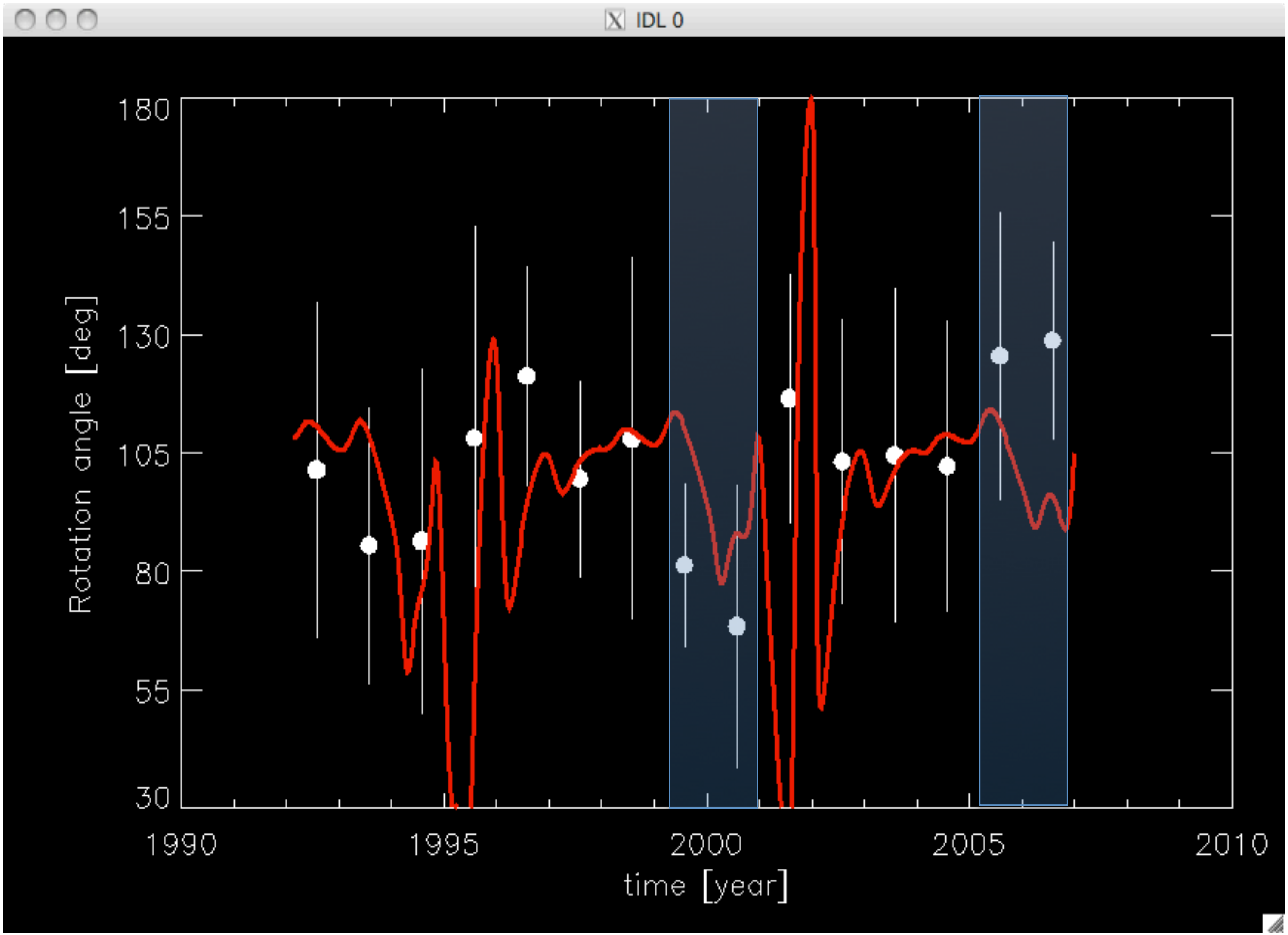
IDL 0
180
155
130
105
80
55
30
Rotation angle [deg]
1990
1995
2000
2005
2010
time [year]

Time dependent direction

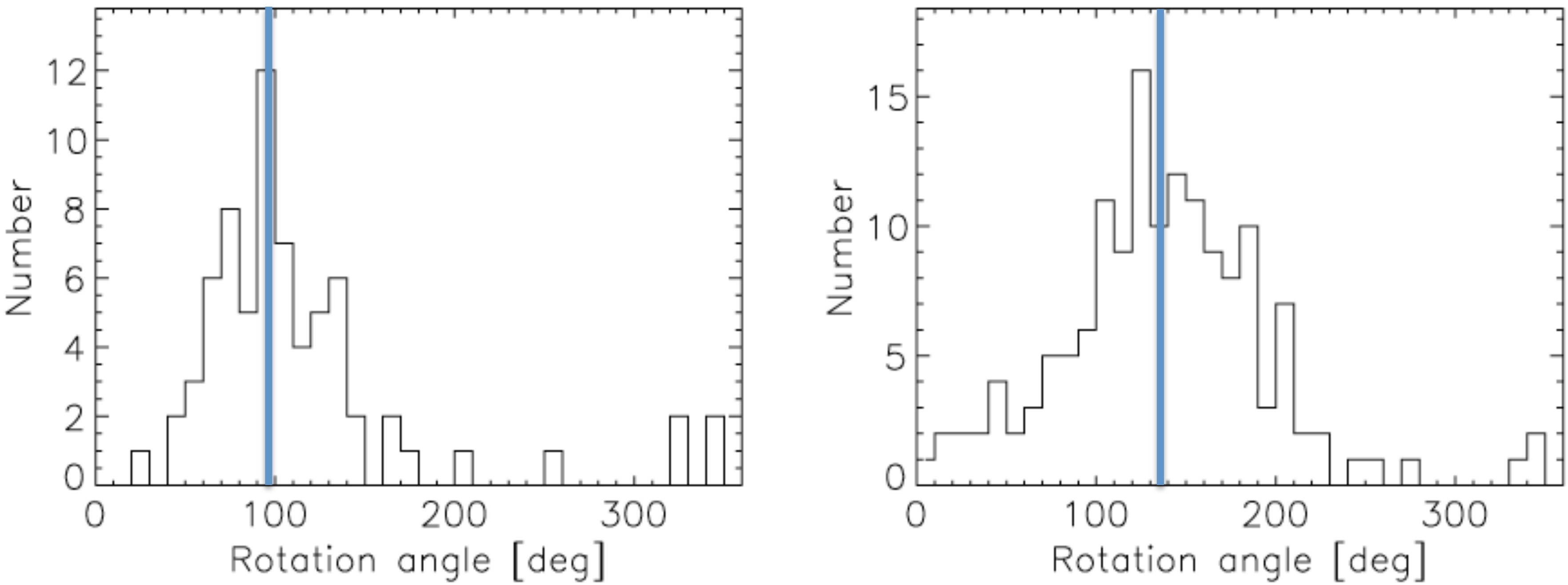

Fig. 4 Distribution of measured impact directions (i.e. spacecraft rotation angle at dust particle impact) of interstellar impactors for two time intervals. *Left:* 1 January 1997 to 31 December 1999; *right:* 1 January 2003 to 31 December 2005. In the earlier time interval the maximum of the distribution is at a rotation angle of 95° very close to the value expected from the interstellar helium flow. In the second interval the maximum is at 135°

Krüger and Grün, 2007

"The reason of this shift remains mysterious ......"

Modeling

Landgraf et al., 200; 2003
ISD:

1) Constant surface potential: +5 V
2) Specific density 2.5 g/cc
3) Start @ 100 AU with 25.3 km/s

Heliosphere

4) IMF parker spiral
5) Wavy current sheet with 22 year periodicity without averaging (cosmic ray propagation model)
6) Capture particles in a slab centered on the orbital plane of Ulysses (+/- 0.5 AU)
7) Capture velocity vectors in a $(1\ \text{AU})^3$ box around Ulysses

Animation

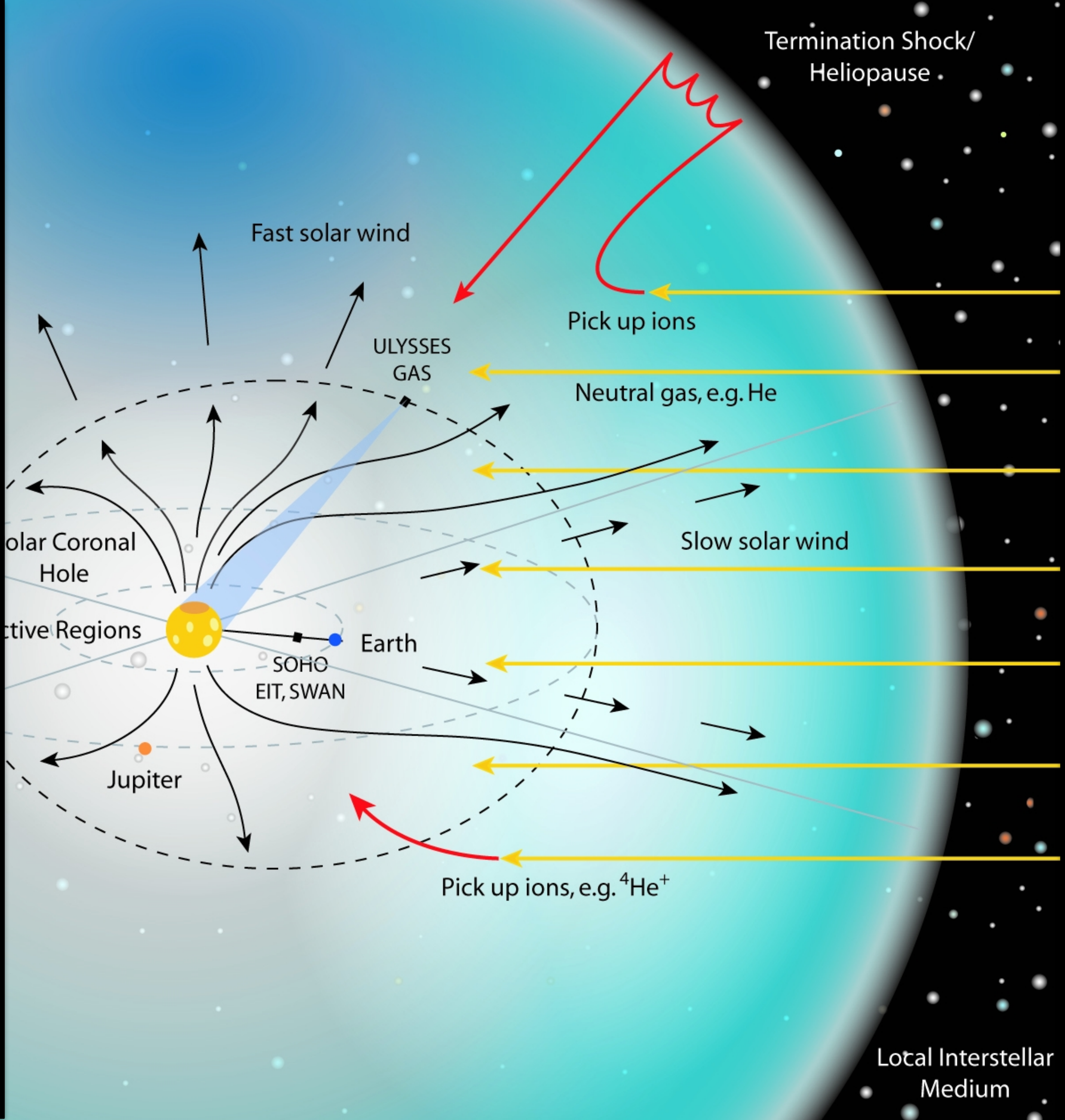

Termination Shock/
Heliopause
Fast solar wind
ULYSSES
GAS
Pick up ions
Neutral gas, e.g. He
Slow solar wind
olar Coronal
Hole
ctive Regions
Earth
SOHO
EIT, SWAN
Jupiter
Pick up ions, e.g. $^{4}He^{+}$
Local Interstellar
Medium

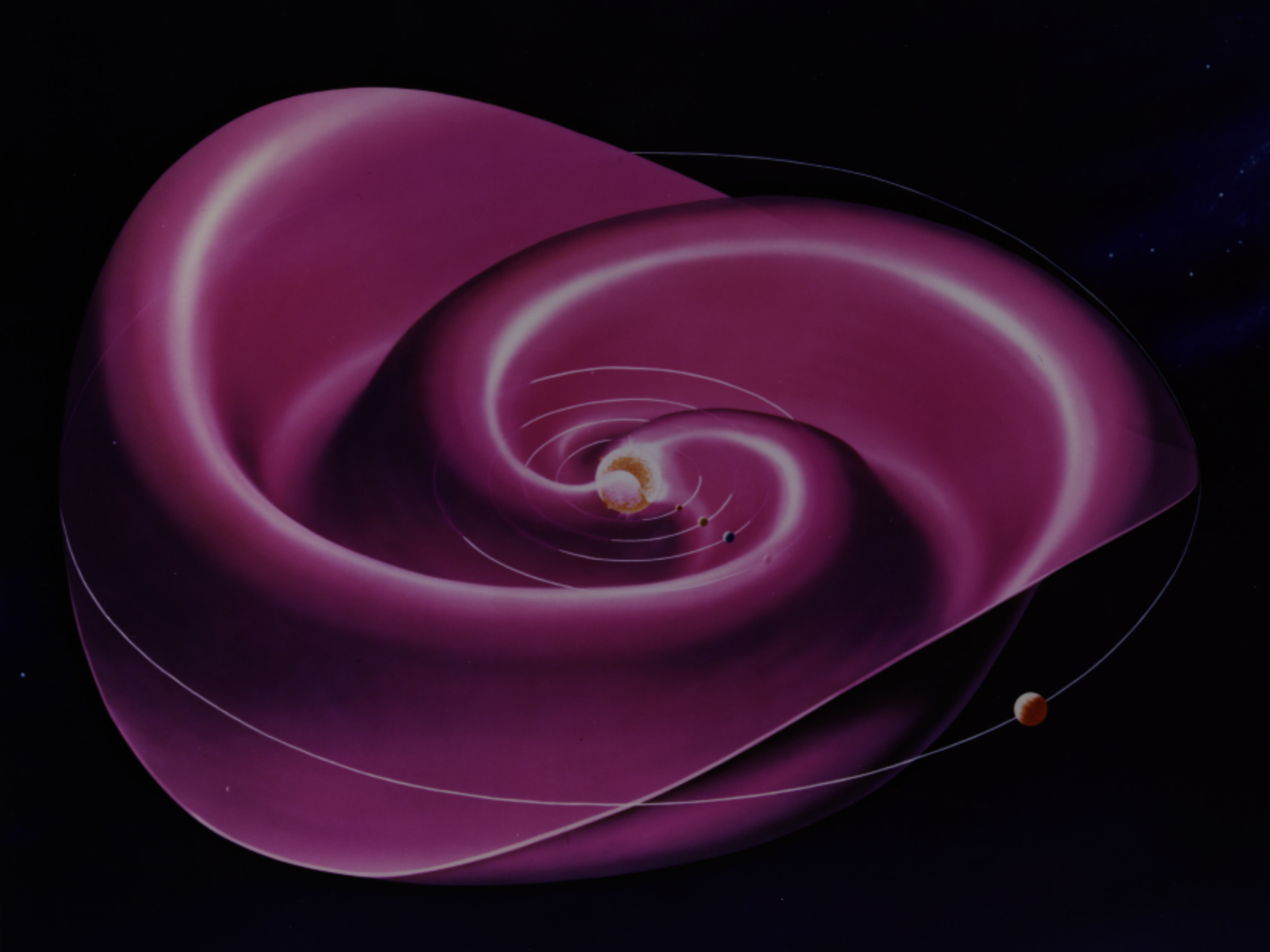

Tilt of the current sheet

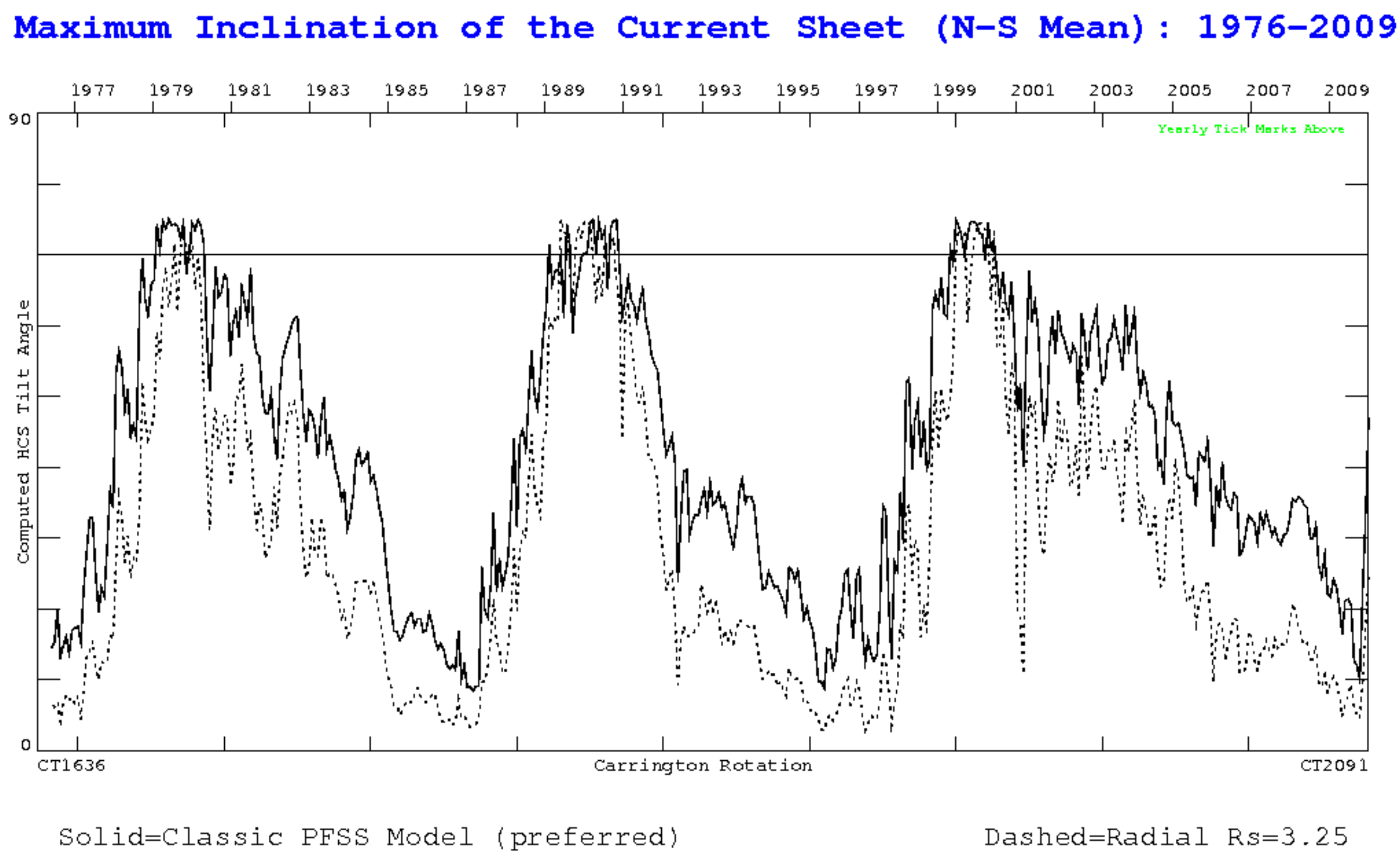

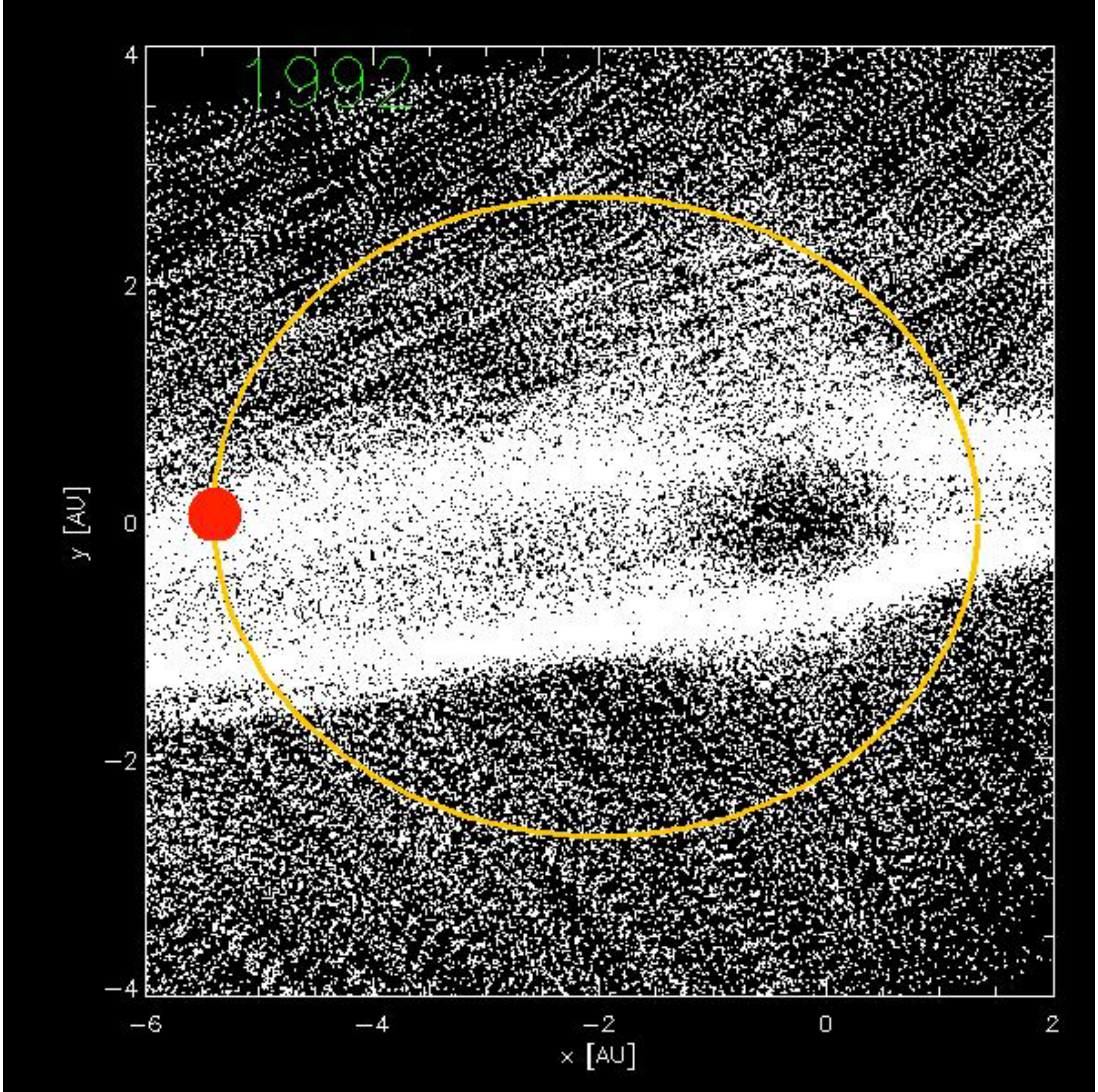
1992
4
2
0
−2
−4
y [AU]
−6
−4
−2
0
2
x [AU]

Flux variability

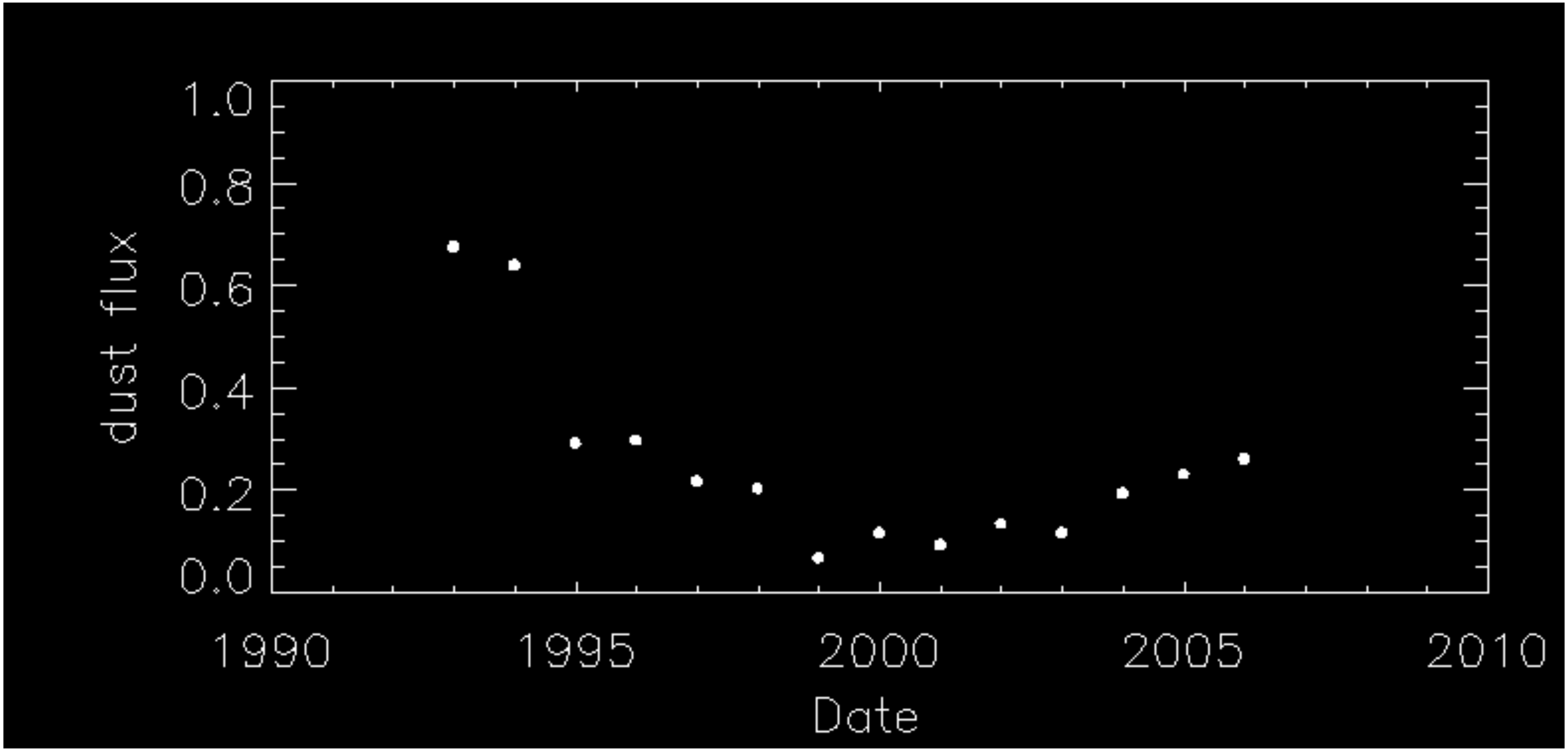

Directional Variability

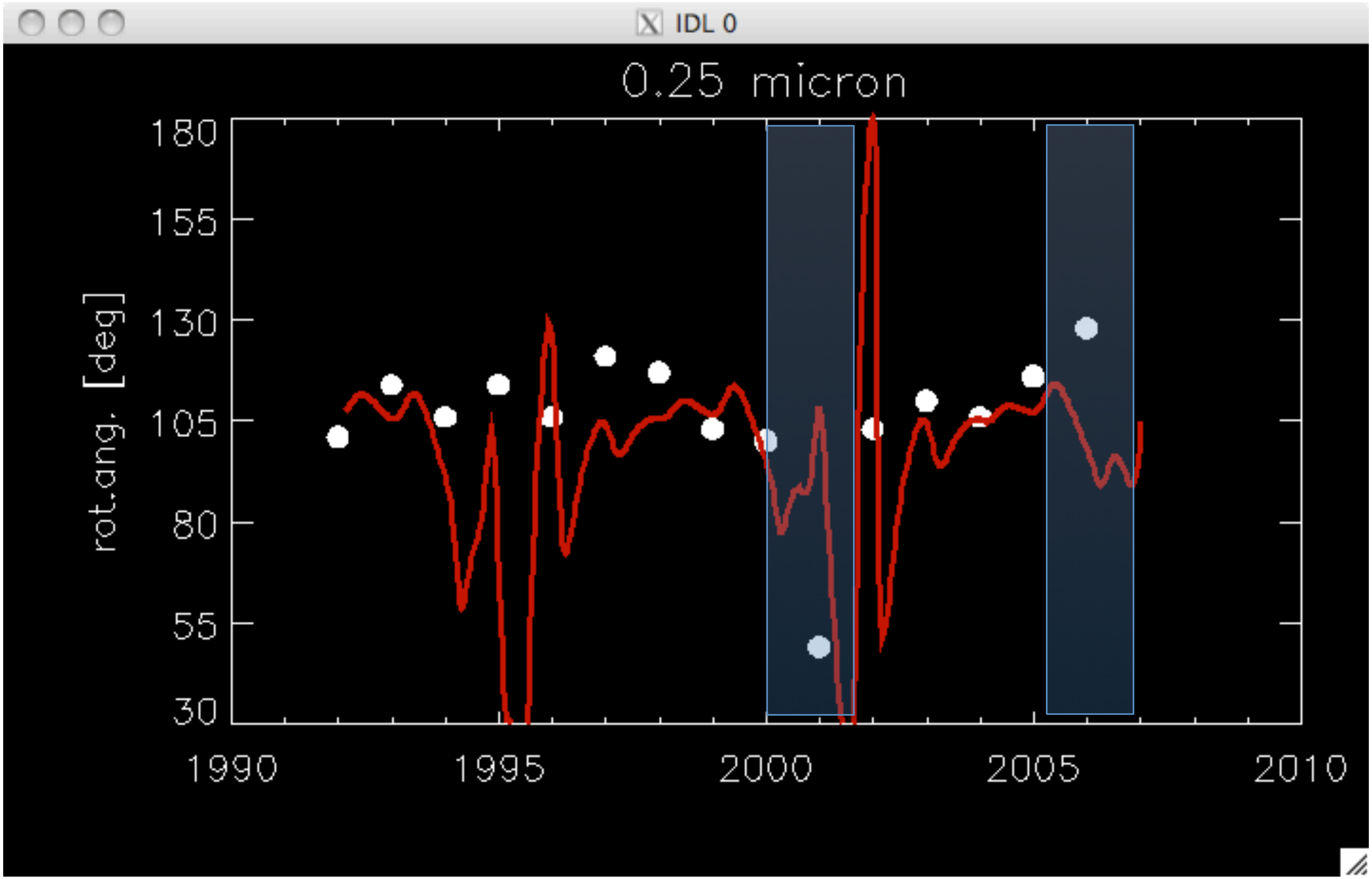

Nano-dust observations

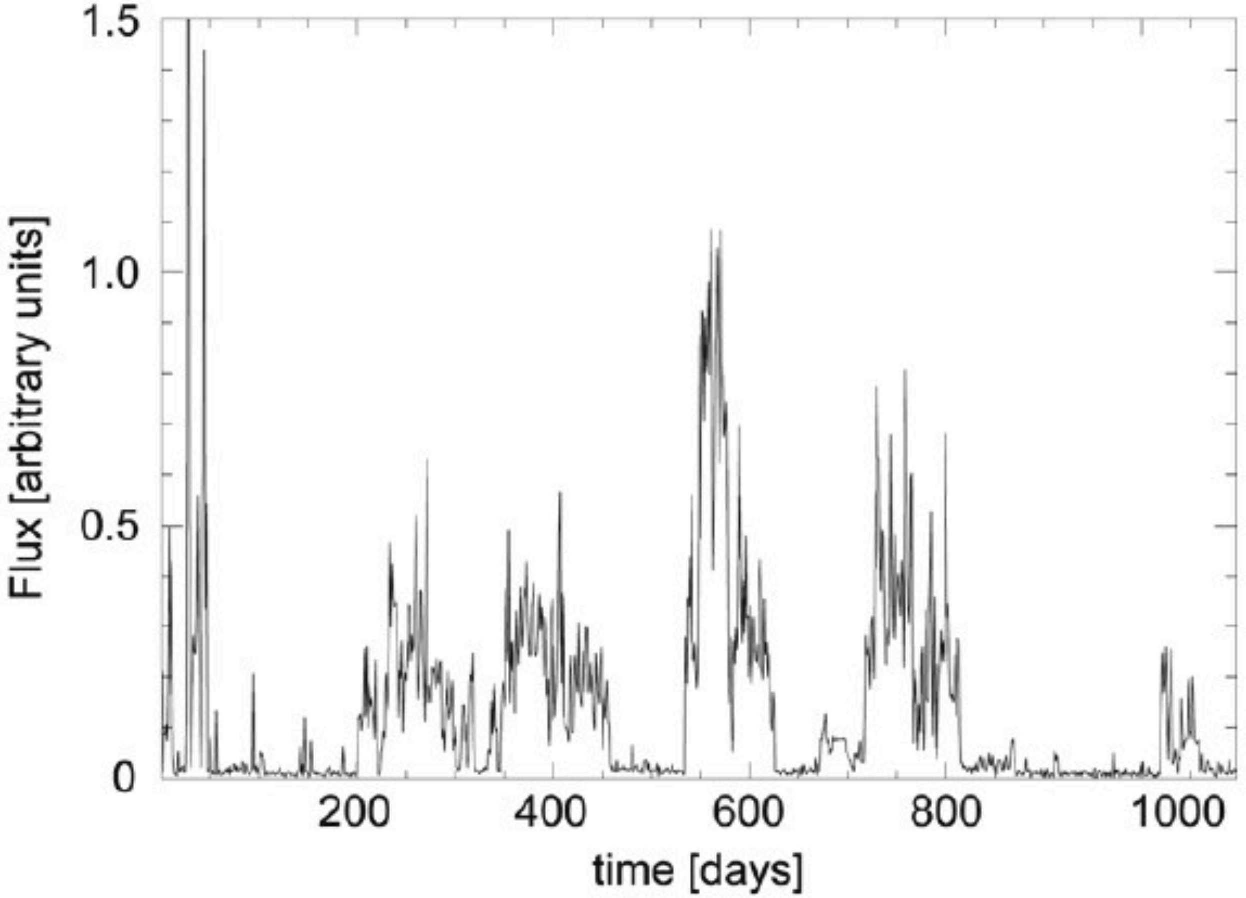

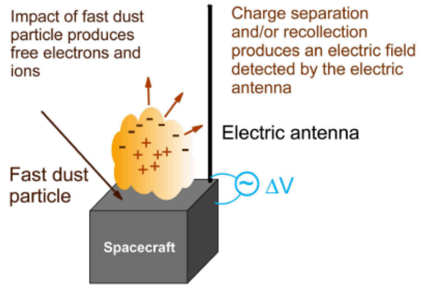

Basics of the electric detection of a fast grain impinging on a spacecraft

Meyer-Vernet et al., 2010

Figure 3. The flux rate of nanodust measured with the plasma wave experiment S/WAVES onboard Stereo A from 2007 to 2009 [30].

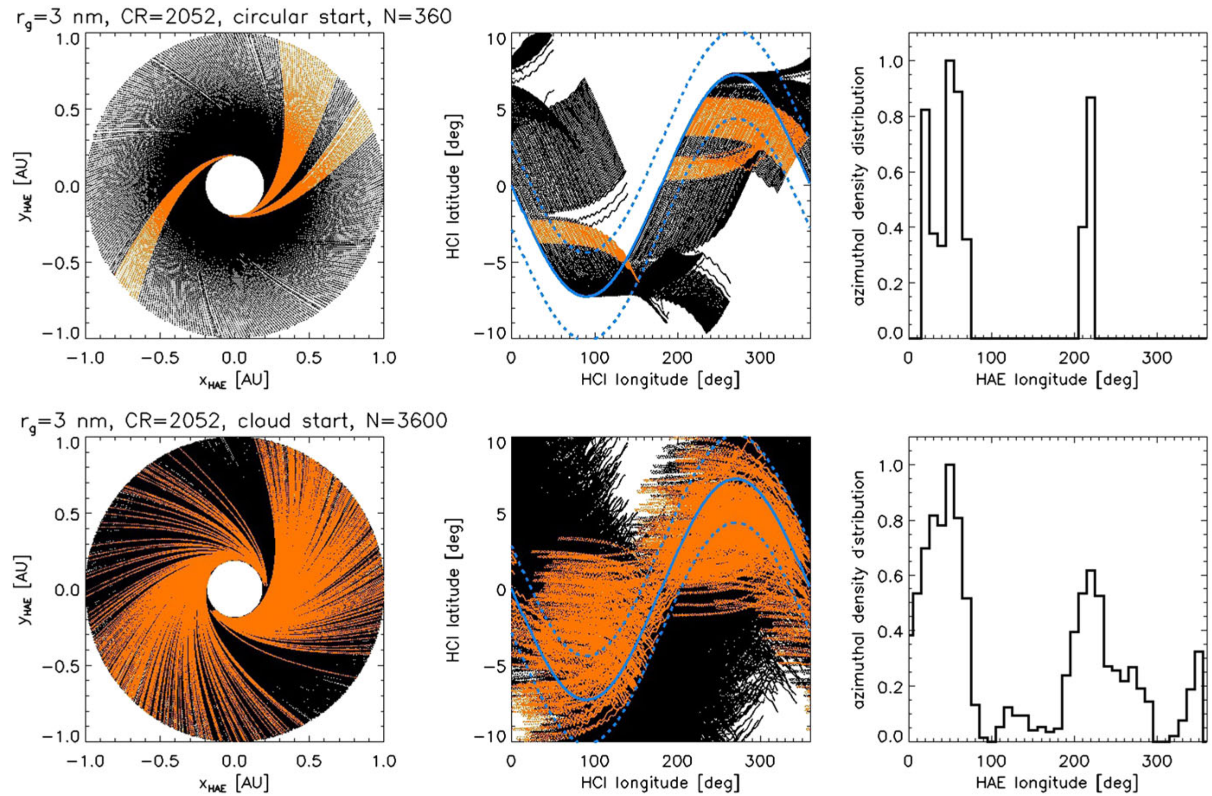

The top row shows the trajectories of 360 particles with radii $r_g = 3$ nm, started uniformly distributed along a circle in the ecliptic plane at $r = 0.2$ AU in the (left column) Heliocentric Aries Ecliptic (HAE) (x, y) plane projection, in the (middle column) HCI θ, ϕ coordinates, and the (right column) azimuthal dust density distribution in HAE. The orange lines represents the trajectories that can be detected near the ecliptic plane at 1 AU. In the (θ, ϕ) plots, the continuous blue line represents the ecliptic plane and the dashed blue lines show the detectable limits set by $|z| < \Delta z = 0.05$ AU. The bottom row is for a $N = 3600$ particle simulation using initial conditions with random inclinations in the range $0 < i < 10°$, random eccentricities in the range $0 < e < 0.01$ and random orbit orientations $(0 < \omega, \Omega < 2\pi)$.

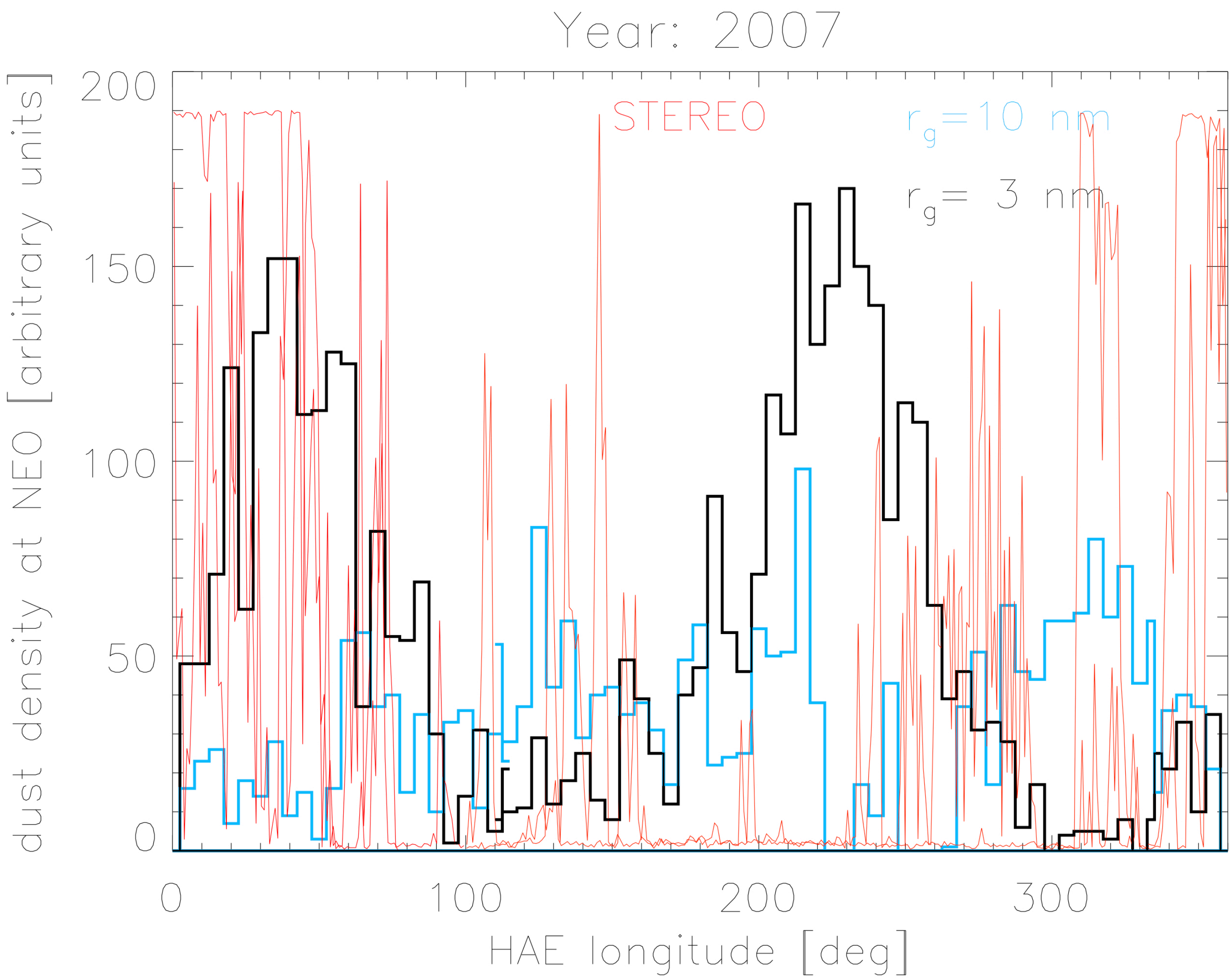

Year: 2007
STEREO
r_g=10 nm
r_g= 3 nm
dust density at NEO [arbitrary units]
HAE longitude [deg]
0
50
100
150
200
0
100
200
300

Instrumentation: Impact detector

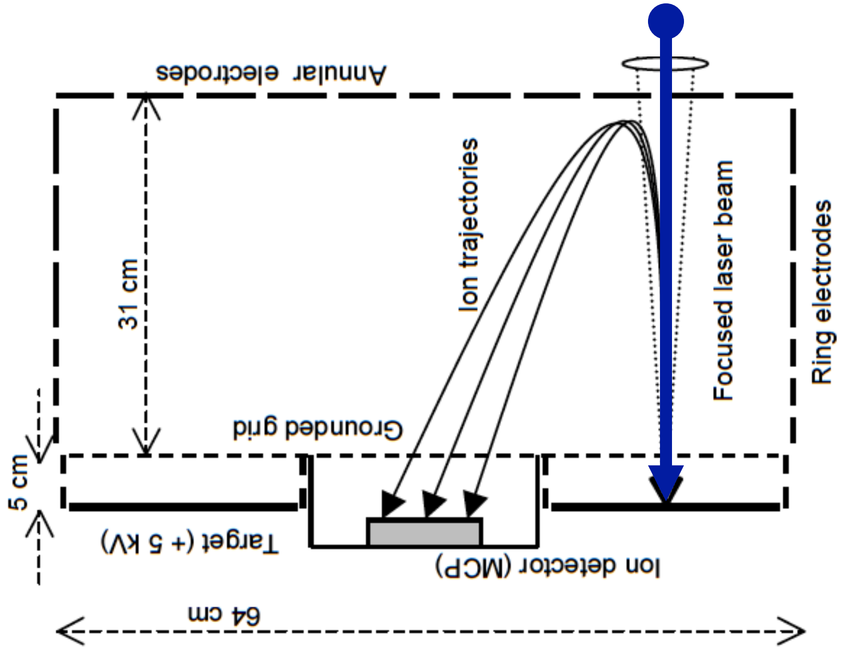

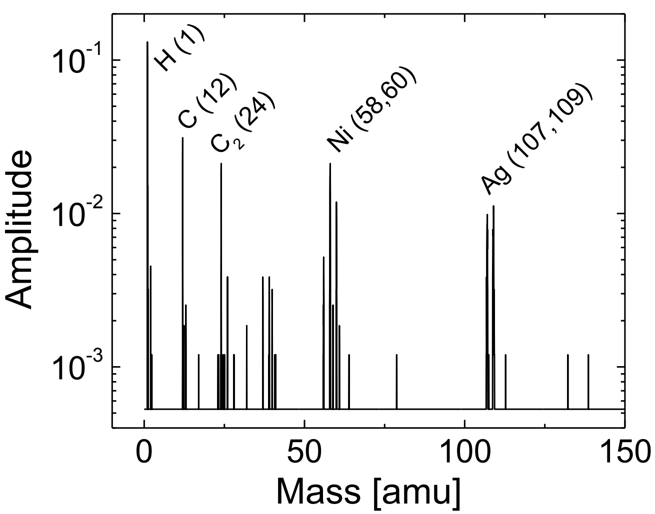

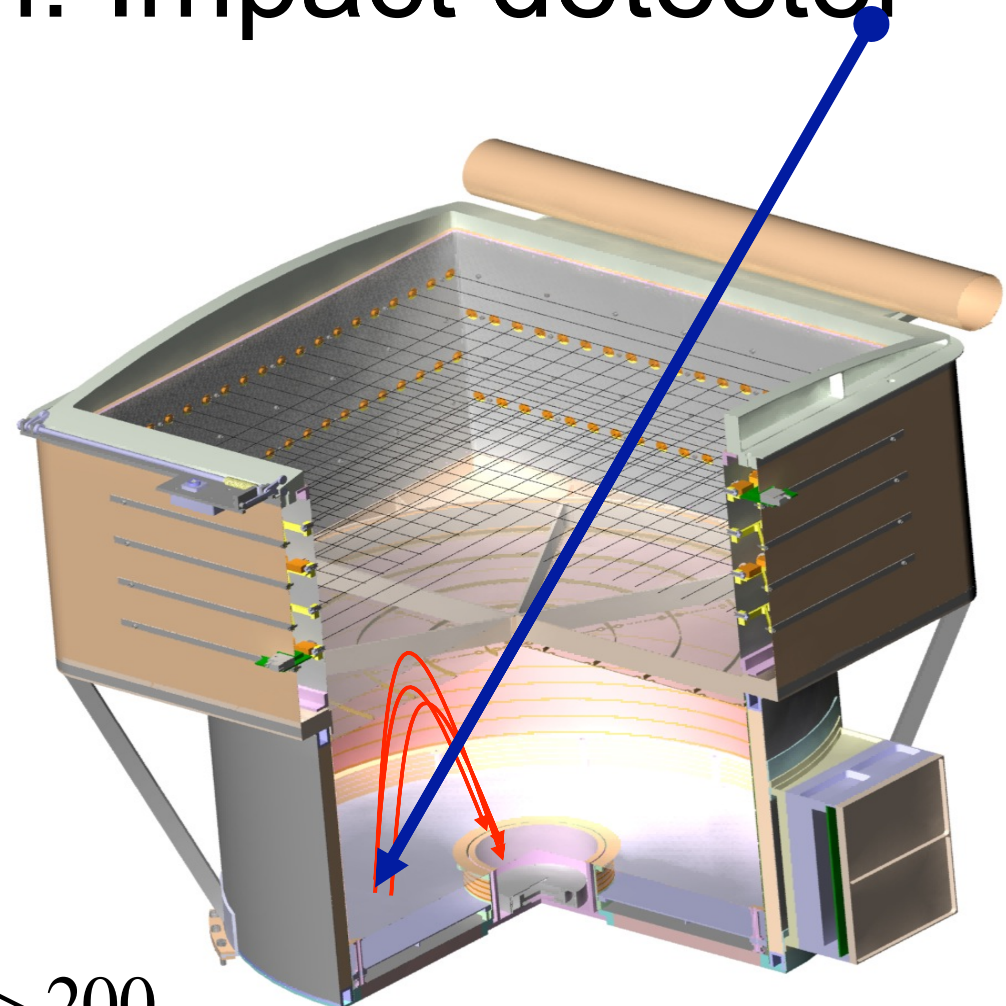

$$\frac{M}{\Delta M} > 200$$

Dust tomography of the heliosphere!

Chemical/isotopic composition of interplanetary and interstellar dust.

SUMMARY

- Dusty plasma issues are relevant to a number of in situ and remote sensing observations.
- The analysis and interpretation of particles and fields, and dust measurements cannot be done 'one instrument at a time.'
- Dust and dusty plasmas are an important component of the heliosphere